ISTANBUL TECHNICAL UNIVERSITY ★ INSTITUTE OF SCIENCE AND TECHNOLOGY

KALMAN FILTERING APPLICATIONS
ON ATTITUDE DETERMINATION OF ITU-PSAT I SATELLITE

M.Sc. Thesis by
Halil Ersin SOKEN

Department : Aeronautics and Astronautics Engineering

Programme : Aeronautics and Astronautics Engineering

JULY 2009

ISTANBUL TECHNICAL UNIVERSITY ★ INSTITUTE OF SCIENCE AND TECHNOLOGY

**KALMAN FILTERING APPLICATIONS
ON ATTITUDE DETERMINATION OF ITU-PSAT I SATELLITE**

**M.Sc. Thesis by
Halil Ersin SOKEN
(511071117)**

Date of submission :   04 May 2009
Date of defence examination :   03 June 2009

Supervisor (Chairman) :   Prof. Dr. Chingiz HAJIYEV (ITU)
Members of the Examining Committee :   Prof. Dr. Alim Rustem ASLAN (ITU)
Prof. Dr. Metin GOKASAN (ITU)

JULY 2009

İSTANBUL TEKNİK ÜNİVERSİTESİ ★ FEN BİLİMLERİ ENSTİTÜSÜ

İTÜ-PSAT I UYDUSUNUN YÖNELİM KESTİRİMİ ÜZERİNE KALMAN SÜZGEÇLEMESİ UYGULAMALARI

YÜKSEK LİSANS TEZİ
Halil Ersin SÖKEN
(511071117)

Tezin Enstitüye Verildiği Tarih :	**04 Mayıs 2009**
Tezin Savunulduğu Tarih :	**03 Haziran 2009**

Tez Danışmanı :	**Prof. Dr. Çingiz HACIYEV (İTÜ)**
Diğer Jüri Üyeleri :	**Prof. Dr. Alim Rüstem ASLAN (İTÜ)**
	Prof. Dr. Metin GÖKAŞAN (İTÜ)

TEMMUZ 2009

FOREWORD

First of all, I would like to thank to my advisor, Professor Chingiz Hajiyev who has made this study possible with all his supports and feedbacks.

Lastly, at that point, I must signify that, I am grateful to my family, who always believe in me and give me vitality with their endless love.

July 2009   Halil Ersin SÖKEN

                                                    Aerospace Engineer

TABLE OF CONTENTS

ABBREVIATIONS

ADCS	: Attitude Determination and Control System
ADS	: Attitude Determination System
AEKF	: Adaptive Extended Kalman Filter
AEFKF	: Adaptive Extended Fading Kalman Filter
AFKF	: Adaptive Fading Kalman Filter
AUFKF	: Adaptive Unscented Fading Kalman Filter
AUKF	: Adaptive Unscented Kalman Filter
AKF	: Adaptive Kalman Filter
DR	: Dead Reckoning
EKF	: Extended Kalman Filter
EMF	: Earth Magnetic Field
GPS	: Global Positioning System
IAE	: Innovation Based Adaptive Estimation
IGRF	: International Geomagnetic Reference Field
IMU	: Inertial Measurement Unit
KF	: Kalman filter
LEO	: Low Earth Orbit
LKF	: Linear Kalman Filter
MMAE	: Multiple Model Based Adaptive Estimation
OKF	: Optimal Kalman Filter
RAE	: Residual Based Adaptive Estimation
UKF	: Unscented Kalman Filter

x

LIST OF TABLES

LIST OF FIGURES

KALMAN FILTERING APPLICATIONS ON ATTITUDE DETERMINATION OF ITU-PSAT I SATELLITE

SUMMARY

Especially after 1990s, space industry have gained an overwhelming interest in smaller and lighter spacecrafts. Although that can be explained with several causes, main reason was the desire to achieve space missions with lesser economical demands. Pico satellites and so cubesats, which is a sort of picosatellite with special characteristics, are the yields of this idea. ITU-PSAT I, first satellite of Istanbul Technical University, can be considered as a part of this concept.

Thus far, Kalman filter based attitude estimation algorithms have been used in many space applications. When the issue of pico satellite attitude estimation is taken into consideration, general linear approach to Kalman filter becomes insufficient and Extended Kalman Filters (EKF) are the types of filters, which are designed in order to overrun this problem. However, when magnetometers are one of the onboard measurement devices as it is for ITU-PSAT I, the nonlinearity degree of the attitude estimation system increases because of the arisen nonlinear measurement model as well as inherent nonlinear dynamics of the satellite. Therefore, EKF may give inaccurate results. Unscented Kalman Filter (UKF) that does not require linearization phase and so Jacobians can be preferred instead of EKF in such circumstances. In addition to the attitude states of a satellite, EKF and UKF can be also used to identify satellite dynamics parameters such as unknown constant disturbance torques and measurement device biases.

Nevertheless, both EKF and UKF are nonrobust (sensitive to failure) against the failure of the measurement system. However, if the Kalman filter algorithm is built with an adaptive manner, such that, faulty measurements do not affect attitude estimation process, accurate estimation results even in case of measurement malfunctions can be guaranteed. Two relatively new technique for such concept can be shown as adaptive Kalman filters (AKF) built in the base of filter gain correction with single and multiple fading factors.

In this thesis, various Kalman filter algorithms for the attitude estimation of a pico satellite in different mission periods are developed. State estimation performances of both EKF and UKF are examined when the magnetometers are the only onboard measurement sensors. Identification of the parameters e.g. unknown constant external torques, magnetometer bias and gyro bias is achieved in case of Inertial Measurement Unit (IMU) usage as an additional sensor. Besides, Adaptive Unscented Fading Kalman Filter (AUFKF) with single and multiple fading factors are proposed so as to secure filter robustness against measurement malfunctions. Developed Kalman filter algorithms are tested as a part of the attitude determination system of ITU PSAT I satellite by the use of simulations.

İTÜ-PSAT I UYDUSUNUN YÖNELİM KESTİRİMİ ÜZERİNE KALMAN SÜZGEÇLEMESİ UYGULAMALARI

ÖZET

Özellikle 1990lar'dan sonra, uzay endüstrisi nispeten daha küçük ve hafif olan uzay araçlarına karşı kaçınılmaz bir ilgi kazandı. Bu durum bir çok nedenle açıklanabilmesine rağmen, temel sebep uzay görevlerini daha az ekonomik isterlerle gerçekleştirebilmekti. Piko uydular ve bu tip uyduların özel bir türü olan küp uydular bu fikrin bir getirisidir. İstanbul Teknik Üniversitesinin ilk uydusu olan İTÜ-PSAT I de bu düşüncenin bir parçası olarak ele alınabilir.

Günümüze değin, Kalman süzgeci temeline dayanan yönelim kestirim algoritmaları bir çok uzay görevinde kullanılmıştır. Piko uydu yönelim kestirimi konusu düşünüldüğünde, Kalman süzgeçlemesine doğrusal yaklaşım yetersiz kalır. Genişletilmiş Kalman Süzgeci (GKS) bu problemi çözmek için geliştirilmiştir. Lakin, İTÜ-PSAT I uydusu için geçerli olduğu gibi, uydu üzerinde taşınan sensörlerden biri manyetometreler olunca, uydunun doğasında var olan doğrusal olmayan dinamiklerin yanısıra ortaya çıkan doğrusal olmayan ölçüm modellemesi sebebiyle, doğrusal olmama durumunun derecesinde artış gözlenir. Buna bağlı olarak da GKS'nin doğru sonuçlar vermemesi olağandır. Bu tarz durumlarda GKS'nin yerine doğrusallaştırma safhasına ve Jacobian hesaplamalarına ihtiyaç duymayan Sezgisiz Kalman Süzgeci (SKS) tercih edilebilir. GKS ve SKS'yi uydunun yönelim durum değişkenlerinin yanısıra, bilinmeyen sabit bozuntu torkları ve ölçüm cihazı kayımları gibi uydu dinamiğine ait parametreleri tanılamak için kullanmak da mümkündür.

Bununla beraber, hem GKS hem de SKS ölçüm sisteminin hatalarına karşı dayanıksızdırlar (hataya karşı duyarlıdırlar). Fakat Kalman süzgeci algoritması hatalı ölçümlerin kestirim sürecini etkilemeyeceği şekilde uyarlamalı bir anlayışla oluşturulursa, ölçüm sisteminin arıza durumları için dahi doğru kestirim sonuçları sağlanabilir. Bu tür bir anlayış için yeni sayılabilecek iki teknik, tek ve çoğul zayıflatıcı faktörlü süzgeç kazanç düzeltimi temel alınarak geliştirilmiş uyarlamalı Kalman süzgeçleridir.

Bu tezde, farklı görev dilimleri içerisinde bir piko uydunun yönelim kestirimini gerçekleştirmek için çeşitli Kalman süzgeci algoritmaları geliştirilmiştir. GKS ve SKS'nin durum değişkeni kestirim performansları manyetometrenin tek ölçüm cihazı olarak kullanıldığı durum için incelenmiştir. Ataletsel Ölçüm Birimi (AÖB) ek bir sensör olarak kullanıldığında bilinmeyen sabit dış torklar, manyetometre ve jiroskop kayımları gibi parametreler tanılanmıştır. Aynı zamanda, süzgecin ölçüm bozuntularına karşı dayanıklılığını sağlamak adına tek ve çoğul zayıflatıcı faktörlü Uyarlamalı Sezgisiz Zayıflatıcı Kalman Süzgeci (USZKS) algoritmaları önerilmiştir. Geliştirilen Kalman süzgeci algoritmaları, simülasyonlar yardımıyla İTÜ-PSAT I sisteminin yönelim belirleme sisteminin bir parçası olarak test edilmiştir.

1. INTRODUCTION

In this section, importance of the thesis is stated by introducing the main motivation and purpose of doing such study together with the literature survey, which examines past and recent similar studies as an argument.

1.1 Motivation and Purpose of the Thesis

Since the world's first Earth orbiting artificial satellite, Sputnik I, was launched on 4 October 1957, humankind has always been on a track to reach to the better in space missions. Until now, technology improved unexpectedly and today, there are more than 500 satellites on orbit where many of them are more functional and generally lesser in size and weight than their pioneers.

In astronautics, as a satellite specification, pico refers to the satellites which have mass no more than 1 kg. These types of satellites are the outcomes of a search for lighter, smaller and so cheaper spacecrafts and recently, they have been mostly considered as a part of the research projects of the organizations like universities [1].

Cubesats are special pico satellites with cubic dimensions of $10cm \times 10cm \times 10cm$. Idea was first proposed by Professor Robert Twigs from Stanford University in 1999. They are also referred as S3-SAT in the light of their main utilization purpose; student-space-study satellites [2]. By the use of cubesats, university like organizations have an opportunity to produce their own satellite, educate their students/personnel practically and demonstrate their capability to develop new technologies. Presently, there are several running cubesats projects all over the world including ITU-PSAT I.

ITU-PSAT I is the first satellite project of Istanbul Technical University. Main aim of the project is to educate students of the Astronautical Engineering Department by giving them a chance to gain practical experience in the basis of their theoretical background. Also it will be an initiative for Turkey in point of view of being the first student designed satellite.

Satellite will carry a low resolution camera for the Earth imaging and meanwhile other sensors. Besides, the ground station located in the university will communicate with the satellite and take the incoming sensor data. Satellite with the approximate weight of 1 kg, will satisfy its energy from the sophisticated solar cells on it [3]. Project is at the last phase as the flight model and space qualification tests continue. Launch is planned to be realized in 2009.

As well as ITU-PSAT I, one of the main problems of cubesat projects is the limited size of the satellites. That is also reflected to the design progress of all subsystems of them as attitude determination and control system (ADCS). When the ADCS is limited in size and mass (also in point of view of energy budget for some missions), that means the number of onboard devices going to be used must be as low as possible. However, that does not annihilate the requirement of precise attitude determination and control in most cases. Hence, the question is, is there any possible way to determine and control attitude of a cubesat accurately despite using a limited number of onboard sensors and actuators? Besides, what happens if the measurements are not reliable because of device biases or any kind of malfunctions?

Main motivation behind this study is to deal with these engineering design problems. Since the attitude of the ITU-PSAT will not be controlled, control part of the ADCS is not necessary but the question is still valid for the attitude determination procedure of the satellite. Aim is to find out if there is possibility to develop an efficient and reliable attitude determination system (ADS) for a pico satellite. While doing this, a scheme based on Kalman filtering will be followed and in general, relatively new techniques like UKF will be used.

Developing an accurate Kalman filter algorithm which is adaptive against the measurement faults can be stated as the main purpose of the thesis. Via the comparison of the EKF and UKF, the superior attitude estimation algorithm will be detected firstly. Then, alongside with the attitude states of the satellite, parameters e.g. unknown constant external torques, magnetometer and gyro biases will be identified. By that way, it will be guaranteed that the both process and measurement models are true and free of errors. At last, as the main objective, the most appropriate adaptive Kalman filter algorithm for the pico satellite, which secures its accurate estimation characteristic even in case of measurement malfunctions, will be developed.

1.2 Literature Survey

Kalman filter plays an important role in the attitude estimation procedure of the spacecrafts since it was firstly proposed [4]. Regarding the obstacles met during development process of the attitude estimation systems, various types of Kalman filters have been developed. One of these difficulties is the inherent nonlinear dynamics and kinematics of the satellites similarly to the many real world systems. Extended Kalman Filter is proposed so as to overcome this problem and it is used instead of linear Kalman filter for estimating the attitude of the satellite [5].

On the other hand, EKF has some disadvantages, especially for the highly nonlinear systems. Generally this is caused by the mandatory linearization phase of EKF procedure and so Jacobians derived with that purpose. For most of the applications, generation of Jacobians is hard, time consuming and prone to human errors [6, 7]. Nonetheless, linearization brings about an unstable filter performance when the time step intervals for update are not sufficiently small and that, results with the filter divergence [8]. Per contra, small time step intervals increase the computational burden because of the larger number of Jacobian calculations. As a result of these facts, EKF may be efficient only if the system is almost linear on the timescale of update intervals [7].

A relatively new Kalman filtering technique, which does not have the shortcomings of EKF for nonlinear systems, is Unscented Kalman Filter. UKF generalizes Kalman filter for both linear and nonlinear systems and in case of nonlinear dynamics, UKF may afford considerably more accurate estimation results than the known observer design methodologies such as Extended Kalman Filter. The basic of UKF is the fact that; the approximation of a nonlinear distribution is easier than the approximation of a nonlinear function or transformation [9]. UKF introduces sigma points to catch higher order statistic of the system and by securing higher order information of the system, it satisfies both better estimation accuracy and convergence characteristic [6].

As a spacecraft attitude estimation algorithm, UKF has many implementation examples in literature. In [10, 11] it is used as a state estimator, while both the states and the parameters of the satellite are estimated by UKF in [6, 12]. Besides, in [13] control of the multibody satellites is achieved by the use of UKF. However, in those

studies [6, 10-13] it is not considered as an identification algorithm for the unknown constant components of the external torques (the gravity-gradient, magnetic field pressure and the sun radiation) acting on the pico satellite.

On the other hand, both EKF and UKF have no capability to adapt themselves to the changing conditions of the measurement system. Malfunctions such as abnormal measurements, increase in the background noise etc. affects instantaneous filter outputs and process may result with the failure of the filter. In order to avoid from such condition, the filter must be operated adaptively.

The Kalman filter approach to the state estimation is quite sensitive to any measurement malfunctions (abnormal measurements, sudden shifts in the measurement channel, and other difficulties such as decrease of instrument accuracy, an increase of background noise, etc.). If the condition of the operation of the measurement system does not correspond to the models, used in the synthesis of the filter, then these changes resulting from some possible failures at the measurement channels significantly decrease the effectiveness of the estimation systems. In such cases to recover the possible malfunctions, the Adaptive Kalman Filters (AKF) can be used [14-24].

The basic approaches to the adaptive Kalman filtering problem are Multiple-model-based adaptive estimation (MMAE) [14-16], Innovation-based adaptive estimation (IAE) [17-19] and Residual-based adaptive estimation (RAE) [20, 21]. While in the first approach bank of Kalman filters run in parallel under different models for the filter's statistical information, in the rest the adaptation is done directly to the covariance matrices of the measurement and/or system noises based on the changes in the innovation or residual sequences.

In methods described in [14-16], the faults are assumed to be known, and the Kalman filters are designed for the known sensor/actuator faults. As the MMAE approach requires several parallel Kalman filters, and the faults should be known, it can be used in limited applications.

Estimation of the covariance matrices by IAE and RAE requires the usage of the innovation vectors or residual vectors of m epoch. This increases the storage burden and presents the determination of the width of the moving window m as another problem. Furthermore, IAE and RAE estimators require that the number, type and

distribution of the measurements for all epochs within a window should be consistent. If they do not, the covariance matrices of the measurement noises cannot be estimated based on the innovation or the residual vectors.

The Adaptive KF presented in [22] has been applied to fuse position signals from the GPS and INS for the autonomous mobile vehicles. The Extended Kalman Filter (EKF) and the noise characteristic have been modified using the Fuzzy Logic Adaptive System. In the paper [23], a method of multi-sensor data fusion based on the Adaptive Fuzzy Kalman Filter is presented. This method is applied in fusing position and orientation signals from Dead Reckoning (DR) system and the GPS for landing vehicle navigation. The EKF and the characteristics of the measurement noise are modified by using the Fuzzy Adaptive System, which is based on a covariance matching technique. It has been demonstrated that the Fuzzy Adaptive Kalman Filter gives better results (more accurate) than the EKF [22, 23]. In [24] fuzzy logic-based adaptive Kalman filter is used to build adaptive centralized, decentralized, and federated Kalman filters for adaptive multi sensor data fusion. The adaptation carried out is in the sense of adaptively adjusting the measurement noise covariance matrix of each local filter to fit the actual statistics of the noise profiles present in the incoming measured data. A fuzzy inference system based on a covariance-matching technique is used as the adaptation mechanism in the paper. The simulation results show that the proposed architectures by authors are effective in situations where there are several sensors measuring the same parameters, but each one has different measurement dynamic and noise statistics. Although fuzzy logic based adaptive Kalman filter algorithms perform well under specific circumstances, they are knowledge-based systems operating on linguistic variables and these methods, which are based on the human experiences, are not widely applicable to the vital systems such as attitude control systems.

Another concept is to scale noise covariance matrix by multiplying it with a time dependent variable. One of the methods for constructing such algorithm is to use a single adaptive factor as a multiplier to the process or measurement noise covariance matrices [25-30]. In other words, these algorithms, which may be named as Adaptive Fading Kalman Filter (AFKF), can be both used when the information about process or measurement noises is absent [28]. However, estimation performance of the Kalman filter differs for each variable, when it is utilized for complex systems with

multivariable and it may be not sufficient to use single fading factor as a multiplier for the covariance matrices [31]. Single factor may not reflect corrective effects for the faulty measurement to the estimation process, accurately. The technique, which can be implemented to surmount this problem, is to use multiple fading factors to fix the relevant component of the gain matrix, individually. Unfortunately, thus far any investigation about the comparison of the AFKF with the single and multiple fading factors have not been achieved.

In literature, it is possible to meet with a limited number of adaptive unscented Kalman filtering (AUKF) applications, which integrate the mentioned adaptive Kalman filtering algorithms with the unscented Kalman filter. In [32], a cost function is defined in order to minimize the filter computed covariance and the actual innovation covariance. However, presented algorithm requires calculation of partial derivatives and that increases the computational burden as well as being inconsistent with the mentality of UKF. Besides, in [33] a two-stage adaptive UKF is proposed in the base of the process noise and measurement noise covariances matrices adaptation. Basically, it applies the methodology presented in [28] to the nonlinear systems by the use of UKF. However, as a disadvantage, it secures the adaptation using only single fading factor and as it is aforementioned, that may be a problem for implementations on complex systems like spacecrafts.

2. PICO SATELLITE MATHEMATICAL MODEL

2.1 Attitude Representations

In his theorem, Leonhard Euler, a Swiss mathematician and physicist, states that "*the most general displacement of a rigid body with one fixed point is a rotation about some axis*" [34]. Moreover, so as to represent this rotation uniquely, at least three parameters are needed. However, there is not a single certain technique to achieve that and several representation methods may be used. In many of these techniques, it is worked with more than three parameters.

Two of commonly used techniques are Euler angles and quaternions (or Euler symmetric parameters). In this thesis, one of these two representation methods have been preferred for the construction of the mathematical model of the pico satellite, depending to the estimation algorithm. Related to their application area, Euler angles and quaternions may be more convenient than each other. Table 2.1 presents a brief comparison between them [34, 35].

Table 2.1: Characteristics of attitude representations of Euler angles and quaternions.

Representation	Number of Parameters	Advantages	Disadvantages
Euler Angles	3	-No redundant parameters -Clear physical interpretation. -Minimal set.	-Trigonometric functions in both rotation matrix and kinematic relations. -Singular for specific rotations. -No convenient product rule.
Quaternions	4	-Convenient product rule. -Simple kinematic relation. -No trigonometric functions. -No singularities.	-No clear physical interpretation. -One redundant parameter.

2.1.1 Euler angles

A transformation from one coordinate frame to another can be carried out by three consecutive rotations about different axes.

While describing the rotation of the axis with respect to another one, rotation matrixes formed by Euler angles are used. The direction cosine matrix of transformation will be the product of these three matrices.

According to [34] there are 12 possible Euler angle representations and so direction cosine matrixes for transformation. They are categorized in two as:

> *Type 1:* Case where three successive rotations take place around three different axes.

> *Type 2:* In this case first and third rotations are performed around same axis and the second one takes place about one of the other two axes.

2.1.1.1 Euler angles for vector transformation

Suppose that $\psi \rightarrow \theta \rightarrow \phi$ rotation order about z, y and x axes, which may be also referred as 3-2-1 Euler angle rotation [33, 35], is followed. That means;

- a rotation ψ about z axis and a rotation matrix of,

$$A_3 = \begin{bmatrix} \cos(\psi) & \sin(\psi) & 0 \\ -\sin(\psi) & \cos(\psi) & 0 \\ 0 & 0 & 1 \end{bmatrix} \tag{2.1}$$

- a rotation θ about y axis and a rotation matrix of,

$$A_2 = \begin{bmatrix} \cos(\theta) & 0 & -\sin(\theta) \\ 0 & 1 & 0 \\ \sin(\theta) & 0 & \cos(\theta) \end{bmatrix} \tag{2.2}$$

- a rotation ϕ about x axis and a rotation matrix of,

$$A_1 = \begin{bmatrix} 1 & 0 & 0 \\ 0 & \cos(\phi) & \sin(\phi) \\ 0 & -\sin(\phi) & \cos(\phi) \end{bmatrix} \tag{2.3}$$

Then the direction cosine matrix (or attitude matrix) that is used for transformation from reference to body frame can be obtained as the product of these three matrices.

$$A_{321} = [A_1][A_2][A_3] =$$

$$\begin{bmatrix} c(\theta)c(\psi) & c(\theta)s(\psi) & -s(\theta) \\ -c(\varphi)s(\psi) + s(\varphi)s(\theta)c(\psi) & c(\varphi)c(\psi) + s(\varphi)s(\theta)s(\psi) & s(\varphi)c(\theta) \\ s(\varphi)s(\psi) + c(\varphi)s(\theta)c(\psi) & -s(\varphi)c(\psi) + c(\varphi)s(\theta)s(\psi) & c(\varphi)c(\theta) \end{bmatrix} \qquad (2.4)$$

Here $c(\cdot)$ and $s(\cdot)$ represent the cosines and sinus functions. Per contra, matrix, which transforms a vector from body to reference frame, is simply the transpose of this matrix as $A_{321}^T = [A_3]^T [A_2]^T [A_1]^T$.

Besides, for the small angle rotations, the sinus functions become $\sin(\psi) \to \psi$, $\sin(\theta) \to \theta$, $\sin(\phi) \to \phi$ as well as the cosines functions approaches to the unity. When these approximations are used and the products of angles, which become insignificant, are ignored as $\psi\theta = \varphi\theta = \cdots = 0$, then the skew symmetric direction cosine matrix for small angles can be gained.

$$A_{321} \approx \begin{bmatrix} 1 & \psi & -\theta \\ -\psi & 1 & \varphi \\ \theta & -\varphi & 1 \end{bmatrix} \qquad (2.5)$$

2.1.1.2 Propagation of Euler angles by time

In order to found kinematic equations, which relate the Euler angles with the angular velocities in body frame, first, derivatives of the Euler angles must be transformed to the body angular rates.

$$\begin{bmatrix} p \\ q \\ r \end{bmatrix} = [A_1][A_2][A_3] \begin{bmatrix} 0 \\ 0 \\ \dot{\psi} \end{bmatrix} + [A_1][A_2] \begin{bmatrix} 0 \\ \dot{\theta} \\ 0 \end{bmatrix} + [A_1] \begin{bmatrix} \dot{\varphi} \\ 0 \\ 0 \end{bmatrix} \qquad (2.6)$$

After the matrix multiplications;

$$p = \dot{\varphi} - \dot{\psi}\sin(\theta) \qquad (2.7)$$

$$q = \dot{\theta}\cos(\varphi) + \dot{\psi}\cos(\theta)\sin(\varphi) \qquad (2.8)$$

$$r = \dot{\psi}\cos(\theta)\cos(\varphi) - \dot{\theta}\sin(\varphi) \qquad (2.9)$$

If these equations are solved for $\dot{\varphi}$, $\dot{\theta}$ and $\dot{\psi}$, then the kinematic equation via Euler angles can be determined.

$$\dot{\varphi} = p + \sin(\varphi)\tan(\theta)\, q + \cos(\varphi)\tan(\theta)\, r \qquad (2.10)$$

$$\dot{\theta} = \cos(\varphi)p - \sin(\varphi)q \qquad (2.11)$$

$$\dot{\psi} = \sin(\varphi)/\cos(\theta)\, q + \cos(\varphi)/\cos(\theta)\, r \qquad (2.12)$$

2.1.2 Quaternions

The quaternion attitude representation is a technique based on the idea that a transformation from one coordinate frame to another may be performed by a single rotation about a vector $\bar{e}$ defined with respect to the reference frame. The quaternion, denoted here by the symbol $\bar{q}$, is a four element vector, the elements of which are functions of vector $\bar{e}$ and the magnitude of the rotation, Φ:

$$q_1 = e_1 \sin\frac{\Phi}{2} \tag{2.13}$$

$$q_2 = e_2 \sin\frac{\Phi}{2} \tag{2.14}$$

$$q_3 = e_3 \sin\frac{\Phi}{2} \tag{2.15}$$

$$q_4 = \cos\frac{\Phi}{2} \tag{2.16}$$

Here e_1, e_2, e_3 are the components of the vector $\bar{e}$ which is to be rotated around with an angle of Φ. As a result by the use of quaternions a transfer from reference frame to body frame can be denoted by a single rotation around a vector defined in the reference frame.

A quaternion with components q_1, q_2, q_3 and q_4 may also be expressed as a four parameter complex number with a real component q_4 and three imaginary components, q_1, q_2 and q_3 as follows:

$$\bar{q} = q_4 + iq_1 + jq_2 + kq_3 \ , \tag{2.17}$$

where i, j, k are hyper-imaginary numbers with characteristics of;

$$i^2 = j^2 = k^2 = -1 \tag{2.18}$$

$$ij = -ji = k \tag{2.19}$$

$$jk = -kj = i \tag{2.20}$$

$$ki = -ik = j \tag{2.21}$$

Also, redundancy of quaternions must be noted as;

$$q_1^2 + q_2^2 + q_3^2 + q_4^2 = 1 \tag{2.22}$$

2.1.2.1 Quaternions for vector transformation

A vector quantity defined in body axes, r_B may be expressed in reference axes as r_R using the quaternion directly. First define a quaternion, r_B^q, in which the complex components are set equal to the components of r_B, and with a zero scalar component, that is, if:

$$r_B = ix + jy + kz \tag{2.23}$$

$$r_B^q = 0 + ix + jy + kz \tag{2.24}$$

This is expressed in reference axes as r_R^q using:

$$r_R^q = \bar{q}\, r_B^q\, \bar{q}^* \tag{2.25}$$

where $\bar{q}^* = (q_4 - iq_1 - jq_2 - kq_3)$,the complex conjugate of $\bar{q}$.

Hence,

$$r_R^q = (q_4 + iq_1 + jq_2 + kq_3)(0 + ix + jy + kz)(q_4 - iq_1 - jq_2 - kq_3)$$

$$= 0 + \{(q_4^2 + q_1^2 - q_2^2 - q_3^2)x + 2(q_1q_2 - q_4q_3)y + 2(q_1q_3 + q_4q_2)z\}i$$

$$+\{2(q_1q_2 + q_4q_3)x + (q_4^2 - q_1^2 + q_2^2 - q_3^2)y + 2(q_2q_3 - q_4q_1)z\}j$$

$$+\{2(q_1q_3 - q_4q_2)x + 2(q_2q_3 + q_4q_1)y + (q_4^2 - q_1^2 + q_2^2 - q_3^2)z\}k \tag{2.26}$$

Alternatively, r_R^q may be expressed in matrix form as follows:

$$r_R^q = A'\, r_B^q \tag{2.27}$$

where $A' = \begin{bmatrix} 0 & 0 \\ 0 & A \end{bmatrix}$, $r_R^q = [0\ r_B]$ and

$$A = \begin{bmatrix} q_1^2 - q_2^2 - q_3^2 + q_4^2 & 2(q_1q_2 + q_3q_4) & 2(q_1q_3 - q_2q_4) \\ 2(q_1q_2 - q_3q_4) & -q_1^2 + q_2^2 - q_3^2 + q_4^2 & 2(q_2q_3 + q_1q_4) \\ 2(q_1q_3 + q_2q_4) & 2(q_2q_3 - q_1q_4) & -q_1^2 - q_2^2 + q_3^2 + q_4^2 \end{bmatrix} \tag{2.28}$$

which is equivalent to writing:

$$r_R = Ar_B \tag{2.29}$$

Here A is the same direction cosine matrix that is used for transformation from body to reference frame.

2.1.2.2 Propagation of quaternions by time

While defining the kinematic equations of motion with quaternions, time dependence of them must be used and that can be derived from the product relation [34].

Multiplication of quaternion is performed in a way not too different from complex number multiplications. However the order of the process must be regarded. By using characteristic of hyper-imaginary numbers;

$$\bar{q}'' = \bar{q}\bar{q}' = (q_4 + iq_1 + jq_2 + kq_3)(q_4' + iq_1' + jq_2' + kq_3') \qquad (2.30)$$

$$\bar{q}'' = (-q_1q_1' - q_2q_2' - q_3q_3' + q_4q_4')$$

$$i(q_1q_4' + q_2q_3' - q_3q_2' + q_4q_1') +$$

$$j(-q_1q_3' + q_2q_4' + q_3q_1' + q_4q_2') +$$

$$k(q_1q_2' - q_2q_1' + q_3q_4' + q_4q_3') \qquad (2.31)$$

If it is written in matrix form,

$$\begin{bmatrix} q_1'' \\ q_2'' \\ q_3'' \\ q_4'' \end{bmatrix} = \begin{bmatrix} q_4' & q_3' & -q_2' & q_1' \\ -q_3' & q_4' & q_1' & q_2' \\ q_2' & -q_1' & q_4' & q_3' \\ -q_1' & -q_2' & -q_3' & q_4' \end{bmatrix} \begin{bmatrix} q_1 \\ q_2 \\ q_3 \\ q_4 \end{bmatrix} \qquad (2.32)$$

Now assume that, $\bar{q}$ and $\bar{q}''$ correspond to the orientation of the body at t and $t + \Delta t$, respectively. Also $\bar{q}'$ is for the representation of position at $t + \Delta t$ in a relative way to the position that has been occupied at t .

$$q_1' \equiv e_1 \sin \frac{\Delta \Phi}{2} \qquad (2.33)$$

$$q_2' \equiv e_2 \sin \frac{\Delta \Phi}{2} \qquad (2.34)$$

$$q_3' \equiv e_3 \sin \frac{\Delta \Phi}{2} \qquad (2.35)$$

$$q_4' \equiv \cos \frac{\Delta \Phi}{2} \qquad (2.36)$$

When the necessary multiplication is done it is obvious that

$$\bar{q}(t + \Delta t) = \left\{ \cos \frac{\Delta \Phi}{2} I + \sin \frac{\Delta \Phi}{2} \begin{bmatrix} 0 & e_3 & -e_2 & e_1 \\ -e_3 & 0 & e_1 & e_2 \\ e_2 & -e_1 & 0 & e_3 \\ -e_1 & -e_2 & -e_3 & 0 \end{bmatrix} \right\} \bar{q}(t) \qquad (2.37)$$

where e_1, e_2, e_3 are the components of rotation axis unit vector and I is the 4×4 identity matrix. After that by small angle approximation

$$cos\frac{\Delta\Phi}{2} \approx 1 \tag{2.38}$$

$$sin\frac{\Delta\Phi}{2} \approx \frac{1}{2}\bar{\omega}_{BR}\Delta t \tag{2.39}$$

It is possible to show that

$$\bar{q}(t+\Delta t) \approx \left\{I + \frac{1}{2}\begin{bmatrix} 0 & r & -q & p \\ -r & 0 & p & q \\ q & -p & 0 & r \\ -p & -q & -r & 0 \end{bmatrix}\Delta t\right\}\bar{q}(t) \tag{2.40}$$

here p, q, r are components of $\bar{\omega}_{BR}$ and they indicate angular velocity of the rigid body with respect to the reference frame. Hence if a skew-symmetric matrix is defined as

$$\Omega(\bar{\omega}_{BR}) = \begin{bmatrix} 0 & r & -q & p \\ -r & 0 & p & q \\ q & -p & 0 & r \\ -p & -q & -r & 0 \end{bmatrix} \tag{2.41}$$

equation becomes

$$\bar{q}(t+\Delta t) \approx \left\{I + \frac{1}{2}\Omega\Delta t\right\}\bar{q}(t) \tag{2.42}$$

Finally it is known that

$$\frac{d\bar{q}(t)}{dt} \cong \frac{\bar{q}(t+\Delta t) - \bar{q}(t)}{\Delta t} = \frac{1}{2}\Omega\bar{q}(t) \tag{2.43}$$

2.1.3 Euler angles and quaternions relationship

Quaternions can be expressed in terms of Euler angles as well as angles can be used to define quaternions. Formulas used for transformation are simple and given below:

- Euler Angle to Quaternion:

$$\begin{bmatrix} q_1 \\ q_2 \\ q_3 \\ q_4 \end{bmatrix} = \begin{bmatrix} \cos\left(\frac{\theta}{2}\right)\cos\left(\frac{\psi}{2}\right)\sin\left(\frac{\varphi}{2}\right) - \sin\left(\frac{\theta}{2}\right)\sin\left(\frac{\psi}{2}\right)\cos\left(\frac{\varphi}{2}\right) \\ \sin\left(\frac{\theta}{2}\right)\cos\left(\frac{\psi}{2}\right)\sin\left(\frac{\varphi}{2}\right) + \cos\left(\frac{\theta}{2}\right)\sin\left(\frac{\psi}{2}\right)\cos\left(\frac{\varphi}{2}\right) \\ \sin\left(\frac{\theta}{2}\right)\cos\left(\frac{\psi}{2}\right)\cos\left(\frac{\varphi}{2}\right) + \cos\left(\frac{\theta}{2}\right)\sin\left(\frac{\psi}{2}\right)\sin\left(\frac{\varphi}{2}\right) \\ \cos\left(\frac{\theta}{2}\right)\cos\left(\frac{\psi}{2}\right)\cos\left(\frac{\varphi}{2}\right) - \sin\left(\frac{\theta}{2}\right)\sin\left(\frac{\psi}{2}\right)\sin\left(\frac{\varphi}{2}\right) \end{bmatrix} \tag{2.44}$$

- Quaternion to Euler Angle:

$$\varphi = \sin^{-1}\big(2(q_2\,q_3 + q_1\,q_4)\big) \tag{2.45}$$

$$\theta = \tan^{-1}\left(\frac{q_3+q_2}{q_4+q_1}\right) + \tan^{-1}\left(\frac{q_3-q_2}{q_4-q_1}\right) \tag{2.46}$$

$$\psi = \tan^{-1}\left(\frac{q_3+q_2}{q_4+q_1}\right) - \tan^{-1}\left(\frac{q_3-q_2}{q_4-q_1}\right) \tag{2.47}$$

2.2 Pico Satellite Dynamics

The fundamental equation of the satellite dynamics relates the time derivative of the angular momentum vector with the overall torque affecting the satellite [34];

$$\frac{d\bar{L}}{dt} = \bar{N} - \bar{\omega}_{BI}\, x\, \bar{L} = J\frac{d\bar{\omega}_{BI}}{dt} \quad , \tag{2.48}$$

$$\bar{L} = J\bar{\omega}_{BI} \quad , \tag{2.49}$$

where $\bar{L}$ is the angular momentum vector, $\bar{N}$ is the external torque vector, $\bar{\omega}_{BI}$ is the angular velocity vector of the body frame with respect to the inertial frame and J is the moment of inertia matrix. When the vectors of $\bar{L}$ and $\bar{\omega}_{BI}$ are parallel, as the rotation is about the principal axis of the satellite, then the moment of inertia matrix is formed of principal moments of inertia as

$$J = \begin{bmatrix} J_x & 0 & 0 \\ 0 & J_y & 0 \\ 0 & 0 & J_z \end{bmatrix}. \tag{2.50}$$

Note that, this condition is an obligation for the rotation without nutation [34].

By the use of (2.48) and (2.49), main equation for the dynamics part of the pico satellite mathematical model can be gained;

$$\frac{d\bar{\omega}_{BI}}{dt} = J^{-1}(\bar{N} - \bar{\omega}_{BI} \times J\bar{\omega}_{BI}). \tag{2.51}$$

Besides, if the vectors are decomposed into their components as

$$\bar{\omega}_{BI} = \begin{bmatrix} \omega_x\ \omega_y\ \omega_z \end{bmatrix}^T, \tag{2.52}$$

$$\bar{N} = \begin{bmatrix} N_x\ N_y\ N_z \end{bmatrix}^T, \tag{2.53}$$

open form of (2.51) can be given as

$$J_x\frac{d\omega_x}{dt} = N_x + \big(J_y - J_z\big)\omega_y\omega_z, \tag{2.54}$$

14

$$J_y \frac{d\omega_y}{dt} = N_y + (J_z - J_x)\omega_z\omega_x, \qquad (2.55)$$

$$J_z \frac{d\omega_z}{dt} = N_z + (J_x - J_y)\omega_x\omega_y, \qquad (2.57)$$

One the most dominant external torque that affects Low Earth Orbit (LEO) satellites like ITU-PSAT I is the gravity gradient torque. This torque is inherent for LEO satellites and can not be neglected when the satellite model is built [36, 37]. Gravity gradient torque components can be determined as;

$$\begin{bmatrix} N_x \\ N_y \\ N_z \end{bmatrix} = -3\frac{\mu}{r_0^3} \begin{bmatrix} (I_y - I_z)A_{23}A_{33} \\ (I_z - I_x)A_{13}A_{33} \\ (I_x - I_y)A_{13}A_{23} \end{bmatrix}. \qquad (2.58)$$

Here μ is the gravitational constant, r_0 is the distance between the centre of mass of the satellite and the Earth and A_{ij} represents the corresponding element of the direction cosine matrix.

2.3 Pico Satellite Kinematics

Related to the chosen attitude representation, derived equations of the satellite kinematics may be different. In this study, as a part of the preferred representations, Euler angles and quaternions, two different version of pico satellite kinematics can be given.

2.3.1 Kinematics with Euler angles

When the Euler angles are used as the attitude representation technique, Kinematic equations of motion of the pico satellite can be expressed in matrix form as

$$\begin{bmatrix} \dot{\varphi} \\ \dot{\theta} \\ \dot{\psi} \end{bmatrix} = \begin{bmatrix} 1 & s(\varphi)t(\theta) & c(\varphi)t(\theta) \\ 0 & c(\varphi) & -s(\varphi) \\ 0 & s(\varphi)/c(\theta) & c(\varphi)/c(\theta) \end{bmatrix} \begin{bmatrix} p \\ q \\ r \end{bmatrix} \qquad (2.59)$$

Here, $c(\cdot), s(\cdot)$ and $t(\cdot)$ stand for the cosines, sinus and the tangent functions successively and p, q, and r are the components of $\bar{\omega}_{BR}$ vector which indicates the angular velocity of the body frame with respect to the reference frame;

$$\bar{\omega}_{BR} = [p \quad q \quad r]^T, \qquad (2.60)$$

In satellite attitude estimation problems, generally it is worked with the angular velocity of the body frame with respect to the inertial frame since the satellite's

orientation with respect to the inertial coordinates is more significant for the designer, especially when the Earth orbiting spacecrafts are the point at issue. Nonetheless, on board inertial measuring instruments like gyros gives measurement outputs in the body frame with respect to the inertial frame [36]. Hence, $\bar{\omega}_{BI}$ and $\bar{\omega}_{BR}$ must be related. That association is possible by the equation of;

$$\bar{\omega}_{BR} = \bar{\omega}_{BI} + A \begin{bmatrix} 0 \\ -\omega_0 \\ 0 \end{bmatrix}. \tag{2.61}$$

where A represents the direction cosine matrix constituted of trigonometric functions of Euler angles. Note that, A matrix may vary in accordance with the chosen axis sequence for the Euler angle rotation as well as the kinematic equations. Here matrix is given for 3-2-1 Euler angle rotation of [34].

$A = A_{321} =$

$$\begin{bmatrix} c(\theta)c(\psi) & c(\theta)s(\psi) & -s(\theta) \\ -c(\varphi)s(\psi) + s(\varphi)s(\theta)c(\psi) & c(\varphi)c(\psi) + s(\varphi)s(\theta)s(\psi) & s(\varphi)c(\theta) \\ s(\varphi)s(\psi) + c(\varphi)s(\theta)c(\psi) & -s(\varphi)c(\psi) + c(\varphi)s(\theta)s(\psi) & c(\varphi)c(\theta) \end{bmatrix}. \tag{2.62}$$

Also, ω_0 denotes the angular velocity of the orbit with respect to the inertial frame, found as $\omega_0 = (\mu/r_0^3)^{1/2}$, where μ is the gravitational constant and r_0 is the distance between the centre of mass of the satellite and the Earth.

2.3.2 Kinematics with quaternions

Kinematic equations of the pico satellite with quaternions is based on the time derivation of quaternions and it can be given by the equation of:

$$\frac{d\bar{q}}{dt} = \frac{1}{2}\Omega(\bar{\omega}_{BR})\bar{q} \tag{2.63}$$

Here $\Omega(\bar{\omega}_{BR})$ is the skew symmetric matrix, formed of elements of the angular velocity vector in body frame with respect to the reference frame as [34];

$$\Omega = \begin{bmatrix} 0 & r & -q & p \\ -r & 0 & p & q \\ q & -p & 0 & r \\ -p & -q & -r & 0 \end{bmatrix} \tag{2.64}$$

If the $\Omega(\bar{\omega}_{BR})$ matrix is written in terms of angular velocity vector in body frame with respect to the inertial frame, $\bar{\omega}_{BI}$, then the equations that are going to be used for attitude estimation process can be determined. Simplified versions of these equations are [6]:

$$\dot{q}_1 = \frac{1}{2}\left[\omega_x q_4 - \omega_y q_3 + \omega_z q_2 + \omega_0 q_3\right] \tag{2.65}$$

$$\dot{q}_2 = \frac{1}{2}\left[\omega_x q_3 + \omega_y q_4 - \omega_z q_1 + \omega_0 q_4\right] \tag{2.66}$$

$$\dot{q}_3 = \frac{1}{2}\left[-\omega_x q_2 + \omega_y q_1 + \omega_z q_4 - \omega_0 q_1\right] \tag{2.67}$$

$$\dot{q}_4 = \frac{1}{2}\left[-\omega_x q_1 - \omega_y q_2 - \omega_z q_3 - \omega_0 q_2\right] \tag{2.68}$$

3. MODELS FOR MEASUREMENT SENSORS

In this section, measurement sensor models for ITU-PSAT I attitude estimation procedure are presented. The Earth magnetic field is modelled so as to simulate magnetometer measurements and determine magnetic field tensor vector, which is going to be used for Kalman filter observation vector prediction, while the model for IMU is derived in order to gain gyro outputs.

Performing measurements with magnetometers and/or gyros and so having the magnetic field and/or an inertial sensor as the attitude estimation reference source have various advantages and drawbacks. Table 3.1 summarizes these characteristics [34, 35]:

Table 3.1: Characteristics of the attitude estimation reference sources.

Reference	Performance	Advantages	Disadvantages
Magnetic Field (Magnetometers)	Accuracy of 0.5 deg- 5 deg	-Economical. -Low power. -Always available for LEO spacecrafts.	-Poor accuracy. -Good only for near Earth satellites. -Limited by modelling accuracy. -Orbit and attitude are strongly coupled. -Spacecraft must be magnetically clean (or in flight calibration must be done). -Sensitive to biases.
Inertial Space (Gyros)	Drift rate of 0.002deg/h - 1deg/h	-No need for external sensors. -Orbit independent. -High accuracy for limited time intervals. -Easily done onboard.	-Senses change in orientation (orientation rate) only. -No absolute measurement. -Subject to drift. -Wear and friction caused by rapidly moving parts. -Relatively high power and mass.

For all of the attitude estimation scenarios, magnetometers are used as one of the measurement sensors. Nonetheless, in case of torque, magnetometer bias and gyro bias identification, gyros (or IMU), are used as the supplementary device.

3.1 The Earth Magnetic Field Modelling

In literature there are more than one methods for modelling the Earth magnetic field (EMF). One of them is to use directly the data of International Geomagnetic Reference Field (IGRF) [38], as it is given in [39].

On the other hand, analytical calculation of the magnetic field is also possible, as it is realized in this study. As the satellite navigates along its orbit, magnetic field vector differs in a relevant way with the orbital parameters. If those parameters are known, then, magnetic field tensor vector that affects satellite can be shown as a function of time, analytically [6, 34]. Note that, these terms are obtained in the orbit reference frame.

$$H_1(t) = \frac{M_e}{r_0^3}\{cos(\omega_0 t)\,[cos(\epsilon)\,sin(i) - sin(\epsilon)\,cos(i)\,cos(\omega_e t)] -$$

$$sin(\omega_0 t)\,sin(\epsilon)\,sin\,(\omega_e t)\} \tag{3.1}$$

$$H_2(t) = -\frac{M_e}{r_0^3}[cos(\epsilon)\,cos(i) + sin(\epsilon)\,sin(i)\,cos(\omega_e t)] \tag{3.2}$$

$$H_3(t) = \frac{2M_e}{r_0^3}\{sin(\omega_0 t)\,[cos(\epsilon)\,sin(i) - sin(\epsilon)\,cos(i)\,cos(\omega_e t)] +$$

$$2\,sin(\omega_0 t)\,sin(\epsilon)\,sin\,(\omega_e t)\} \tag{3.3}$$

Here

- $M_e = 7.943\ x\ 10^{15} Wb.m$; the magnetic dipole moment of the Earth,

- $\mu = 3.98601\ x\ 10^{14} m^3/s^2$; the Earth Gravitational constant,

- $i = 97°$; the simulation value for the orbit inclination of ITU-PSAT I,

- $\omega_e = 7.29\ x\ 10^{-5} rad/s$; the spin rate of the Earth,

- $\epsilon = 11.7°$; the magnetic dipole tilt,

- $r_0 = 6{,}928{,}140 \, m$; the distance between the centre of mass of the satellite and the Earth (simulation value if the altitude of ITU-PSAT I is accepted as $550 \, km$).

Three onboard magnetometers of pico satellite measures the components of the magnetic field vector in the body frame. Therefore for measurement model, which characterizes the measurements in body frame, gained magnetic field terms must be transformed by the use of direction cosine matrix, A. Overall measurement model may be given as;

$$\begin{bmatrix} H_x(\{\bar{q}/\varphi, \theta, \psi\}, t) \\ H_y(\{\bar{q}/\varphi, \theta, \psi\}, t) \\ H_z(\{\bar{q}/\varphi, \theta, \psi\}, t) \end{bmatrix} = A \begin{bmatrix} H_1(t) \\ H_2(t) \\ H_3(t) \end{bmatrix} \tag{3.4}$$

where, $H_1(t), H_2(t)$, and $H_3(t)$ represents the Earth magnetic field vector components in orbit frame as a function of time and $H_x(\{\bar{q}/\varphi, \theta, \psi\}, t), H_y(\{\bar{q}/\varphi, \theta, \psi\}, t)$, and $H_z(\{\bar{q}/\varphi, \theta, \psi\}, t)$ shows the Earth magnetic field vector components in body frame as a function of time and varying attitude quaternions / Euler angles.

3.2 Model for IMU

Inertial Measurement Unit (IMU) consists of three rate gyros aligned through three axes, orthogonally to each other. Rate gyros supply directly the angular rates of the body frame with respect to the inertial frame. Hence the model for rate gyros can be given as;

$$\bar{\omega}_{BI\_Meas} = \bar{\omega}_{BI} + \bar{b}_g + \eta_1. \tag{3.5}$$

where, $\bar{\omega}_{BI\_Meas}$ is the measured angular rates of the satellite, $\bar{b}_g$ is the gyro bias formed of three bias components of three different gyros as $\bar{b}_g = [b_x \quad b_y \quad b_z]^T$ and η_1 is the zero mean Gaussian white noise with the characteristic of

$$E[\eta_k \eta_j^T] = I_{3x3} \sigma_g^2 \delta_{kj} , \tag{3.6}$$

Here, I_{3x3} is the identity matrix with the dimension of 3×3 , σ_g is the standard deviation of each rate gyro and δ_{kj} is the Kronecker delta function as,

$$\delta_{kj} = \begin{cases} 1, & k = j \\ 0, & k \neq j \end{cases} \tag{3.7}$$

Nevertheless, characteristic of gyro bias is given as:

$$\frac{d\bar{b}_g}{dt} = \eta_2 \qquad (3.8)$$

where, η_2 is also the zero mean Gaussian white noise.

4. KALMAN FILTERING APPLICATIONS

In this section, algorithms of Kalman filter (KF) types that are going to be used for ITU-PSAT I attitude estimation process are introduced. In order to form a base for the further Kalman filter studies, linear Kalman filter algorithm is also given.

After the first part that presents the Kalman filter algorithms in a general scheme, application procedures of these filters to the attitude estimation process of the ITU-PSAT I are proposed. Thus, it is aimed at clarifying the study for the reader.

4.1 Optimal Kalman Filters

For Kalman filters, optimality means that the filter's gain is derived optimally. Optimal Kalman Filter (OKF) uses filter gain of case, where expected value of the square of the magnitude of error in posterior state estimation is minimized. In other words, filter runs under some certain optimization law defined by minimization rule of indicated vector and so it has the optimal gain. If this optimal gain is modified in order to adapt filter to the changing conditions, that means filter is not optimal anymore and can be called as adaptive Kalman filter.

Under these circumstances, linear Kalman filter (LKF), extended Kalman filter and unscented Kalman filter are all optimal unless an adaptation process is run on their gains.

4.1.1 Linear Kalman filter

Linear Kalman filter is the filter type which may be utilized for linear systems in point of view of both system process model and measurement model. Related to this statement, it cannot be used for attitude estimation procedure of a satellite since the satellite dynamics are inherently nonlinear. Besides, as in case, measurement model of the satellite may be nonlinear too.

However, linear Kalman filter is the fundamental of other Kalman filter types that are going to be used for the attitude estimation of ITU-PSAT. Hence, its algorithm should be presented to make the latter studies more understandable.

First, let introduce the process and observation models for a dynamical system in the state space form as follow (note that, system is not controlled):

$$x_k = F_k x_{k-1} + G_k w_k \qquad (4.1)$$

$$y_k = H_k x_k + v_k, \qquad (4.2)$$

where, F_k is the system dynamics matrix, B_k is the control distribution matrix, x_k is the state vector, y_k is the measurement vector, G_k is the transition matrix of system noises, H_k is the measurement matrix and w_k and v_k are successively, white Gaussian system process and measurement noises;

$$E\left[w_k w_j^T\right] = Q_k \delta_{kj} , \qquad (4.3)$$

$$E\left[v_k v_j^T\right] = R_k \delta_{kj} , \qquad (4.4)$$

$$E\left[w_k v_j^T\right] = 0. \qquad (4.4)$$

Here, Q_k is the process noise covariance matrix, R_k is the measurement noise covariance matrix and δ_{kj} is the Kronecker delta function.

After that, optimal Kalman filter (OKF) can be given by those following steps [40]:

State prediction:

$$\tilde{x}_{k/k-1} = F_k \hat{x}_{k-1/k-1} \qquad (4.5)$$

Covariance prediction:

$$P_{k/k-1} = F_k P_{k-1/k-1} F_k^T + G_k Q_k G_k^T \qquad (4.6)$$

Innovation:

$$\tilde{e}_k = y_k - H_k \tilde{x}_{k/k-1} \qquad (4.7)$$

Optimal Kalman Gain:

$$K_k = P_{k/k-1} H_k^T \left(H_k P_{k/k-1} H_k^T + R_k\right)^{-1} \qquad (4.8)$$

State estimation:

$$\hat{x}_{k/k} = \tilde{x}_{k/k-1} + K_k \tilde{e}_k \qquad (4.9)$$

Covariance estimation:

$$P_{k/k} = (I - K_k H_k) P_{k/k-1}. \qquad \textbf{(4.10)}$$

Here $\tilde{x}_{k/k-1}$ is the predicted state vector, $P_{k/k-1}$ is the predicted covariance matrix, $\tilde{e}_k$ is the innovation sequence, K_k is the optimal Kalman gain, $\hat{x}_{k/k}$ is the estimated state vector and $P_{k/k}$ is the estimated covariance matrix for discrete step k. Subscript $k/k-1$ denotes that computation is done in current step k by using measurements of step $k-1$. Same as, subscript $k-1/k-1$ means the variable has computed at the step $k-1$ by taking measurements of step $k-1$ into consideration.

4.1.2 Extended Kalman filter

Extended Kalman filter is the version of Kalman filter developed for systems with nonlinear system process or/and measurement models. It is simply based on derivation of the system dynamics and measurement matrices constituted of partial derivatives (the Jacobians).

First step of extended Kalman filter algorithm design procedure must be describing the real world by a set of non-linear equations and these equations may be shown in state-space form as a set of first order non-linear differential equations [40].

$$\dot{x} = f(x(t), t) + w \qquad \textbf{(4.11)}$$

where x is the system state vector, $f(x)$ is nonlinear functions of these state and w is the white process noise.

Besides, measurement equation needed for Kalman filter application is also non-linear function of the states and

$$y = h(x(t), t) + v \qquad \textbf{(4.12)}$$

where y is the measurement vector, $h(x)$ is the nonlinear functions that relates the systems states with the measurements and v is the white measurement noise.

The f function can be used for prediction of states from the last outputs of the Kalman filter (estimated states) and h function can be operated to find out predicted measurements from predicted states. However in order to participate these functions in the process they must be first linearized. Hence Jacobian matrices constituted of partial derivatives with respect to the states must be derived.

$$f(x(t), t) \approx f(\hat{x}(t), t) + \frac{\partial f(x)}{\partial x}\bigg|_{\hat{x},u} \delta x \qquad (4.13)$$

$$h(x(t), t) \approx h(\tilde{x}(t), t) + \frac{\partial h(x)}{\partial x}\bigg|_{\tilde{x}} \delta x \qquad (4.14)$$

And then

$$F = \frac{\partial f(x)}{\partial x}\bigg|_{\hat{x},u} \qquad (4.15)$$

$$H = \frac{\partial h(x)}{\partial x}\bigg|_{\tilde{x}} \qquad (4.16)$$

Here F is system dynamics matrix, H is measurement matrix, $\hat{x}$ is the estimated state from the previous step, u is the control vector, and $\tilde{x}$ is the predicted state of the present step. To find out F and H matrixes in discretized form an approximation with Taylor series expansion for $e^{F\Delta t}$ and $e^{H\Delta t}$ can be done and generally first two terms of such expansion is sufficient for efficient result. Hence;

$$F_k = I + F\Delta t \qquad (4.17)$$

$$H_k = I + H\Delta t \qquad (4.18)$$

where F_k and H_k are system dynamics and measurement matrices in discretized form, I is the identity matrix and Δt is the sampling time in second.

Remaining progress of EKF is identical with the linear case and equations of (4.5)-(4.10) are used for prediction and update phases of the filter. However, remind that, at each iteration, the Jacobians must be recalculated in accordance with the changing state prediction and estimation values.

4.1.3 Unscented Kalman filter

In order to utilize Kalman filter for nonlinear systems without any linearization step, the unscented transform and so Unscented Kalman Filter is one of the techniques. UKF uses the unscented transform, a deterministic sampling technique, to determine a minimal set of sample points (or sigma points) from the *a priori* mean and covariance of the state. Then, these sigma points go through nonlinear transformation. The *posterior* mean and the covariance are obtained from these transformed sigma points [12].

As it is stated, UKF procedure begins with the determination of $2n + 1$ sigma points with a mean of $\hat{x}(k|k)$ and a covariance of $P(k|k)$. For an n dimensional state vector, these sigma points are obtained by

$$\chi_0(k|k) = \hat{x}(k|k) \tag{4.19}$$

$$\chi_i(k|k) = \hat{x}(k|k) + \left(\sqrt{(n + \kappa)[P(k|k) + Q(k)]}\right)_i \tag{4.20}$$

$$\chi_{i+n}(k|k) = \hat{x}(k|k) - \left(\sqrt{(n + \kappa)[P(k|k) + Q(k)]}\right)_i, \tag{4.21}$$

where, $\chi_0(k|k), \chi_i(k|k)$ and $\chi_{i+n}(k|k)$ are sigma points, $Q(k)$ is the process noise covariance matrix, n is the state number and κ is the scaling parameter which is used for fine tuning and the heuristic is to chose that parameter as $n + \kappa = 3$ [8]. Also, i is given as $i = 1 \dots n$.

Next step of the UKF process is transforming each sigma point by the use of system dynamics,

$$x_i(k + 1|k) = f[x_i(k|k), k]. \tag{4.22}$$

Then these transformed values are utilized for gaining the predicted mean and the covariance [10].

$$\hat{x}(k + 1|k) = \frac{1}{n + \kappa}\left\{\kappa\chi_0(k + 1|k) + \frac{1}{2}\sum_{i=1}^{2n} \chi_i(k + 1|k)\right\} \tag{4.23}$$

$$P(k + 1|k) = \frac{1}{n+\kappa}\{\kappa[x_0(k + 1|k) - \hat{x}(k + 1|k)] \cdot$$
$$[x_0(k + 1|k) - \hat{x}(k + 1|k)]$$
$$+ \frac{1}{2}\sum_{i=1}^{2n}[x_i(k + 1|k) - \hat{x}(k + 1|k)] \cdot$$
$$[x_i(k + 1|k) - \hat{x}(k + 1|k)]^T\} \tag{4.24}$$

Here, $\hat{x}(k + 1|k)$ is the predicted mean and $P(k + 1|k)$ is the predicted covariance. Nonetheless, predicted observation vector is,

$$\hat{y}(k + 1|k) = \frac{1}{n + \kappa}\left\{\kappa y_0(k + 1|k) + \frac{1}{2}\sum_{i=1}^{2n} y_i(k + 1|k)\right\}. \tag{4.25}$$

where,

$$y_i(k + 1|k) = h[x_i(k + 1|k), v(k), k].$$ **(4.26)**

After that, observation covariance matrix is determined as,

$$P_{yy}(k + 1|k) = \frac{1}{n+\kappa} \{\kappa[y_0(k + 1|k) - \hat{y}(k + 1|k)] \cdot$$

$$[y_0(k + 1|k) - \hat{y}(k + 1|k)]$$

$$+ \frac{1}{2} \sum_{i=1}^{2n} [y_i(k + 1|k) - \hat{y}(k + 1|k)] \cdot$$

$$[y_i(k + 1|k) - \hat{y}(k + 1|k)]^T\}$$ **(4.27)**

where innovation covariance is

$$P_{vv}(k + 1|k) = P_{yy}(k + 1|k) + R(k + 1).$$ **(4.28)**

Here $v(k)$ is the white Gaussian measurement noise and $R(k + 1)$ is the measurement noise covariance matrix. On the other hand the cross correlation matrix can be obtained as,

$$P_{xy}(k + 1|k) = \frac{1}{n+\kappa} \{\kappa[x_0(k + 1|k) - \hat{x}(k + 1|k)] \cdot$$

$$[y_0(k + 1|k) - \hat{y}(k + 1|k)]$$

$$+ \frac{1}{2} \sum_{i=1}^{2n} [x_i(k + 1|k) - \hat{x}(k + 1|k)] \cdot$$

$$[y_i(k + 1|k) - \hat{y}(k + 1|k)]^T\}.$$ **(4.29)**

Following part is the update phase of UKF algorithm. At that phase, first by using measurements, $y(k + 1)$, residual term (or innovation sequence) is found as

$$e(k + 1) = y(k + 1) - \hat{y}(k + 1|k),$$ **(4.30)**

and then Kalman gain is computed via equation of,

$$K(k + 1) = P_{xy}(k + 1|k)P_{vv}^{-1}(k + 1|k).$$ **(4.31)**

At last, updated states and covariance matrix are determined by,

$$\hat{x}(k + 1|k + 1) = \hat{x}(k + 1|k) + K(k + 1)e(k + 1)$$ **(4.32)**

$$P(k + 1|k + 1) = P(k + 1|k) - K(k + 1)P_{vv}(k + 1|k)K^T(k + 1).$$ **(4.33)**

Here, $\hat{x}(k+1|k+1)$ is the estimated state vector and $P(k+1|k+1)$ is the estimated covariance.

4.2 Adaptive Fading Kalman Filters

As it is aforementioned if the Kalman filter is modified in order to secure filter's robustness against the estimation system malfunctions, that means filter is not optimal anymore and can be called as adaptive Kalman filter.

In this part of the section, two different adaptive Kalman filter algorithms with the filter gain correction for the case of measurement malfunctions are introduced. By the use of defined variables named as fading factor, the faulty measurements are taken into the consideration with a small weight and the estimations are corrected without affecting the characteristic of the accurate ones. As they use fading factors to correct the estimation process, presented AKFs may be named as adaptive fading Kalman filter (AFKF). In this study, Adaptive Fading Kalman Filter (AFKF) algorithms with single and multiple fading factors are proposed.

4.2.1 Adaptive fading Kalman filter with single fading factor

In normal operation conditions, where any kind of measurement malfunction is not observed, any of the optimal Kalman filters, i.e. linear Kalman filter, extended Kalman filter and unscented Kalman filter, gives sufficiently good estimation results. However, when the measurements are faulty because of malfunctions in the estimation system such as abnormal measurements, sudden shifts or step-like changes in the measurement channel etc. filter estimation outputs become inaccurate.

Therefore, an adaptive Kalman filter algorithm, which brings the fault tolerance to the filter and secures accurate estimation results in case of faulty measurements without affecting the remaining good estimation characteristic, should be introduced. This part presents the adaptation scheme, which can be applied to LKF and EKF.

Base of the adaptive Kalman filter is the comparison of real and theoretical values of the covariance of the innovation sequence [29]. When the operational condition of the measurement system mismatches with the model used in the synthesis of the filter, then the Kalman filter gain changes according the differentiation in the

covariance matrix of the innovation sequence. Under these circumstances, covariance matrix of the innovation sequence differs as:

$$P_{e_k} = H_k P_{k/k-1} H_k^T + S_k R_k, \tag{4.34}$$

and so the Kalman gain becomes

$$K_k = P_{k/k-1} H_k^T \left(H_k P_{k/k-1} H_k^T + S_k R_k \right)^{-1} \tag{4.35}$$

Here S_k is the adaptive factor or the single fading factor (SFF).

Due to the approach, the Kalman gain is changed when the predicted observation $H_k \tilde{x}_{k/k-1}$ is considerably different from the actual observation y_k, because of the significant changes in the operational condition of the measurement system. In other word, if the real value of filtration error exceeds the theoretical error as

$$tr\{\tilde{e}_k \tilde{e}_k^T\} \geq tr\{H_k P_{k/k-1} H_k^T + R_k\} \tag{4.36}$$

filter must be run adaptively. Here $tr(\cdot)$ denotes the trace of the related matrix.

In order to determine adaptive factor, S_k, let substitute (4.34) into the (4.36) and put in that adaptation begins at the point where condition (4.36) is satisfied,

$$tr\{\tilde{e}_k \tilde{e}_k^T\} = tr\{H_k P_{k/k-1} H_k^T\} + S_k tr\{R_k\} \tag{4.37}$$

Then, in light of $tr\{\tilde{e}_k \tilde{e}_k^T\} = \tilde{e}_k^T \tilde{e}_k$ equality, S_k can be written as

$$S_k = \frac{\tilde{e}_k^T \tilde{e}_k - tr\{H_k P_{k/k-1} H_k^T\}}{tr\{R_k\}} \tag{4.38}$$

If there is some kind of malfunction in the measurement system, that means the condition (4.36) is met, then it brings out an increase in the adaptive factor S_k. Higher S_k causes a smaller Kalman gain (4.35) because of the covariance of the innovation sequence (4.34) which is also increased in adaptive case. Consequently, small Kalman gain value reduces the effect of the faulty innovation sequence on the state estimation process (4.9). In all other cases, where measurement system operates normally, adaptive factor takes the value of $S_k = 1$ and so filter runs optimally.

Nevertheless, adaptive algorithm is operated only when the measurements are faulty and in all other cases procedure is run optimally with LKF or EKF. Process is controlled by the use of a kind of statistical information. At that point, following two hypotheses may be introduced:

- γ_0; the system is normally operating

- γ_1 ; there is a malfunction in the estimation system.

To detect failures a statistical function may be defined as,

$$\beta_k = \tilde{e}_k^T \left[H_k P_{k/k-1} H_k^T + R_k \right]^{-1} \tilde{e}_k. \tag{4.39}$$

This statistical function has χ^2 distribution with n degree of freedom where n is the dimension of the state vector.

If the level of significance, α, is selected as,

$$P\{\chi^2 > \chi^2_{\alpha,M}\} = \alpha; \quad 0 < \alpha < 1 \tag{4.40}$$

the threshold value, $\chi^2_{\alpha,s}$ can be found. Hence, when the hypothesis γ_1 is correct, the statistical value of β_k will be greater than the threshold value $\chi^2_{\alpha,s}$, i.e.:

$$\begin{aligned} \gamma_0 &: \beta_k \leq \chi^2_{\alpha,s} && \forall k \\ \gamma_1 &: \beta_k > \chi^2_{\alpha,s} && \exists k \end{aligned} \tag{4.41}$$

4.2.2 Adaptive fading Kalman filter with multiple fading factors

As it is discussed, it is possible to adapt filter by using single adaptive factor as a corrective term on the filter gain [29], but that is not a healthy procedure as long as the filter performance differs for each state for the complex systems with multivariable [31]. The preferred method is to use an adaptive matrix built of multiple fading factors (MFF) to fix the relevant term of the Kalman gain matrix, individually.

In order to determine the adaptive matrix, an innovation based process may be followed. It is known that, Kalman filter innovation sequence can be determined by (4.7). Then, as the next step, real and theoretical values of the innovation covariance matrix must be compared as,

$$\frac{1}{\mu} \sum_{j=k-\mu+1}^{k} \tilde{e}_k \tilde{e}_k^T = H_k P_{k/k-1} H_k^T + R_k. \tag{4.42}$$

Here, μ is the width of the moving window. In case, where the system operates normally, the real and the theoretical innovation covariance matrix values match as

in (4.42). However, when there is a measurement malfunction in the estimation system, the real error will exceed the theoretical one. Hence, if an adaptive matrix, S_k, is added in to the algorithm as,

$$\frac{1}{\mu} \sum_{j=k-\mu+1}^{k} \tilde{e}_k \tilde{e}_k^T = H_k P_{k/k-1} H_k^T + S_k R_k, \tag{4.43}$$

then, it can be determined by the formula of,

$$S_k = \left(\frac{1}{\mu} \sum_{j=k-\mu+1}^{k} \tilde{e}_k \tilde{e}_k^T - H_k P_{k/k-1} H_k^T \right) R_k^{-1}. \tag{4.44}$$

In case of normal operation, the adaptive matrix will be a unit matrix as $S_k = I$. Here I represents the unit matrix.

Nonetheless, as the μ is a limited number because of the number of the measurements and the computations performed with computer implies errors such as the approximation errors and the round off errors; S_k matrix, found by the use of (4.44) may not be diagonal and may have diagonal elements which are "negative" or lesser than "one" (actually, that is physically impossible).

Therefore, in order to avoid such situation, composing adaptive matrix by the following rule is suggested:

$$S^* = diag(s_1^*, s_2^*, \dots, s_n^*) \tag{4.45}$$

where,

$$s_i^* = max\{1, S_{ii}\} \qquad i = 1, n . \tag{4.46}$$

Here, S_{ii} represents the ith diagonal element of the matrix S. Apart from that point, if the measurements are faulty, S_k^* will change and so affect the Kalman gain matrix;

$$K_k = P_{k/k-1} H_k^T \left(H_k P_{k/k-1} H_k^T + S_k^* R_k \right)^{-1} . \tag{4.47}$$

Therefore, in case of any kind of malfunctions, related element of the adaptive matrix, which corresponds to the faulty component of the measurement vector, increases and that brings out a smaller Kalman gain, which reduces the effect of the innovation on the state update process. As a result, more accurate estimation results can be obtained.

Nevertheless, the adaptive algorithm is again operated only when the measurements are faulty and in all other cases procedure is run optimally with regular OKF. Same statistical information with the single fading factor based algorithm, which is defined by (4.39)-(4.41), is used as the supervision criteria.

4.2.3 Adaptation procedure of unscented Kalman filter

Since the filtration algorithm of the UKF is different from LKF and EKF, its adaptation procedure must be given separately. In this part, adaptive unscented fading Kalman filter (AUFKF) algorithms with the single and multiple fading factors are proposed.

4.2.3.1 Adaptation with single fading factor

Adaptive algorithm affects characteristic of filter only when the condition of the measurement system does not correspond to the model used in the synthesis of the filter. Otherwise filter works with regular UKF algorithm (4.19)-(4.33) in an optimal way. Same as the case with LKF and EKF, adaptation occurs as a change in the covariance matrix of the innovation sequence,

$$P_{vv}(k + 1|k) = P_{yy}(k + 1|k) + S(k)R(k + 1) \qquad \textbf{(4.48)}$$

where $S(k)$ is the adaptive factor calculated in the base of innovation sequence, $e(k + 1)$ analyses. In adaptive case filter gain becomes

$$K(k + 1) = P_{xy}(k + 1|k)\big[P_{yy}(k + 1|k) + S(k)R(k + 1)\big]^{-1} \qquad \textbf{(4.49)}$$

The gain matrix is changed when the condition of

$$tr[e(k + 1)e^T(k + 1)] \geq tr\big[P_{yy}(k + 1|k) + R(k + 1)\big] \qquad \textbf{(4.50)}$$

is the point at issue. Here $tr(\cdot)$ is the trace of the related matrix. Left hand side of (4.50) represents the real filtration error while the right hand side is the accuracy of the innovation sequence known as a result of priori information [29]. When the predicted observation vector $\hat{y}(k + 1|k)$ is reasonably different from measurement vector, $y(k + 1)$, real filtration error exceeds the theoretical one. Hence gain matrix must be fixed hereafter by the use of adaptive algorithm and so adaptive factor $S(k)$. In order to calculate adaptive factor equality of

$$tr[e(k + 1)e^T(k + 1)] = tr\big[P_{yy}(k + 1|k) + S(k)R(k + 1)\big] \qquad \textbf{(4.51)}$$

is used. Equation (4.51) can be rewritten as

$$tr[e(k+1)e^T(k+1)] = tr[P_{yy}(k+1|k)] + S(k)tr[R(k+1)] \qquad \textbf{(4.52)}$$

If the knowledge of

$$tr[e(k+1)e^T(k+1)] = e^T(k+1)e(k+1) \qquad \textbf{(4.53)}$$

is taken into consideration (36) becomes

$$e^T(k+1)e(k+1) = tr[P_{yy}(k+1|k)] + S(k)tr[R(k+1)]. \qquad \textbf{(4.54)}$$

As a result, adaptive factor can be obtained as

$$S(k) = \frac{e^T(k+1)e(k+1) - tr[P_{yy}(k+1|k)]}{tr[R(k+1)]}. \qquad \textbf{(4.55)}$$

Adaptive factor rises in case of malfunctions. That makes up an increment in covariance matrix of innovation sequence and a decrement in Kalman gain as it can be seen from (4.48) and (4.49). Consequently, faulty measurements are regarded with a small weight in the identification process and filter outputs are not affected.

On the other hand, adaptive algorithm is used only in case of faulty measurements and in all other cases procedure is run optimally with regular Unscented Kalman filter. Same checkout procedure is used with the one presented in 4.2.1. However, note that, this time statistical function is build in a convenient way with the UKF as

$$\beta_k = e^T(k+1)[P_{yy}(k+1|k) + R(k+1)]^{-1}e(k+1) \qquad \textbf{(4.56)}$$

4.2.3.2 Adaptation with multiple fading factors

As in other cases, AUFKF with multiple fading factors runs when the condition of the measurement system mismatches with the model used in the synthesis of the filter. Otherwise filter works with optimal UKF algorithm. For a normally operating system, the real and the theoretical innovation covariance matrix values match as in (4.57).

$$\frac{1}{\mu} \sum_{j=k-\mu+1}^{k} e(k+1)e(k+1)^T = P_{yy}(k+1|k) + R(k+1), \qquad \textbf{(4.57)}$$

here, μ is the width of the moving window.

However, when there is a measurement malfunction in the estimation system, the real error will exceed the theoretical one. Hence, if an adaptive matrix, $S(k)$, is added into the algorithm as,

$$\frac{1}{\mu} \sum_{j=k-\mu+1}^{k} e(k+1)e(k+1)^T = P_{yy}(k+1|k) + S(k)R(k+1),$$ (4.58)

then, it can be determined by the formula of,

$$S(k) = \left(\frac{1}{\mu} \sum_{j=k-\mu+1}^{k} e(k+1)e(k+1)^T - P_{yy}(k+1|k) \right) R(k+1)^{-1}.$$ (4.59)

In case of normal operation, the adaptive matrix will be a unit matrix as $S(k) = I$. Here I represents the unit matrix.

Nonetheless, as μ is a limited number because of the number of the measurements and the computations performed with computer implies errors such as the approximation errors and the round off errors; $S(k)$ matrix, found by the use of (4.59) may not be diagonal and may have diagonal elements which are "negative" or lesser than "one" (actually, that is physically impossible).

Therefore, in order to avoid such situation, composing adaptive matrix by the following rule is suggested:

$$S^* = diag(s_1^*, s_2^*, ..., s_n^*)$$ (4.60)

where,

$$s_i^* = max\{1, S_{ii}\} \qquad i = 1, n .$$ (4.61)

Here, S_{ii} represents the ith diagonal element of the matrix S. Apart from that point, if the measurements are faulty, $S^*(k)$ will change and so affect the Kalman gain matrix;

$$K(k+1) = P_{xy}(k+1|k) \left[P_{yy}(k+1|k) + S^*(k)R(k+1) \right]^{-1} .$$ (4.62)

In case of any kinds of malfunctions, the related element of the adaptive matrix, which corresponds to the faulty component of the measurement vector, increases and that brings out a smaller Kalman gain, which reduces the effect of the faulty

innovation term on the state update process (4.32). As a result, accurate estimation results can be obtained even in case of measurement malfunctions.

On the other hand, adaptive algorithm is used only in case of faulty measurements and in all other cases procedure is run optimally with regular Unscented Kalman filter. Checkout is satisfied by the procedure formed of (4.56) with (4.40) and (4.41).

4.3 Kalman Filtering for Attitude Estimation

Throughout the study, several Kalman filter algorithms are proposed for the attitude estimation of a pico satellite. In this part, utilization methodology of these algorithms for ITU-PSAT I is investigated.

Generally, by the use of optimal EKF or UKF, attitude parameters of a satellite can be estimated. In this sense, acquiring information about the attitude angles (in Euler angles or quaternions) and the angular rates of the satellite may be sufficient. Nevertheless, for general scheme, it is assumed that all the torques, affecting the satellite, are known and measurement sensors, i.e. magnetometers and gyros are bias free. However, that is not a realistic approach, since these unknown terms always has an effect on the estimation accuracy. One of the techniques to overrun this problem is to take these unknown parameters into account and estimate them as well as the attitude angles and the angular rates.

On the other hand, performing a Kalman filter algorithm for estimation of more states means a degrading filter performance by time. In other words, estimating parameters as less as possible may bring about more precise Kalman filter results. Hence, the filter algorithms for the estimation of the unknown constant components of the external torques and the magnetometer and gyro biases should be run for short durations.

If these torque and bias terms do not change significantly for a period of time (since the external torques and the bias of the magnetometers are assumed to be constant and the bias of the gyros changes only within a limited bound), then it is possible to utilize Kalman filter algorithms that identify them, initially, and then use the general scheme for the estimation of only attitude and the angular rates. If it is needed, estimations of these parameters may be corrected by running the relevant Kalman filter algorithm periodically.

Besides, as it is mentioned, Kalman filter algorithms must be built adaptively so as to be not affected by the measurement malfunctions. Thus, main aim is to develop an accurate adaptive Kalman filter where the formerly estimated parameters such as torques and biases are taken into consideration. Table 4.1 gives the details of the mentioned Kalman filter algorithms.

Table 4.1: Characteristics of Kalman filter algorithms.

Filter Type	Measurement Sensors	Estimated parameters	No. of estimated parameters[1]
Filter for attitude parameter estimation	3 magnetometers	Attitude angles + attitude rates	6 or7
Filter for torque estimation	3 magnetometers+ 3gyros	Attitude angles+attitude rates+ constant components of the unknown external torques	9 or 10
Filter for magnetometer bias estimation	3 magnetometers+ 3gyros	Attitude angles+attitude rates+ magnetometer biases	9 or 10
Filter for gyro bias estimation	3 magnetometers+ 3gyros	Attitude angles+attitude rates+ gyro biases	9 or 10
Adaptive Kalman filter for parameter estimation	3 magnetometers	Attitude angles + attitude rates	6 or 7

4.3.1 Attitude parameter estimation scenario

In this scenario, only attitude angles and the angular rates of the pico satellite are estimated. For two different versions of attitude representation, Euler angles and quaternions, estimated state vectors are individually, formed as;

- Euler angles

$$\bar{x} = [\varphi \quad \theta \quad \psi \quad \omega_x \quad \omega_y \quad \omega_z]^T \tag{4.63}$$

---

[1] If quaternions is chosen as an attitude representation, one more parameter is required to be estimated, since there are 4 quaternion components instead of 3 Euler angles.

- Quaternions

$$\bar{x} = [q_1 \quad q_2 \quad q_3 \quad q_4 \quad \omega_x \quad \omega_y \quad \omega_z]^T \qquad \textbf{(4.64)}$$

4.3.2 Torque estimation scenario

In this scenario, along with the attitude angles and the angular rates, the unknown constant components of the external torques (magnetic field pressure and the sun radiation) are also estimated. Since the estimated torque components are constant, it is possible to say that

$$\frac{d\bar{N}}{dt} = 0 \qquad \textbf{(4.65)}$$

where $\bar{N}$ is the vector of constant unknown external torques as in (2.53).

Under these, circumstances estimated state vector will be

$$\bar{x} = [\varphi \quad \theta \quad \psi \quad \omega_x \quad \omega_y \quad \omega_z \quad N_x \quad N_y \quad N_y]^T \qquad \textbf{(4.66)}$$

Note that, torque estimation scenario is achieved with only Euler angle representation.

4.3.3 Magnetometer bias estimation scenario

As well as attitude angles and the angular rates, magnetometer biases are also estimated in this scenario. It is assumed that, bias of each magnetometer is constant such that

$$\frac{d\bar{b}_m}{dt} = 0 \quad . \qquad \textbf{(4.67)}$$

Here $\bar{b}_m$ is the magnetometer bias vector as;

$$\bar{b}_m = [b_{m_x} \quad b_{m_y} \quad b_{m_z}]^T \qquad \textbf{(4.68)}$$

As a result, the estimated state vector is

$$\bar{x} = [\varphi \quad \theta \quad \psi \quad \omega_x \quad \omega_y \quad \omega_z \quad b_{m_x} \quad b_{m_y} \quad b_{m_z}]^T \quad . \qquad \textbf{(4.69)}$$

Note that, magnetometer bias estimation scenario is achieved with only Euler angle representation.

4.3.4 Gyro bias estimation scenario

This time, instead of magnetometer bias, biases of the three onboard gyroscopes are estimated along with the Euler angles and the angular rates. Characteristic of gyro biases is same as the model given with (3.8). It may be repeated for convenience

$$\frac{d\bar{b}_g}{dt} = \eta_2 \tag{4.70}$$

where

$$\bar{b}_g = \begin{bmatrix} b_{g_x} & b_{g_y} & b_{g_z} \end{bmatrix}^T \tag{4.71}$$

Then the estimated state vector can be given as,

$$\bar{x} = \begin{bmatrix} \varphi & \theta & \psi & \omega_x & \omega_y & \omega_z & b_{g_x} & b_{g_y} & b_{g_z} \end{bmatrix}^T \tag{4.72}$$

Note that, gyro bias estimation scenario is achieved with only Euler angle representation.

4.3.5 Scenario for estimation in case of measurement malfunctions

In that last case, again only attitude angles and the angular rates of the pico satellite are estimated, but as a difference with the initial scenario, this time filter is built adaptively. Estimated state vectors are same with the ones given by (4.63) and (4.64).

5. SIMULATIONS

In this last section of the thesis, results of the simulations for the attitude estimation of the ITU-PSAT I are presented. Proposed Kalman filter algorithms run as an attitude estimator for the pico satellite and the obtained simulation outputs are given with a discussion on each of them.

Mainly, a scheme as described in 4.3 is followed and it is dealt with five separate scenarios; attitude parameter estimation, torque estimation, magnetometer bias estimation, gyro bias estimation and estimation in case of measurement malfunctions. All of these scenarios are considered for UKF while EKF is used only for attitude estimation and estimation in case of measurement malfunctions.

Also, note that, not all of the figures obtained by the simulations are given in this section. Only, figures which reflect the results clearly are chosen and presented here. If the algorithm is an extensive and important one for the thesis i.e. torque estimation and estimation by AUFKF, then the rest of the figures are put into appendix section.

5.1 Attitude Estimation via Extended Kalman Filter

5.1.1 Attitude parameter estimation

In this simulation, attitude angles and the angular rates of the pico satellite are estimated via EKF. As the attitude representation method, Euler angles are used. Simulations are realized in 10000 steps for a period of 100 seconds with 0.01 seconds of sampling time, Δt.

First part of figures gives EKF parameter identification results and the actual values in a comparing way. Second part of the figures shows the error of the estimation process based on the actual attitude values of the satellite. The last part indicates the variance of the estimation.

As it is seen in Fig.5.1, Fig.5.2 and Fig.5.3, EKF algorithm accurately estimates both the attitude angles and the angular velocities of the satellite with respect to the inertial frame.
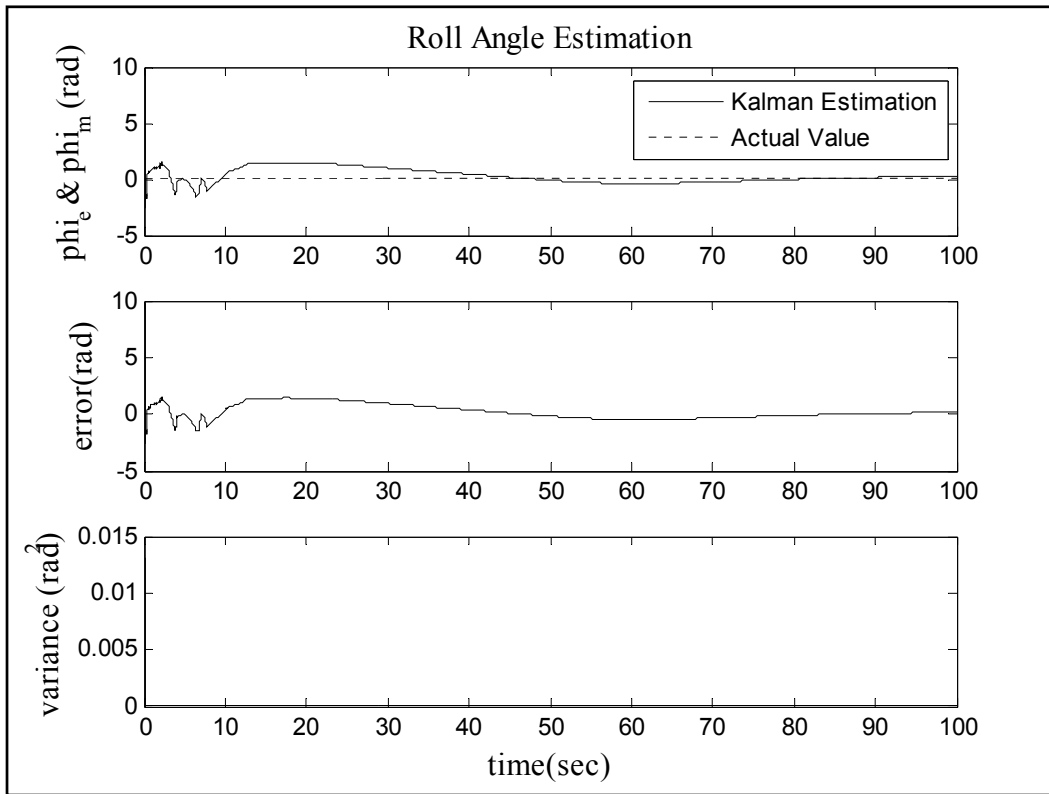
Figure 5.1 : Roll angle estimation by EKF.
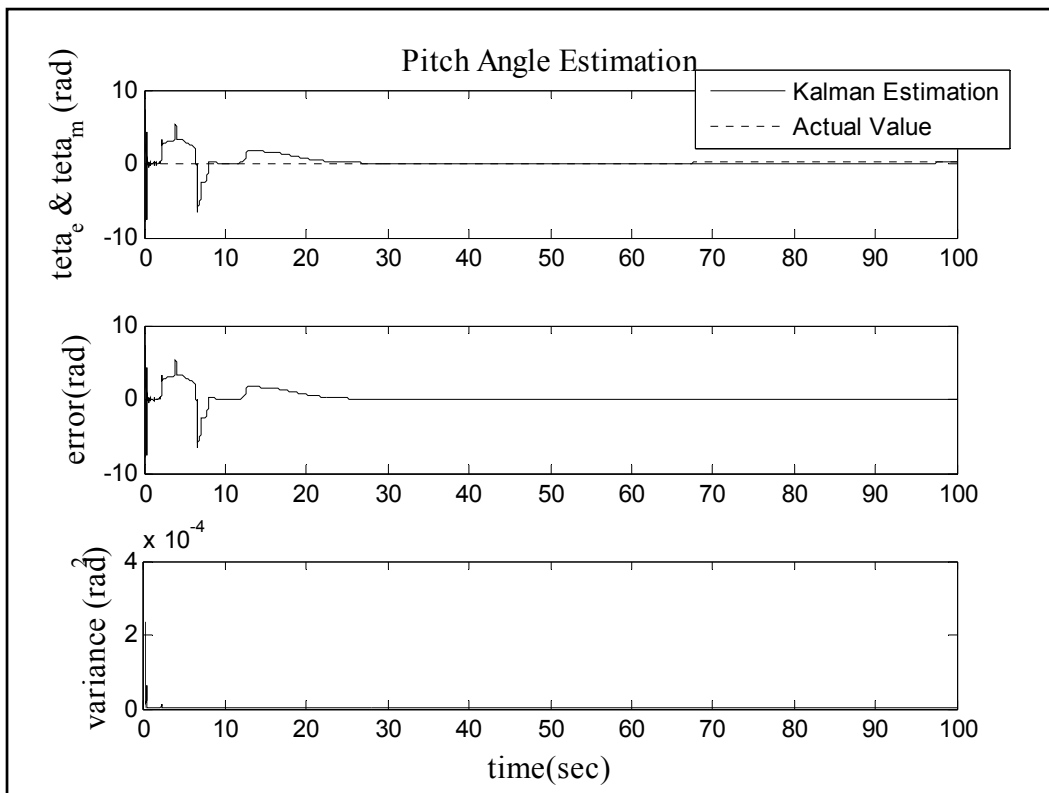
Figure 5.2 : Pitch angle estimation by EKF.
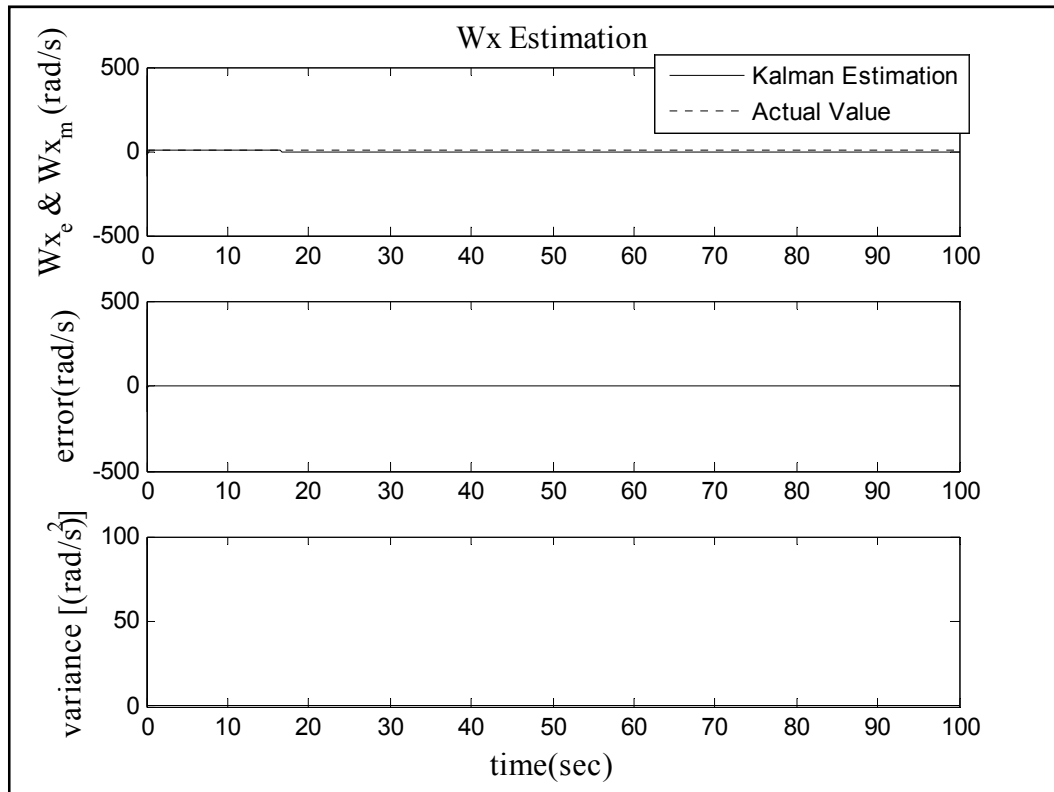
Figure 5.3 : Estimation of angular velocity about "x" axis with EKF.

5.1.2 Estimation in case of measurement malfunctions

As it is explained in the previous sections, both EKF and UKF can be made robust against the measurement malfunctions by the use of proposed adaptive Kalman filter algorithms. This scenario presents the results for an adaptive extended Kalman filter (AEKF) algorithm which is used for estimation in case of measurement faults. Since the filter uses single fading factor to adapt the filter gain, it may be also called as adaptive extended fading Kalman filter (AEFKF) with SFF. Simulations are realized in 10000 steps for a period of 100 seconds with 0.01 seconds of sampling time, Δt.

In case of measurement fault, which is formed by adding a constant term to the measurement of one magnetometer at 40th second, the simulations are also done with EKF so as to compare results with AEKF.

Nonetheless, $\chi^2_{\alpha,s}$ is taken as 12.592 and this value comes from chi-square distribution when the degree of freedom is 6 and the reliability level is %95.

First part of figures gives EKF or AEKF state estimation results and the actual values in a comparing way. Second part of the figures shows the error of estimation process based on the actual attitude estimation values of the satellite. The last part indicates the variance of the estimation.
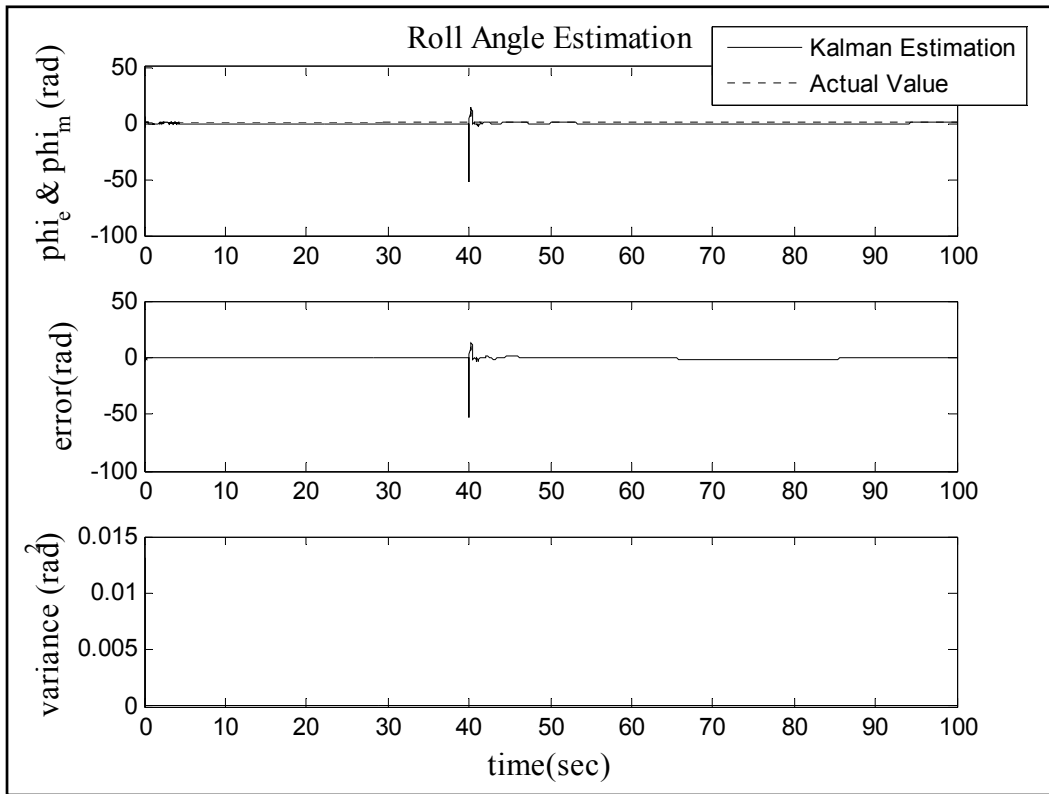
Figure 5.4 : Roll angle estimation by EKF in case of measurement malfunction.
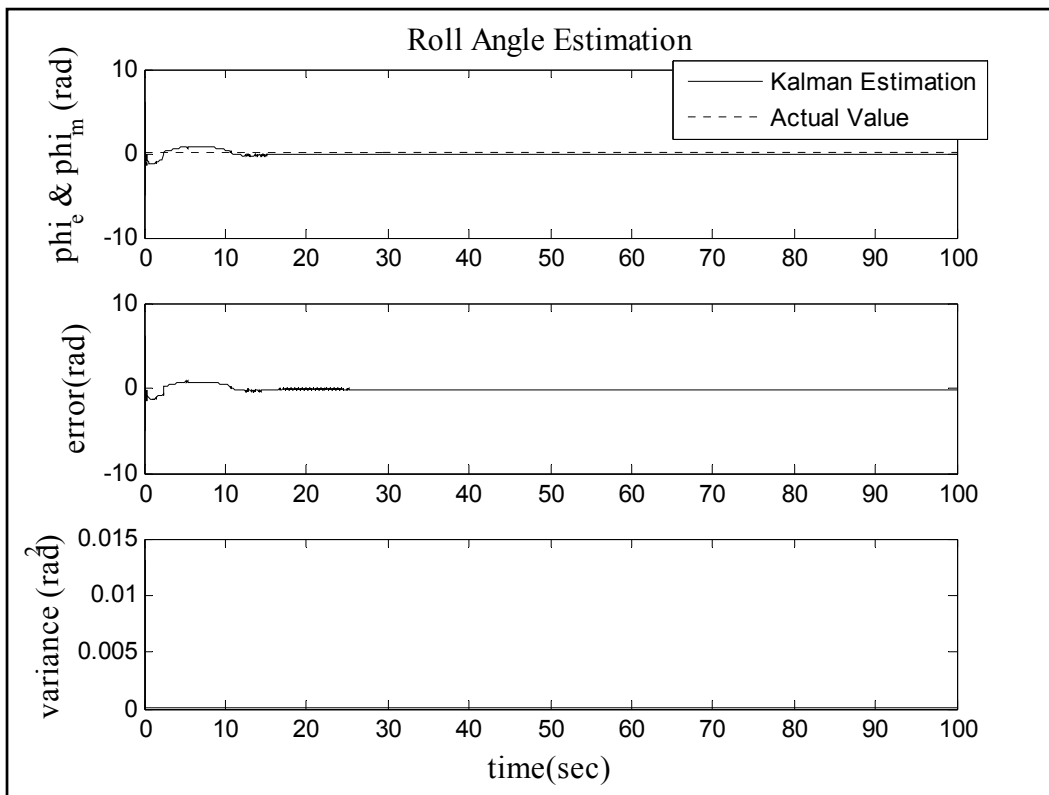
Figure 5.5 : Roll angle estimation by AEKF in case of measurement malfunction.

As the Fig.5.4 shows, when the measurement malfunction is implemented to the system, EKF estimates the roll angle with a great error. Per contra, AEKF secures its estimation characteristic even in case of faulty measurements by reducing the effect of the innovation terms on the state estimation phase (Fig. 5.6). That means, if the measurements have error, the filter gain is decreased due to the adaptive factor which is much larger than 1. Variation of adaptive factor by time proofs that (Fig. 5.7).
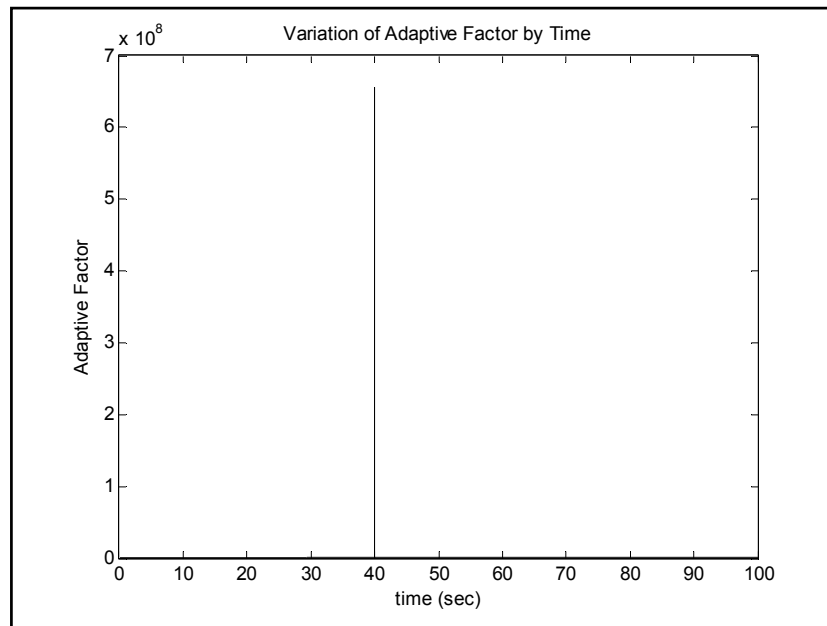
Figure 5.6 : Variation of adaptive factor by time for AEKF.

Similar results have been obtained for the estimation of other attitude parameters.

5.2 Attitude Estimation via Unscented Kalman Filter

5.2.1 Attitude parameter estimation

In this simulation, attitude angles and the angular rates of the pico satellite are estimated via UKF. As the attitude representation method, both Euler angles and the quaternions are used.

First part of figures gives UKF parameter identification results and the actual values in a comparing way. Second part of the figures shows the error of the estimation process based on the actual attitude values of the satellite. The last part indicates the variance of the estimation.

5.2.1.1 Attitude parameter estimation with Euler angles

Simulations are realized in 20000 steps for a period of 2000 seconds with 0.1 seconds of sampling time, Δt.

By examining results, it can be understood that UKF gives accurate estimation results for both Euler angles and the angular velocities (Fig.5.7 and Fig 5.8). Besides if the EKF and UKF algorithms for the attitude estimation are compared, and the data presented in Table 5.1 is regarded, it is possible to say that UKF is more efficient than EKF. Also, UKF algorithms can work with a larger sampling time than EKF algorithms without failing and usually, that brings about a lesser computational burden.
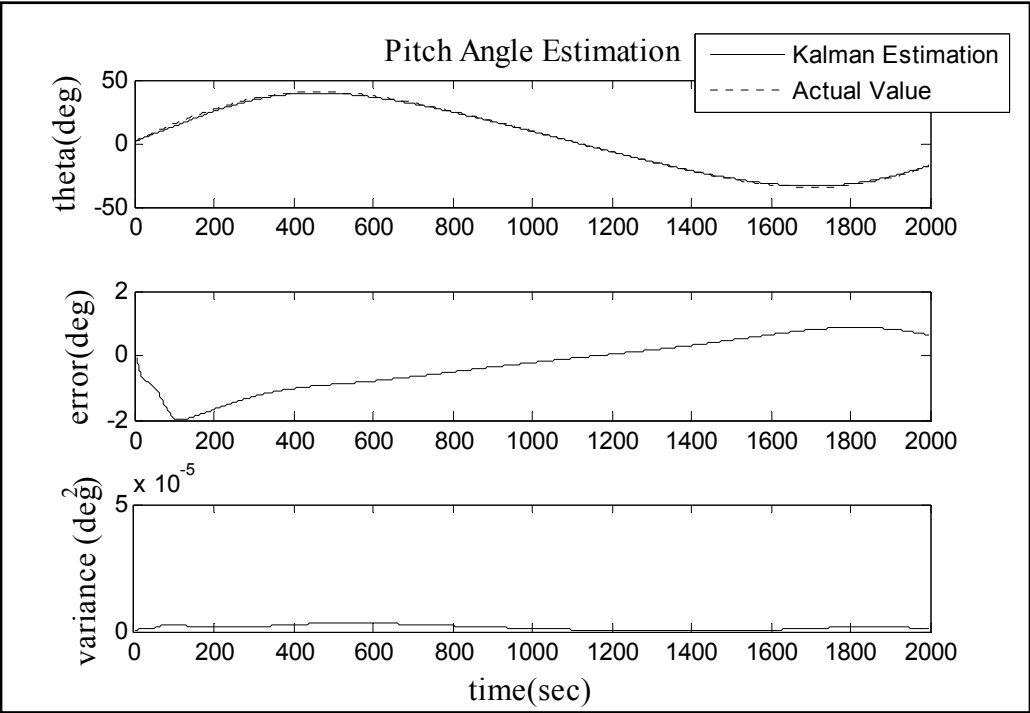
Figure 5.7 : Pitch angle estimation by UKF.
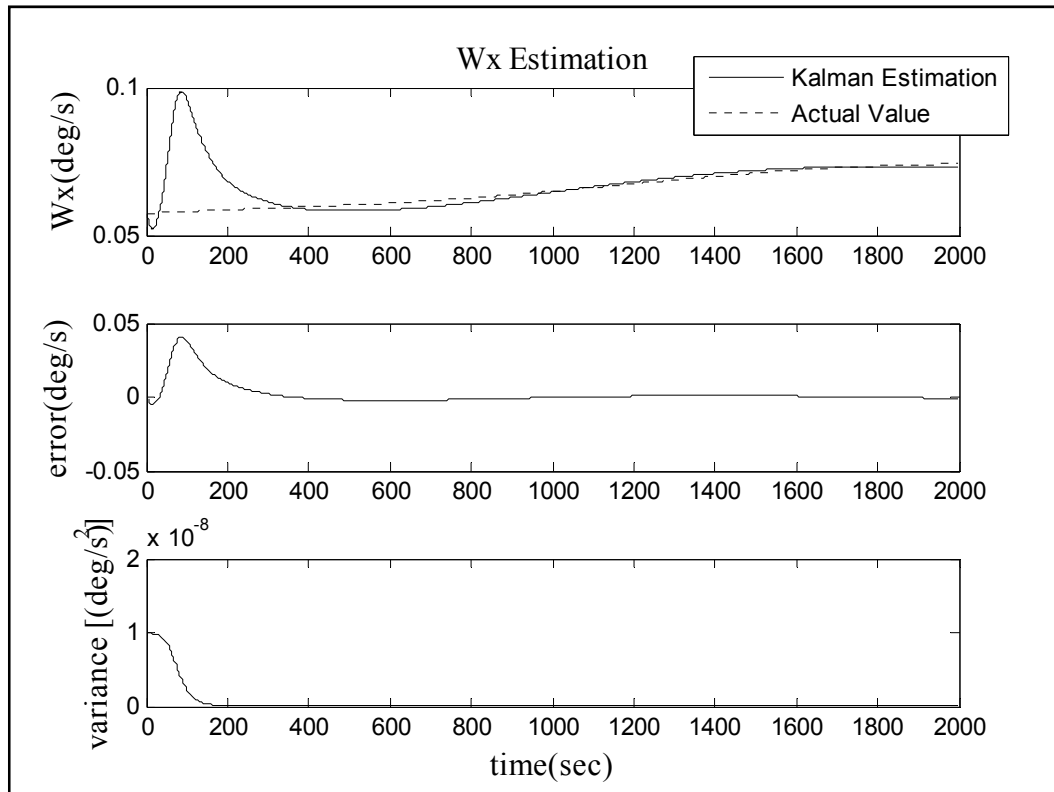
Figure 5.8 : Estimation of angular velocity about "x" axis with UKF.

Table 5.1: Comparison of EKF and UKF estimation performances[2].

Parameter	Absolute Estimation Error Values for EKF	Absolute Estimation Error Values for UKF
φ (*deg*)	9.0644	0.0278
θ (*deg*)	2.7221	0.2191
ψ (*deg*)	8.9144	2.8457
ω_x (*deg/s*)	0.6473	0.0003
ω_y (*deg/s*)	0.8236	0.0018
ω_z (*deg/s*)	1.3286	0.0018

---

[2] Note that, values are gained at time steps where the indicated filter is converged and giving accurate estimation results. Since EKF and UKF can be run for different periods because of the filter characteristics, the results do belong to two separate times.

5.2.1.2 Attitude parameter estimation with quaternions

UKF is also used for attitude estimation when the quaternions are chosen as the attitude parameterization technique. This time simulations are realized with 0.005 seconds of sampling time, Δt, for a period of 50 seconds in 10000 steps.

As it is apparent form Fig.5.9 and 5.10, accurate estimation results may be obtained in this case too. However, as the number of the states to be estimated is increased, UKF with quaternion representation may require more computation than UKF with Euler angles representation. Besides, quaternion representation means one redundant parameter, as a result of the characteristic of (2.22). When this constraint is not taken into consideration, UKF process may break down because of the covariance matrix which becomes singular by time. Hence, to get out of the problem, this constraint must be implicated into model as a dummy measurement,

$$y(q,t) = \begin{bmatrix} H_x(q,t) \\ H_y(q,t) \\ H_z(q,t) \\ q_1^2 + q_2^2 + q_3^2 + q_4^2 - 1 \end{bmatrix}. \tag{5.1}$$
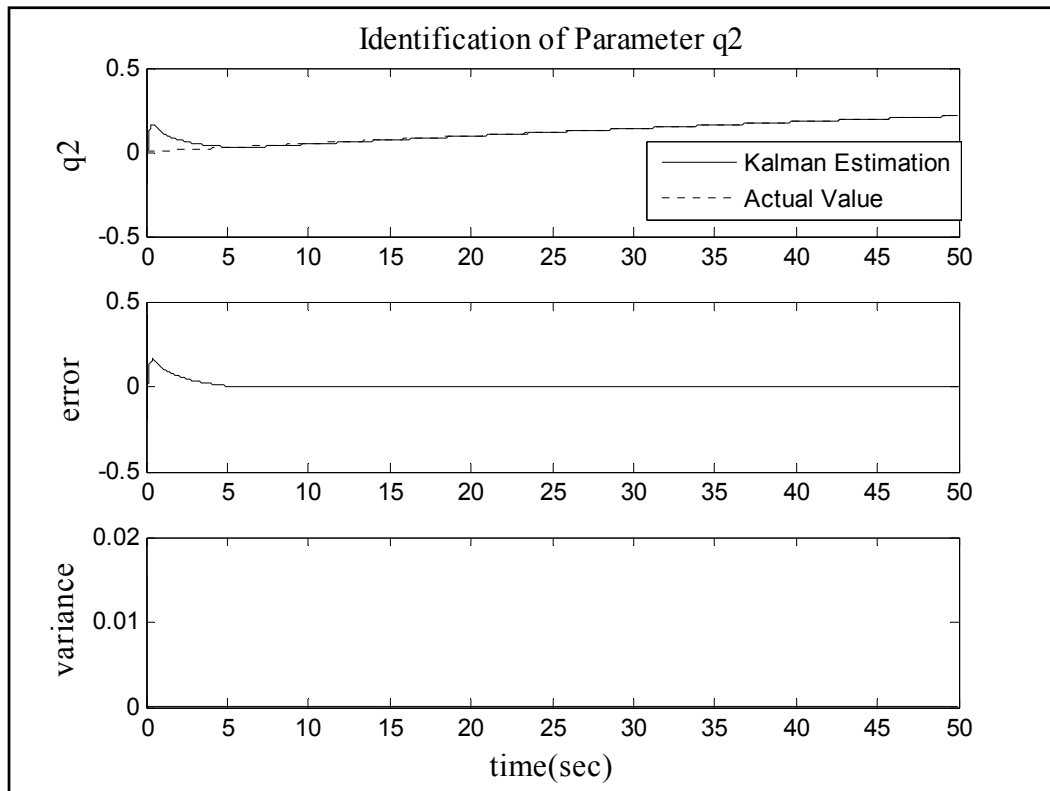
Figure 5.9 : Estimation of parameter "q2" by UKF with quaternion representation.

This redundant parameter makes filter, prone to the divergence. If the constrain is not checked within short periods, filter may fail. That is why; a smaller sampling period is needed as in case.
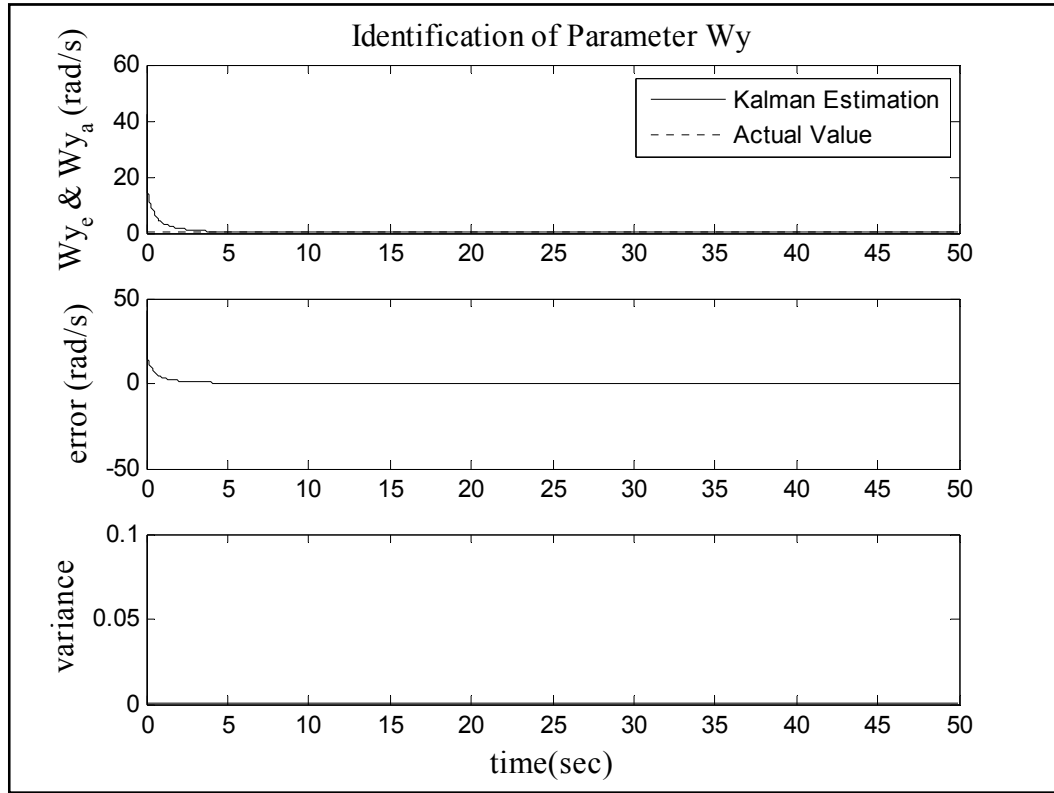
Figure 5.10 : Estimation of angular velocity about "y" axis with UKF with quaternion representation.

5.2.2 Torque estimation

In this estimation scenario, unknown constant components of the external torques affecting the satellite are estimated in addition to the Euler angles and the angular rates. As it is aforementioned, in this case, IMU is also used as a supplementary sensor. Simulations are realized in 20000 steps for a period of 2000 seconds with 0.1 seconds of sampling time, Δt.

First part of figures gives UKF parameter identification results and the actual values in a comparing way. Second part of the figures shows the error of the estimation process based on the actual attitude estimation values of the satellite. The last part indicates the variance of the estimation.

In Fig.5.11, an attitude Euler angle estimation example is given. As it is obvious, UKF accurately estimates the roll angle of the satellite within the bounds of maximum +2/-2 deg. of estimation error and especially after the 1400th second of the

estimation, the filter output becomes highly precise. Besides as it is presented in Fig.5.12, UKF also has a good estimation characteristic for the angular rates.
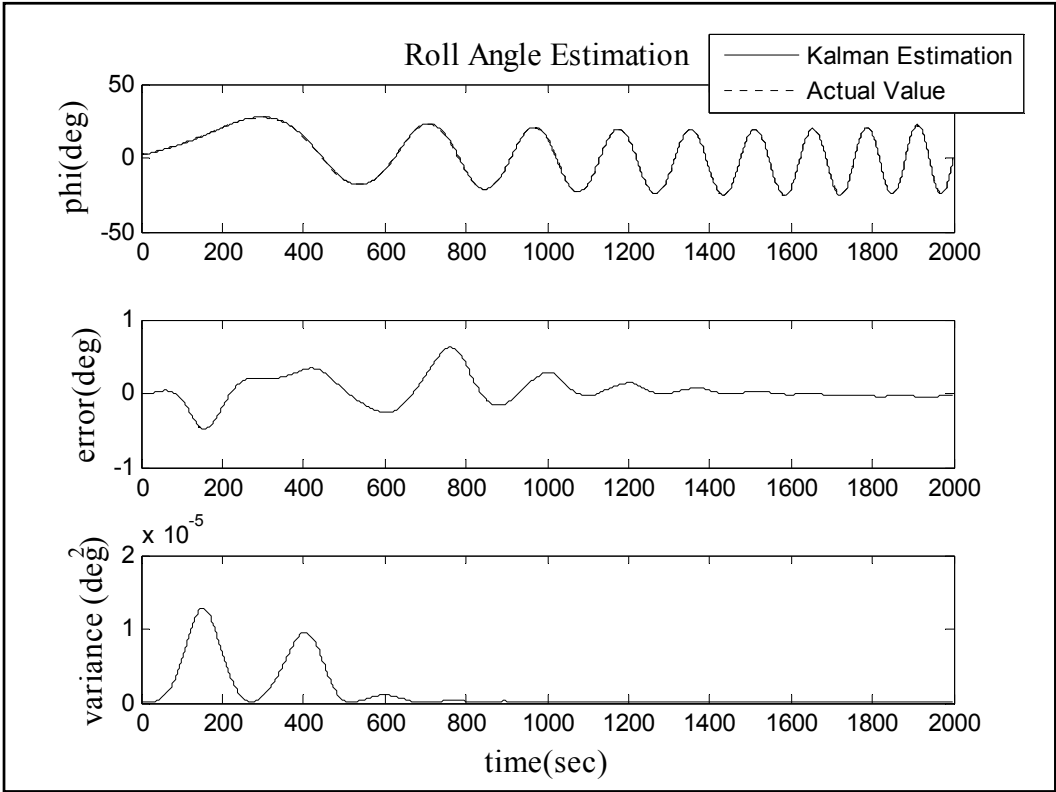
Figure 5.11 : Roll angle estimation by UKF for torque estimation scenario.

Another fact about the UKF algorithm is the exact estimation of the unknown constant components of the external torques, which coincides with the actual value approximately after 250 seconds from the origin (Fig. 5.13). That is also obvious from Fig. 5.14 that reflects the estimation error percentages for torques with respect to the actual values. Therefore, it is possible to say that; proposed UKF algorithm estimates all of the states (Euler angles, angular rates and the unknown constant components of the external torques) accurately.
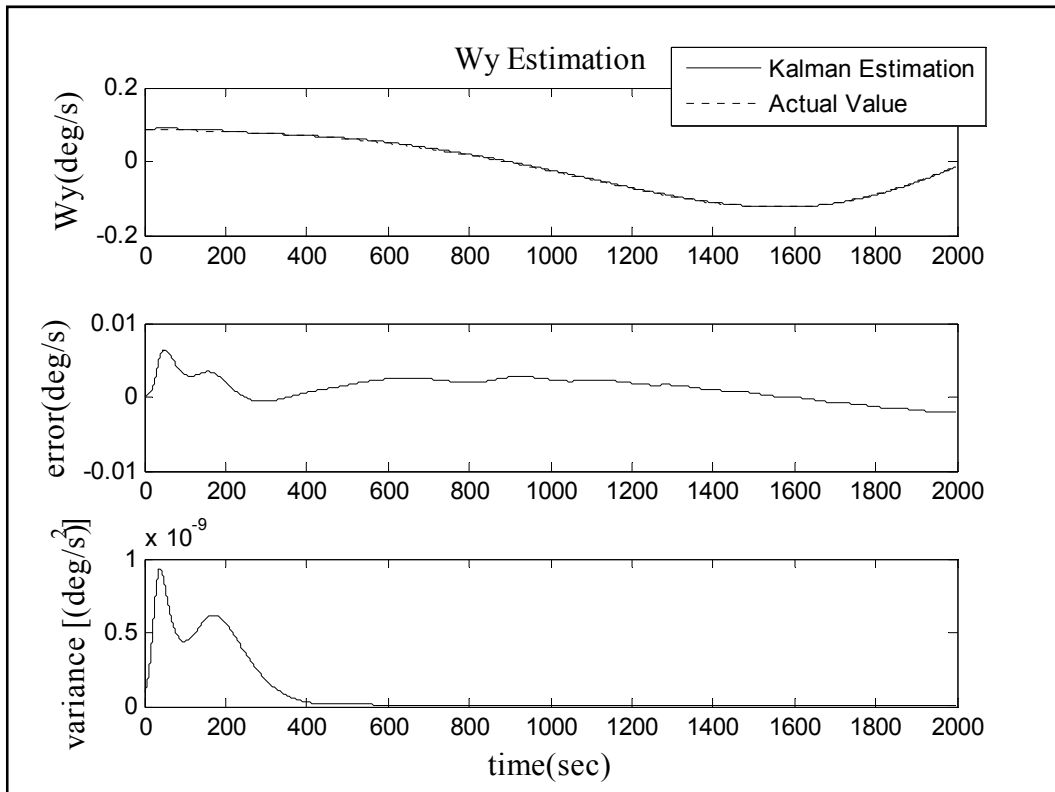
Figure 5.12 : Estimation of angular velocity about "y" axis by UKF for torque estimation scenario.
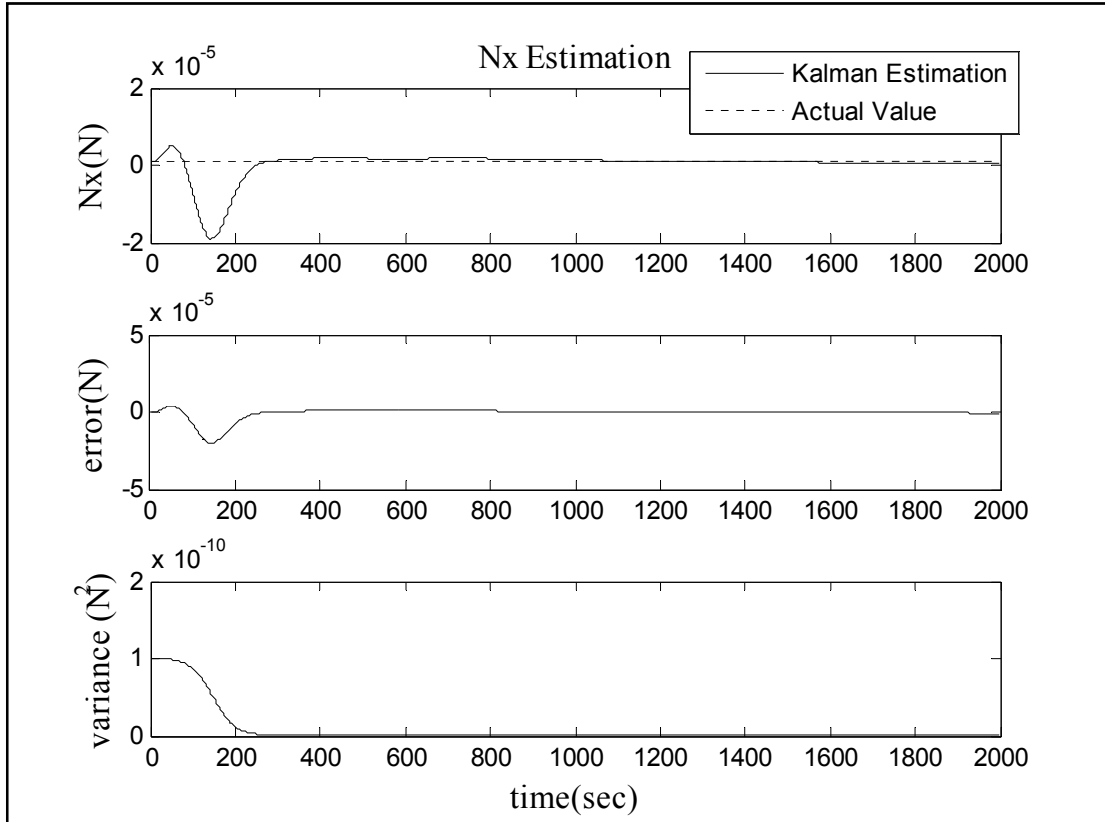
Figure 5.13 : Estimation of constant external torque about "x" axis with UKF.
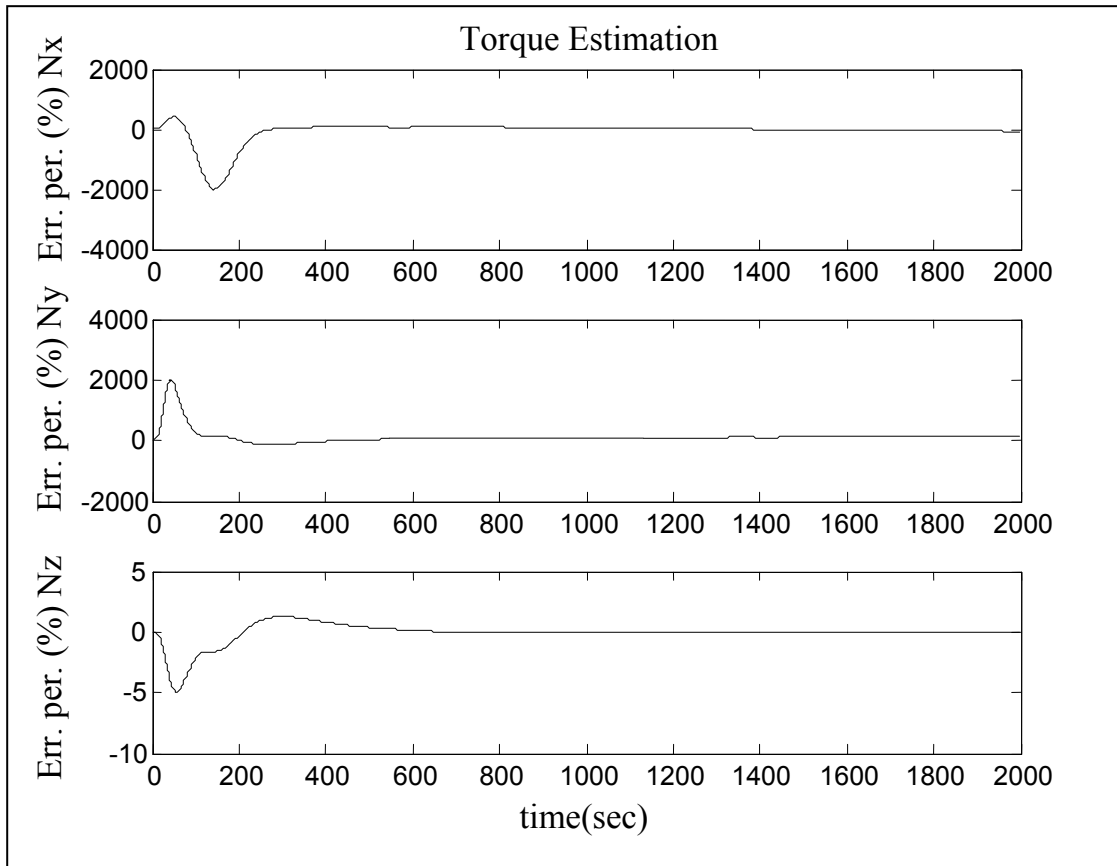
Figure 5.14 : Error percentages for estimations of torques.

5.2.3 Magnetometer bias estimation

In this estimation scenario, magnetometer biases are estimated as well as Euler angles and the angular rates. As it is aforementioned, in this case, IMU is also used as a supplementary sensor. Simulations are realized in 20000 steps for a period of 2000 seconds with 0.1 seconds of sampling time, Δt.

First part of figures gives UKF parameter identification results and the actual values in a comparing way. Second part of the figures shows the error of the estimation process based on the actual attitude estimation values of the satellite. The last part indicates the variance of the estimation.

In this case, UKF again gives accurate estimation results for Euler angles and the angular velocities as it is evident from Fig.5.15 and Fig.5.16. Nonetheless, although it is hard to estimate constant parameters, which do not change by time according to any dynamical rule, UKF algorithm estimates magnetometer biases with a sufficient precision (5.17). For magnetometer bias estimation scenario, filter must be tuned

carefully, in order to obtain good estimation characteristics for both bias terms and the attitude angles and angular rates.
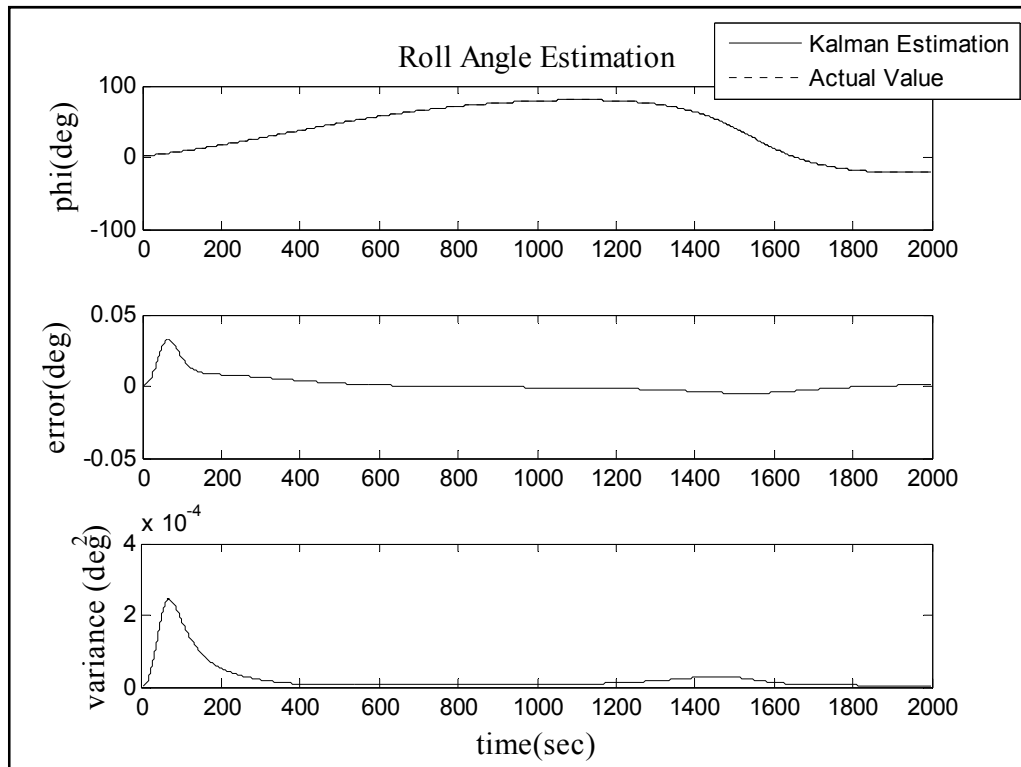
Figure 5.15 : Roll angle estimation by UKF for magnetometer bias estimation scenario.
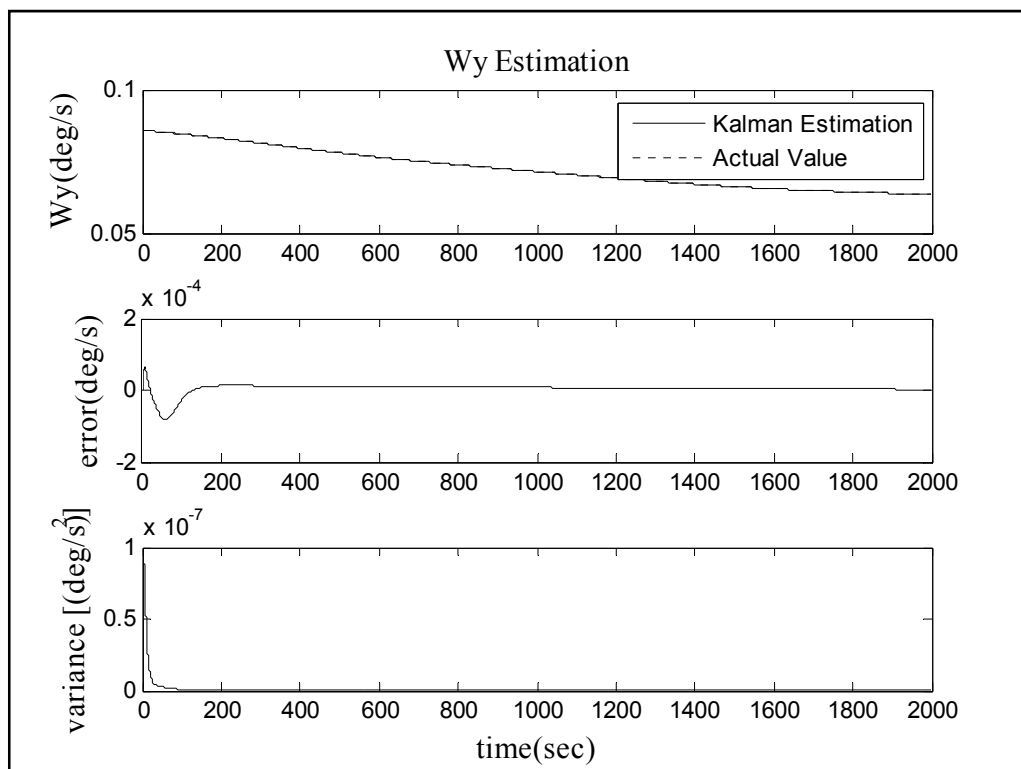
Figure 5.16 : Estimation of angular velocity about "y" axis by UKF for magnetometer bias estimation scenario.
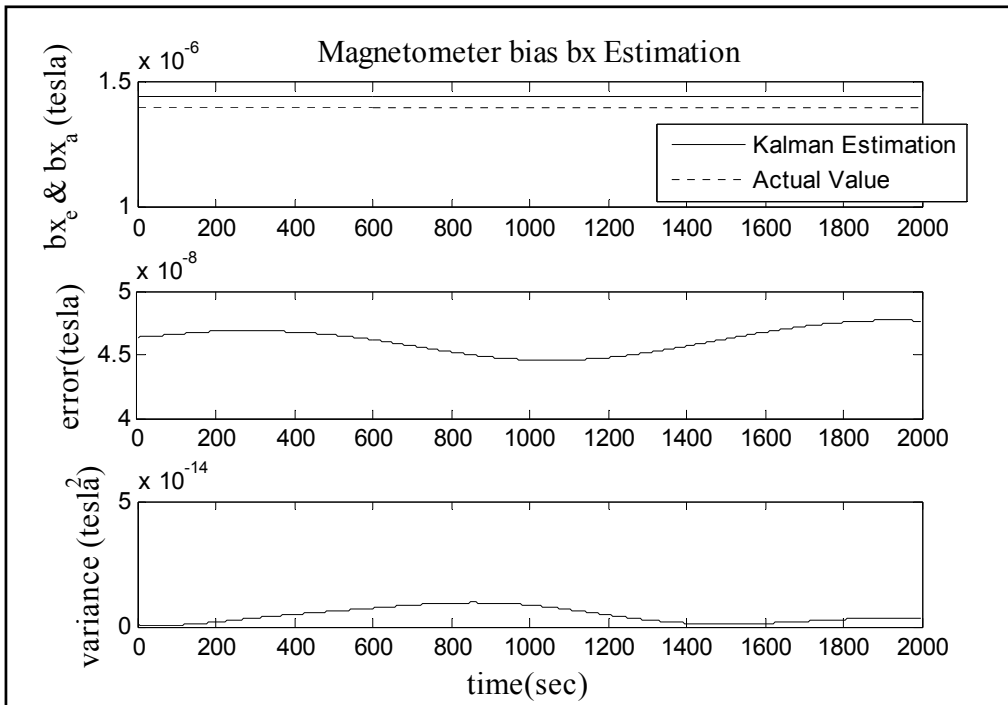
Figure 5.17 : Estimation of bias of the magnetometer which is aligned in "x" axis.

Furthermore, error percentages of magnetometer bias estimation procedure with respect to the actual values of the biases may be given to show how accurately biases can be identified with a fine tuned UKF (Fig. 5.18).
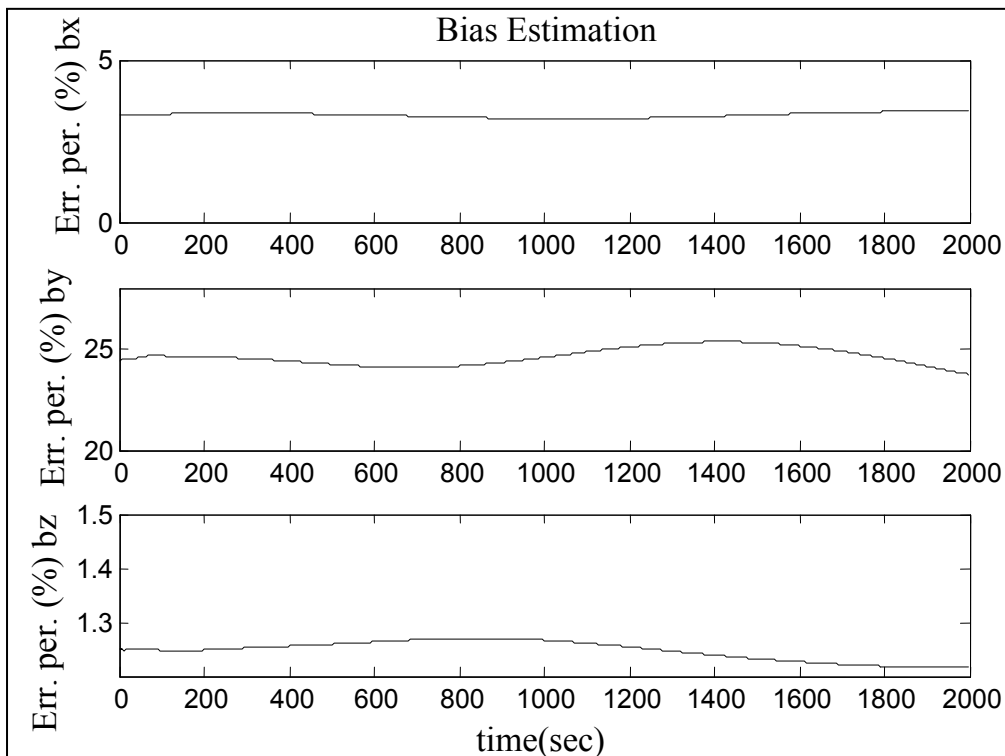
Figure 5.18 : Error percentages for estimations of magnetometer biases.

5.2.4 Gyro bias estimation

This time, gyro biases are estimated instead of magnetometer biases in addition to the attitude angles and the angular rates. Simulations are realized in 20000 steps for a period of 2000 seconds with 0.1 seconds of sampling time, Δt.

First part of figures gives UKF parameter identification results and the actual values in a comparing way. Second part of the figures shows the error of the estimation process based on the actual attitude estimation values of the satellite. The last part indicates the variance of the estimation.
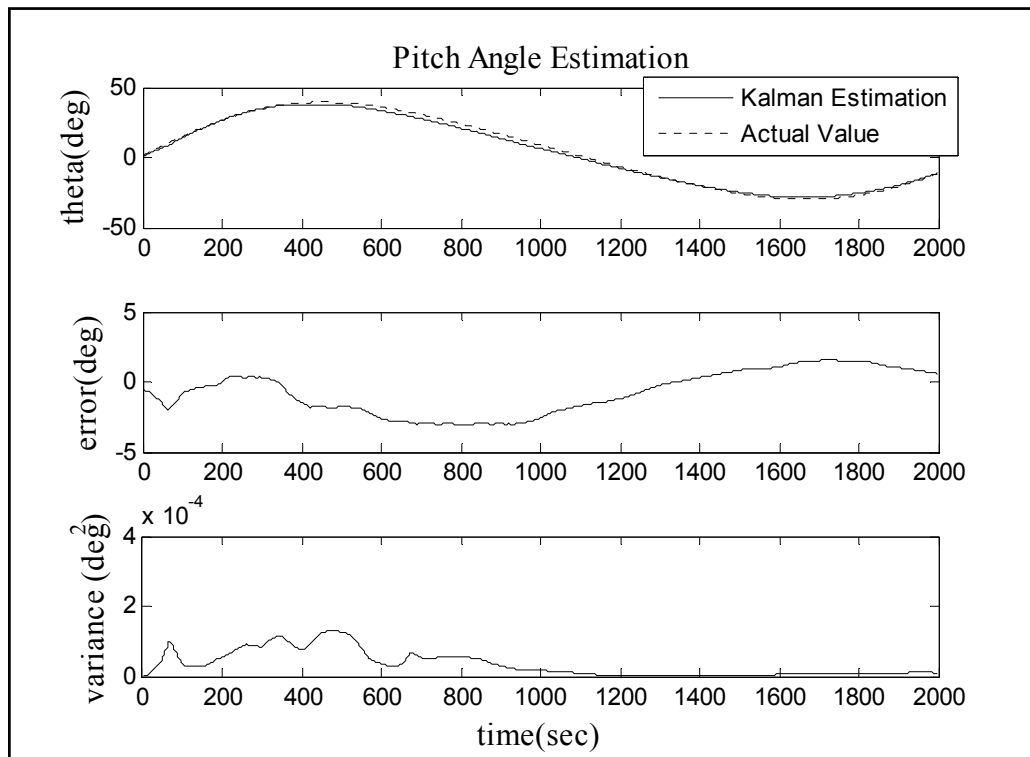
Figure 5.19 : Pitch angle estimation by UKF for gyro bias estimation scenario.

UKF algorithm estimation outputs of both attitude angles and the angular velocities are accurate again (Fig. 5.19 and Fig. 5.20). Nevertheless, by the use of UKF, gyro biases can be also estimated precisely. That is clear in Fig. 5.21. However, as it is valid for magnetometer bias estimation process, UKF for gyro bias is a hard to tune algorithm too. Especially, initial values of the covariance matrix, $P(0/0)$, and the process noise covariance matrix, $Q(k)$ should be determined ably.
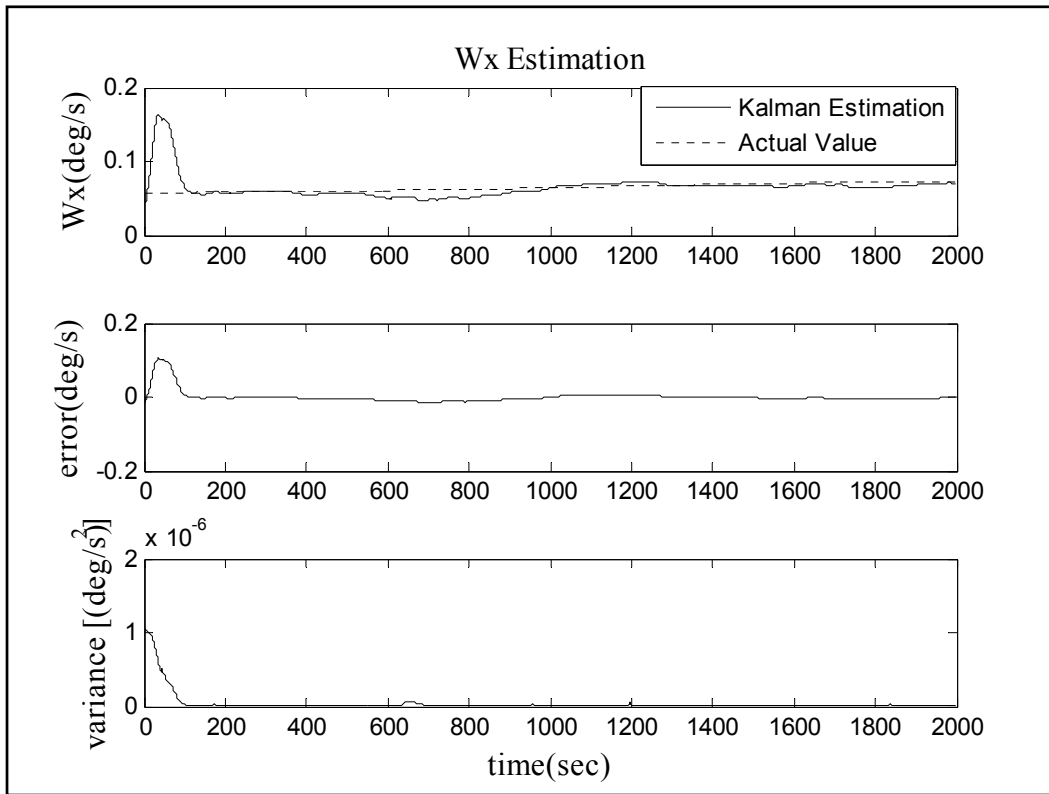
Figure 5.20 : Estimation of angular velocity about "x" axis by UKF for gyro bias estimation scenario.
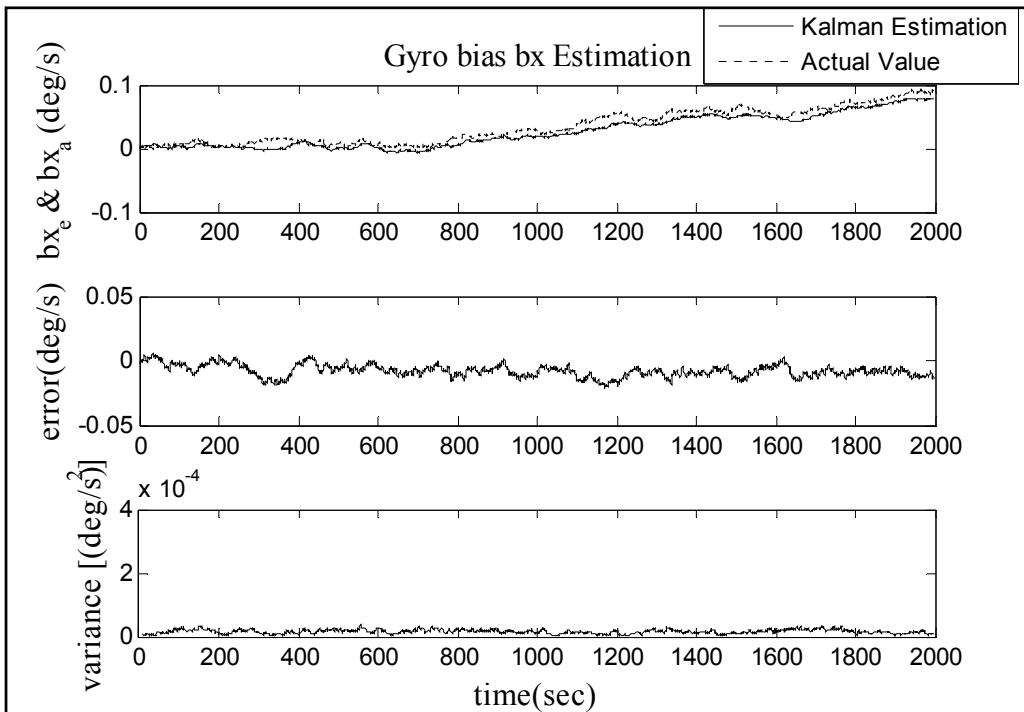
Figure 5.21 : Estimation of bias of the gyro which is aligned in "x" axis.

5.2.5 Estimation in case of measurement malfunctions

In that last scenario, results for AUFKF algorithms with SFF and MFF are presented. Simulations are realized in 20000 steps for a period of 2000 seconds with 0.1 seconds of sampling time, Δt.

During simulations, for testing AUFKF algorithms, two kinds of measurement malfunction scenarios are taken into consideration; instantaneous abnormal measurements, and continuous bias.

Besides, in case of measurement faults, the simulations are also done with UKF so as to compare results with AUFKFs and understand efficiency of the adaptive algorithms in a better way.

Nonetheless, $\chi^2_{\alpha,s}$ is taken as 12.592 and this value comes from chi-square distribution when the degree of freedom is 6 and the reliability level is %95.

First part of figures gives UKF or AUFKF state estimation results and the actual values in a comparing way. Second part of the figures shows the error of estimation process based on the actual attitude estimation values of the satellite. The last part indicates the variance of the estimation.

5.2.5.1 Instantaneous abnormal measurements

Instantaneous abnormal measurements are simulated by adding a constant term to the magnetic field tensor measurement of one magnetometer at the 500th second. As it is seen from Fig. 5.22, Fig. 5.23 and Fig 5.24, both AUFKF algorithms (with SFF and MFF) give more accurate estimation results than UKF in case of the instantaneous abnormal measurements. The results obtained by regular UKF are not reliable when the measurements are gained with an error. However, AUFKFs with SFF and MFF maintain their estimation characteristic for the whole process and afford precise estimation outputs in case of the abnormal measurements, as well as the normal operation condition. Similar results have been obtained when the measurement malfunction is implemented to another magnetometer.

Table 5.2 compares absolute estimation errors of three filters for two different time steps. Note that, highlighted results are gained at seconds where the measurement malfunction is implemented.
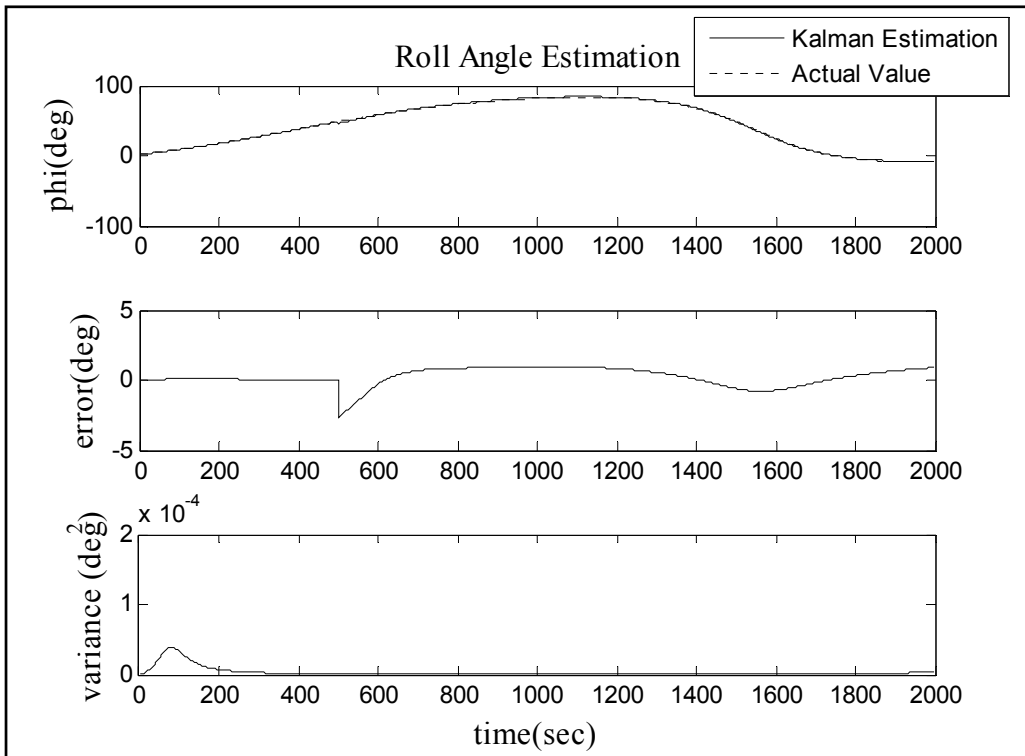
Figure 5.22 : Roll angle estimation by optimal UKF in case of instantaneous abnormal measurements.
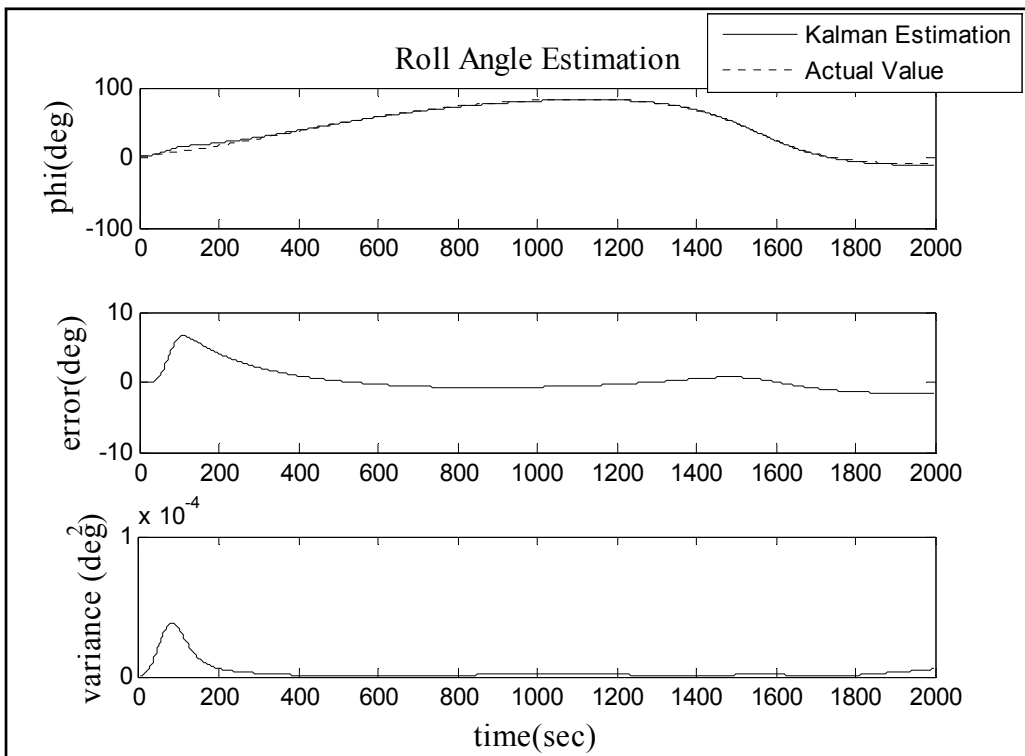
Figure 5.23 : Roll angle estimation by AUFKF with SFF in case of instantaneous abnormal measurements.

58
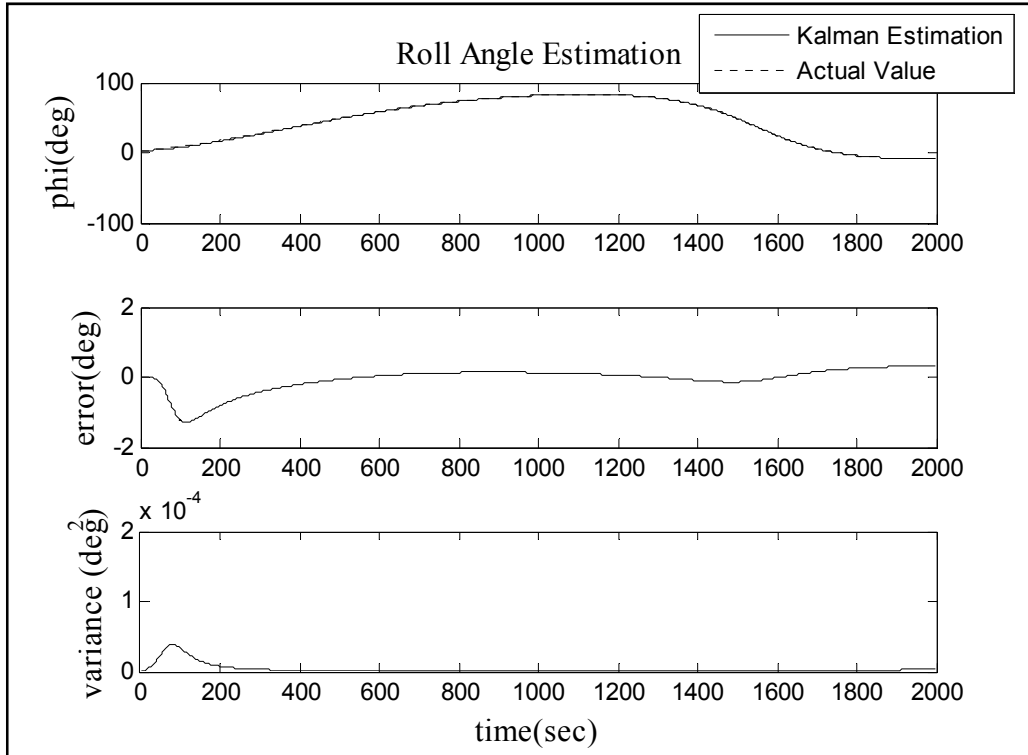
Figure 5.24 : Roll angle estimation by AUFKF with MFF in case of instantaneous abnormal measurements.

Table 5.2: Comparison of absolute estimation errors in case of instantaneous abnormal measurements.

Parameter	Abs. Err. Values for Regular UKF		Abs. Err. Values for AUFKF with SFF		Abs. Err. Values for AUFKF with MFF	
	500 s.	1000 s.	500 s.	1000 s.	500 s.	1000 s.
φ (deg)	2.6941	0.9987	0.1992	0.6871	0.0652	0.1286
θ (deg)	1.1066	0.8125	1.8899	0.3089	0.3746	0.0705
ψ (deg)	0.7437	5.1317	3.5498	4.7176	0.7132	0.9247
ω_x (deg/s)	0.028	0.002	0.0014	0.0018	0.0003	0.0003
ω_y (deg/s)	0.0181	0.0055	0.0037	0.0036	0.0007	0.0007
ω_z (deg/s)	0.0007	0.0005	0.0056	0.0002	0.0013	0.00004

When the measurements are faulty, AUFKF with SFF compensates that by increasing its single fading factor (adaptive factor) and disregarding all of the measurements for these time steps. Besides, AUFKF with MFF secures the robustness of the filter by increasing related fading factors of the adaptive matrix individually. Increment of the related fading factors brings out a decrement in the related components of the Kalman gain, so as to reduce the corrective effect of the

innovation sequences of the faulty measurements on the state estimation process (4.32). Progress may be understood better by examining the graph of the adaptive factor of the AUFKF with SFF (Fig. 5.25) and the adaptive matrix itself of AFKF with MFF at the 500th second (5.2).
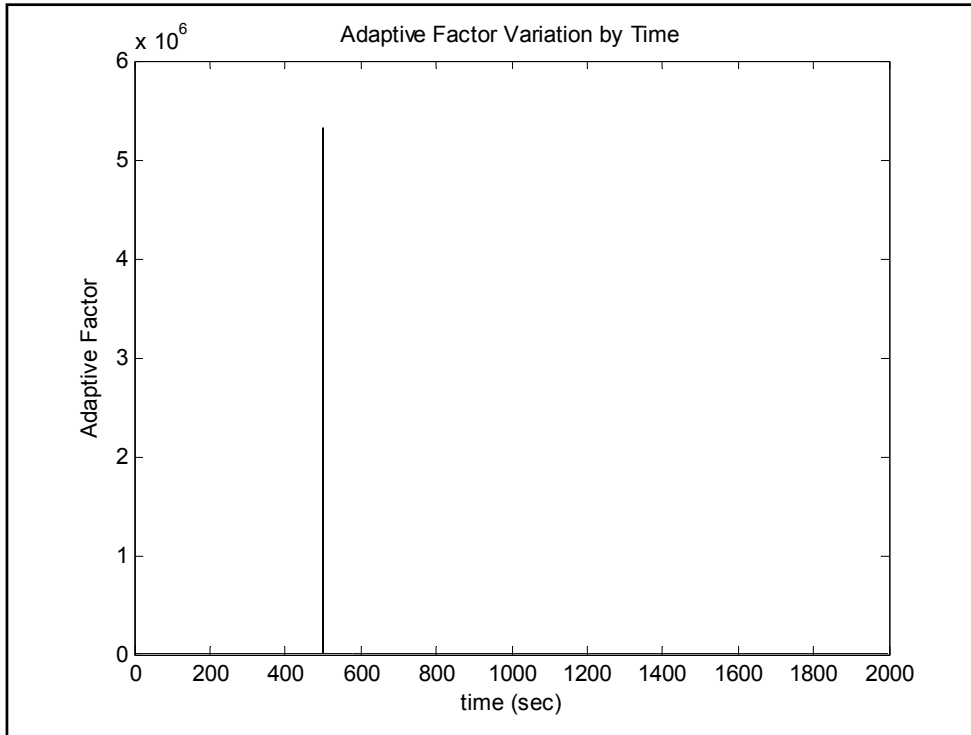
Figure 5.25 : Variation of adaptive factor by time for AUFKF with SFF in case of instantaneous abnormal measurements.

$$S^*(k) = \begin{bmatrix} 16000002 & 0 & 0 \\ 0 & 1 & 0 \\ 0 & 0 & 1.58 \end{bmatrix} \tag{5.2}$$

Even though both of the adaptive Kalman filters give similar estimation results in case of instantaneous abnormal measurements, AUFKF with MFF can be thought as a more advantageous algorithm as it takes the faulty measurements into account individually. Disregarding all of the measurements, as AUFKF with SFF does, affects estimation procedure of the all states. However, since the abnormal measurement is implemented only to the one measurement channel, keeping out the related measurement would be more significant. As a result of the dynamics and the measurement models of the satellite which are nonlinear and constituted of coupled states, any malfunction in one of the magnetometers affects the estimation

characteristic of all states, but not in same degree. Hence, for this kind of measurement malfunction, AUFKF with MFF proves its high performance capability as it can correct estimation characteristic of each state, individually and secure accurate estimation characteristic for all states at the same time.

Proposed AUFKF algorithms are free of computational burden and they can be easily run by simple microprocessors. If the general %10 constrain for the mass and the power consumption of the ADCS of a pico satellite is regarded [2], these algorithms do not brings out an extra requirement and they can be used with the systems suitable for general EKF or UKF processing.

Furthermore, note that it is possible to obtain same kind of results for AUFKF algorithms when they are built with the quaternion representation. Fig. 5.26 and Fig. 5.27 gives UKF and AUFKF with SFF estimation results for a quaternion component in case of instantaneous abnormal measurements.
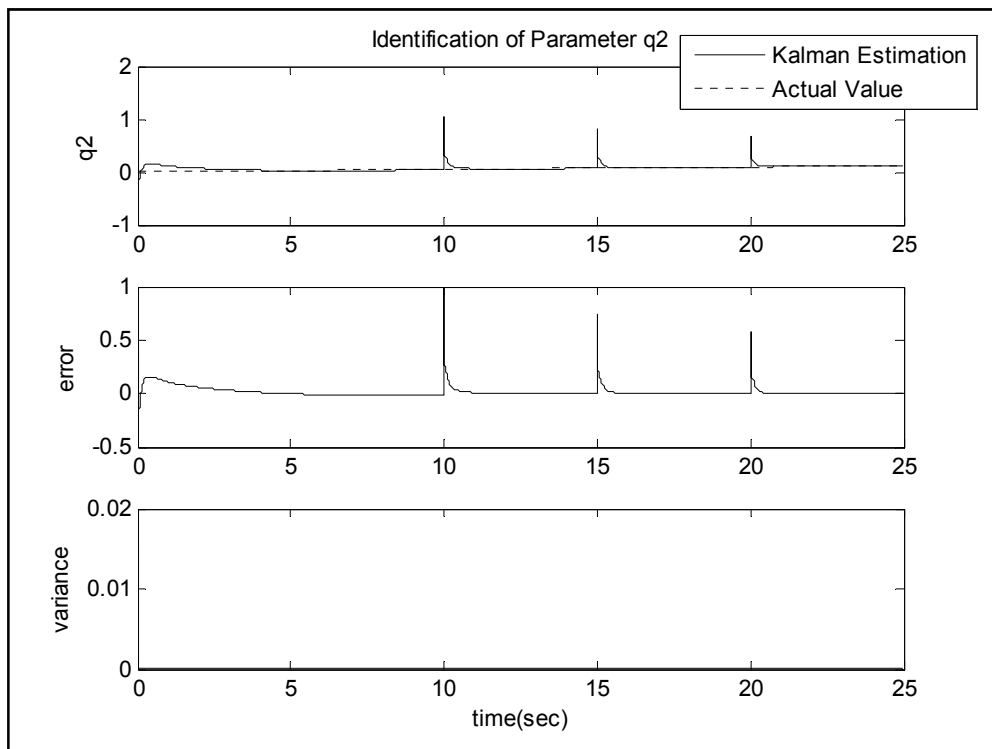
Figure 5.26 : Estimation of parameter "q2" by optimal UKF in case of instantaneous abnormal measurements.
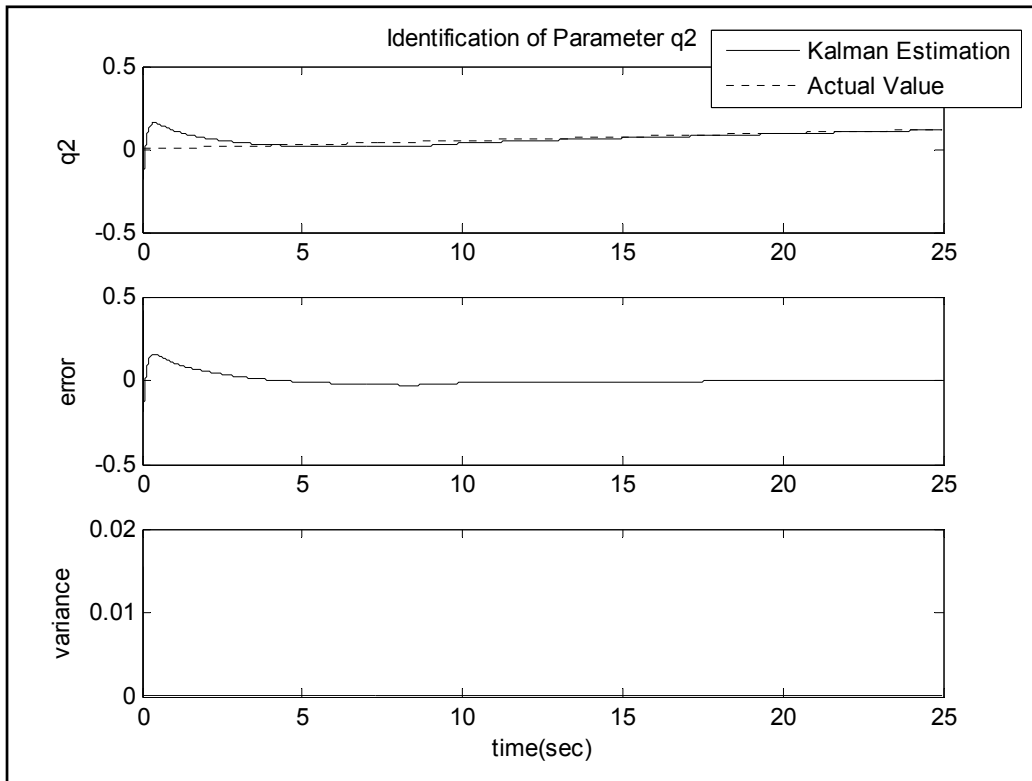
Figure 5.27 : Estimation of parameter "q2" by AUFKF with SFF in case of instantaneous abnormal measurements.

5.2.5.2 Continuous bias at measurements

Continuous bias term is formed by adding a constant term to the measurements of one of the magnetometer in between 500th and 530th seconds. As Fig. 5.28, Fig. 5.29, Fig. 5.30 and Table 5.3 show, again optimal UKF fails about estimating states accurately. Per contra, AUFKF algorithms with SFF and MFF reduce the effect of the innovation sequence and eliminate the estimation error which is caused by the biased measurements of one magnetometer. Besides, by the use of the predicted states which are more weighted than the innovation sequence in (4.32), they secure accurate estimation outputs throughout this period.
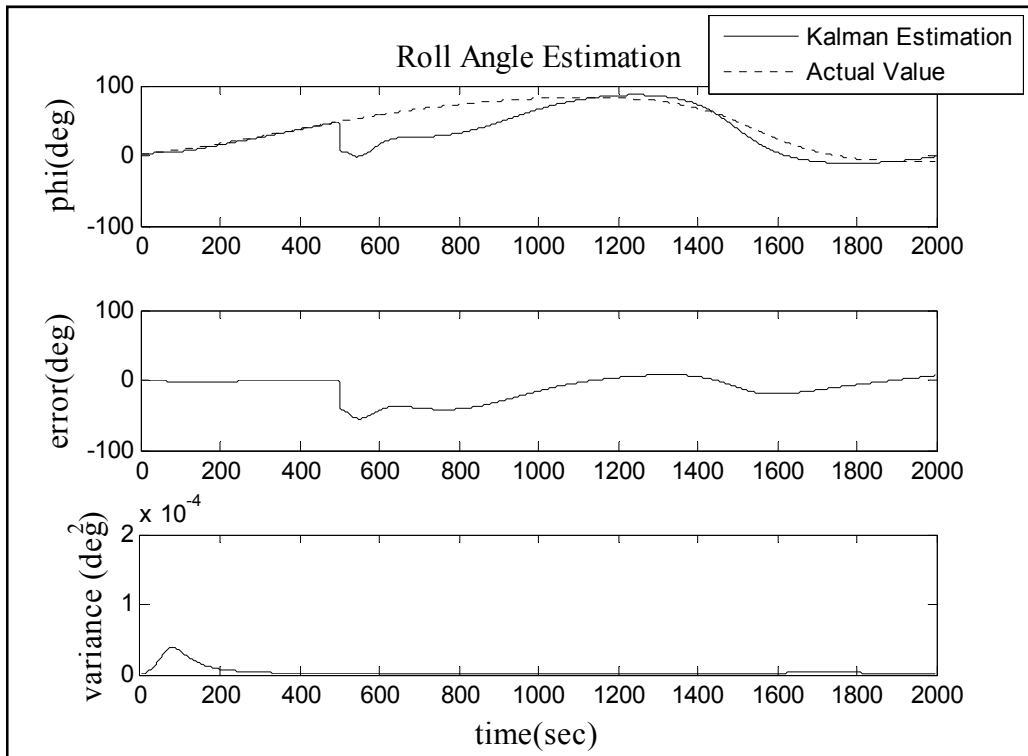
Figure 5.28 : Roll angle estimation by optimal UKF in case of continuous bias at measurements.
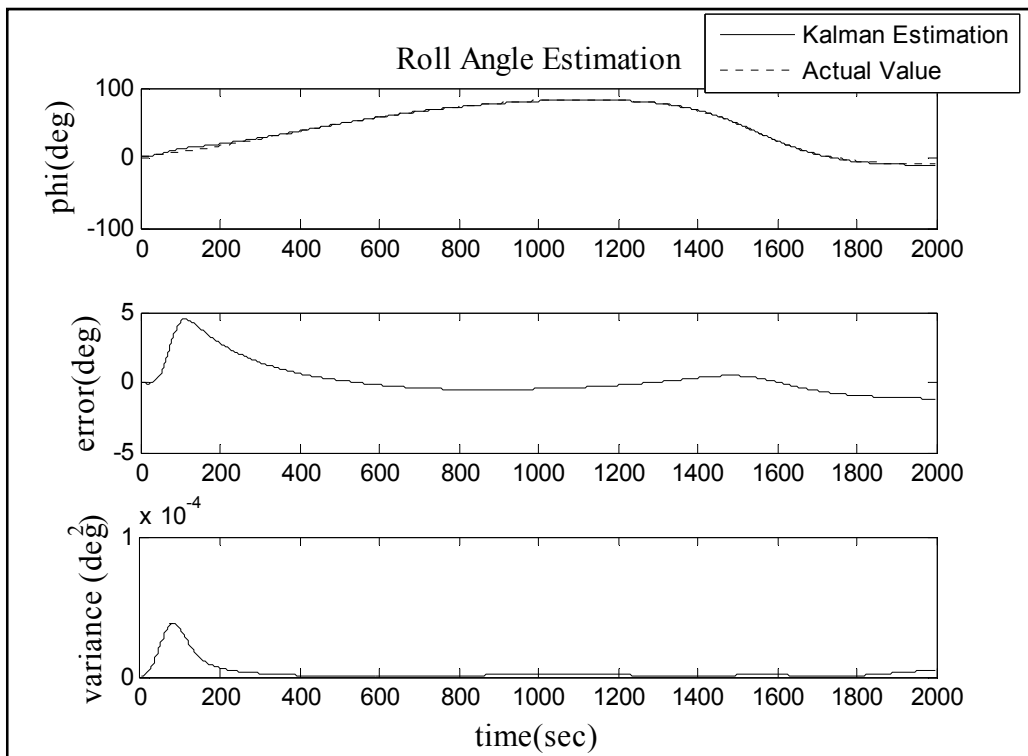
Figure 5.29 : Roll angle estimation by AUFKF with SFF in case of continuous bias at measurements.
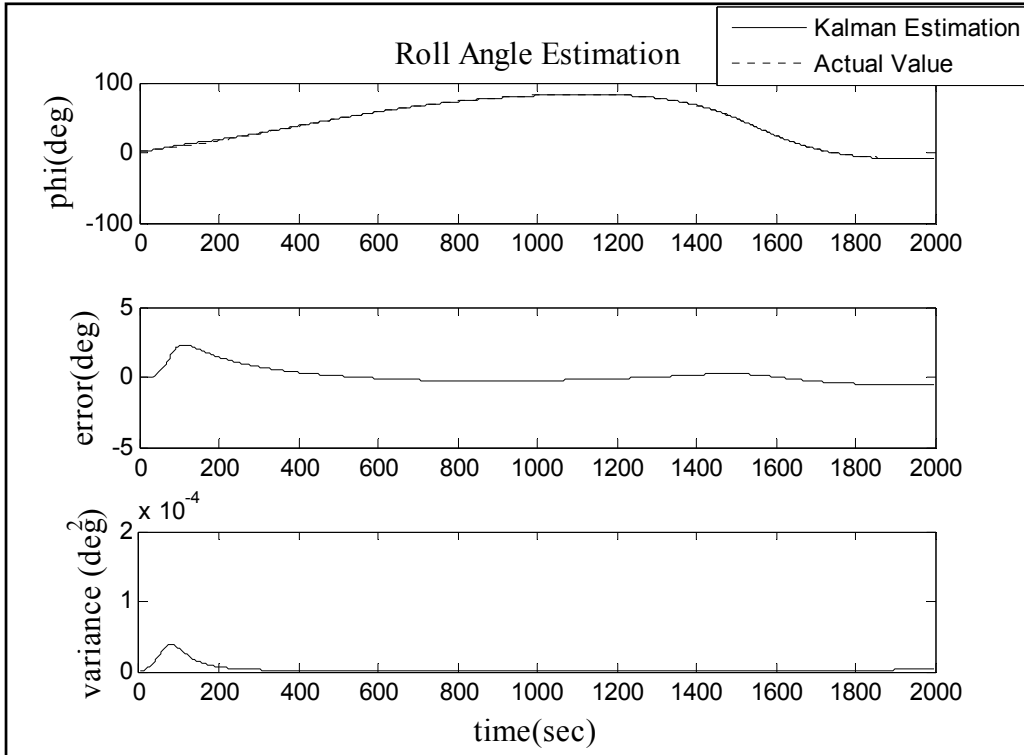
Figure 5.30 : Roll angle estimation by AUFKF with MFF in case of continuous bias at measurements.

Table 5.3: Comparison of absolute estimation errors in case of continuous bias at measurements.

Parameter	Abs. Err. Values for Regular UKF		Abs. Err. Values for AUFKF with SFF		Abs. Err. Values for AUFKF with MFF	
	500 s.	1000 s.	500 s.	1000 s.	500 s.	1000 s.
φ (deg)	5.0535	15.759	0.1571	0.461	0.0928	0.2329
θ (deg)	2.7733	23.431	1.2893	0.2172	0.6617	0.1156
ψ (deg)	1.2492	192.76	2.4375	3.2138	1.256	1.6444
ω_x (deg/s)	0.0558	0.0798	0.0009	0.0012	0.0005	0.0006
ω_y (deg/s)	0.0352	0.2307	0.0025	0.0024	0.0013	0.0013
ω_z (deg/s)	0.0043	0.1422	0.0039	0.0001	0.0021	0.0001

Even though, it can not be stated that AUFKF with MFF is superior than AUFKF with SFF according to the figures (Fig. 5.29 and Fig. 5.30), Table 5.3 shows that estimation outputs of AUFKF with MFF are more precise as it is expected. Already, it is a known fact that individual increase of related fading factors, which corresponds to the faulty measurements, is advantageous than disregarding all measurements at the same time.

64

6. CONCLUSION

In this study, various Kalman filter algorithms for the attitude estimation of ITU-PSAT I satellite in different mission periods are developed. State estimation performances of both EKF and UKF are investigated when the magnetometers are the only onboard measurement sensors. Identification of the parameters e.g. unknown constant external torques, magnetometer bias and gyro bias is achieved in case of Inertial Measurement Unit (IMU) usage as a supplementary sensor. Besides, Adaptive Unscented Fading Kalman Filter (AUFKF) with single and multiple fading factors are proposed so as to secure filter robustness against measurement malfunctions. Developed Kalman filter algorithms are tested as a part of the attitude determination system of ITU PSAT I satellite by the use of simulations.

Individual UKF algorithm gave accurate outputs for the estimation of unknown components of the external torques acting on the satellite, magnetometer bias and the gyro bias, as well as Euler angles and angular rates. The simulation results approve that, the developed UKF based identification algorithms of the attitude dynamics parameters gives sufficiently accurate estimation results to be utilized on a pico satellite. Moreover, they may be considered for other satellite types too.

If EKF and UKF algorithms are compared regarding the satellite attitude estimation problem, it is possible to say that UKF is superior to EKF. Nonetheless, when it is thought in point of view of usage on pico satellites and their limited computer processor capacity, being free of computational burden is an advantage for UKF.

Also adaptive unscented fading Kalman filter algorithms with single fading factor and multiple fading factors for the case of measurement malfunctions are developed. By the use of defined variables named as fading factor, faulty measurements are taken into consideration with small weight and the estimations are corrected without affecting the characteristic of the accurate ones. In the presented AUFKFs, the filter gain correction is performed only in the case of malfunctions in the measurement system.

Proposed AUFKF algorithms are applied for the attitude estimation process of ITU-PSAT I satellite's attitude dynamics model. Algorithms are tested for two different measurement malfunction scenarios and results are compared with the outputs of optimal UKF for the same cases; Instantaneous abnormal measurements and continuous bias at measurements. At both circumstances, UKF becomes faulty while the introduced AUFKF algorithms stand robust to the measurement errors (insensitive to failure). Comparison of simulation results show that, the performance of AUFKF algorithms are significantly better than UKF in the case of measurement malfunctions. On the other hand, if these two adaptive Kalman filter algorithms are compared, it is thought that AUFKF with MFF is more advantageous. However, especially for the attitude estimation problem, further studies on that topic are required.

The proposed approach does not require a priori statistical characteristics of the faults. Furthermore, the presented AUFKF algorithms are simple for practical implementation and their computational burden are not heavy. These characteristics make introduced AUFKF algorithms extremely important in point of view of supplying reliable state estimation for the attitude determination and control system of pico satellites.

REFERENCES

[1]   **Toorian, A., Diaz K., and Lee S.,** 2008. The Cubesat Approach to Space Access. Proceedings of 2008 IEEE Aerospace Conference, 1-14, Montana, USA.

[2]   **Polaschegg, M.,** 2005. Study of a Cube-Sat Mission, *M.Sc.Thesis,* Karl Franzens University of Graz, Graz, Austria.

[3]   **Kurtulus, C., Inalhan, G., and Aslan A.R.,** 2007: İTÜ-pSAT I: Istanbul Technical University Student Pico-Satellite Program. Proceedings of 3rd International Conference on Recent Advances in Space Technologies, 725-732, Istanbul, Turkey.

[4]   **Lefferts, E. J., Markley, F. L., and Shuster M.D.,** 1982: Kalman Filtering for Spacecraft Attitude Estimation. *Journal of Guidance, Control, and Dynamic,* **5**, 417-429.

[5]   **Psiaki, M. L., Martel, F., and Pal, P. K.,** 1990: Three-axis Attitude Determination via Kalman Filtering of Magnetometer Data. *Journal of Guidance, Control, and Dynamics*, **13**, 506-514.

[6]   **Sekhavat, P., Gong, Q., and Ross, I. M.,** 2007. NPSAT I Parameter Estimation Using Unscented Kalman Filter. Proceedings of American Control Conference, 4445-4451, New York, USA.

[7]   **Julier, S. J., and Uhlmann, J. K.,** 2004: Unscented Filtering and Nonlinear Estimation. *Proceedings of IEEE*, **92**, 401-422.

[8]   **Julier, S. J., Uhlmann, J. K., and Durrant-Whyte, H. F.,** 1995. A New Approach for Filtering Nonlinear Systems. Proceedings of American Control Conference, **3**, 1628-1632.

[9]   **Julier, S., Uhlmann, J., and Durrant-Whyte, H. F.,** 2000: A New Method for the Nonlinear Transformation of Means and Covariances in Filters and Estimators. *IEEE Transactions on Automatic Control*, **45**, 477-482.

[10]   **Crassidis, J. L., and Markley, F. L.,** 2003: Unscented Filtering for Spacecraft Attitude Estimation. *Journal of Guidance, Control, and Dynamics*, **26**, 536-542.

[11]   **Soken, H. E., and Hajiyev, Ch.,** 2008. Unscented Kalman Filter Based Attitude Estimation of ITU-PSAT I Satellite Using Magnetometer Measurements. Proceedings of the International Workshop on Small Satellites, New Missions, and New Technologies, 72-76, Istanbul, Turkey.

[12]   **Dyke, M.C., Schwartz, J. L., and Hall, C. D.,** 2004. Unscented Kalman Filtering for Spacecraft Attitude State and Paremeter Estimation.

Proceedings of the AAD/AIAA Space Flight Mechanics Conference. no.AAS 04-115, Hawaii, USA.

[13] **Fisher, J., and Vadali, S.R.,** 2008: Gyroless Attitude Control of Multibody Satellites Using an Unscented Kalman Filter. *Journal of Guidance, Control, and Dynamics,* **31**, 245-251.

[14] **White, N. A., Maybeck, P. S., and DeVilbiss S. L.,** 1998: MMAE Detection Of Interference/Jamming and Spoofing in a DGPS-Aided Inertial System. *IEEE Transactions on Aerospace and Electronic Systems,* **34**, 1208-1217.

[15] **Zhang, Y., and Li, X.R.,** 1997. Detection and Diagnosis of Sensor and Actuator Failures Using Interacting Multiple-Model Estimator. Proceeding of the 36th IEEE Conference on Decision and Control, **5**, 4475-4480

[16] **Maybeck, P. S.,** 1999. Multiple Model Adaptive Algorithms for Detecting and Compensating Sensor and Actuator/Surface Failures in Aircraft Flight Control Systems. *International Journal of Robust and Nonlinear Control,* **9**, 1051-1070.

[17] **Mehra, R. K.,** 1970**.** On the identification of variance and adaptive Kalman filtering. *IEEE Transactions on Automatic Control,* **15**, 175-184.

[18] **Maybeck, P. S.,** 1982: Stochastic Models, Estimation, and Control, Vol. I and II. Academic Press, New York, USA.

[19] **Salychez, O. S.,** 1994. Special Studies in Dynamic Estimation Procedures with Case Studies in Inertial Surveying, *ENGO 699.26 lecture notes,* Department of Geomatics Engineering, University of Calgary, Canada.

[20] **Mohamed, A. H., and Schwarz, K. P.,** 1999: Adaptive Kalman Filter for INS/GPS. *Journal of Geodesy,* **73**, 193-203.

[21] **Wang, J., Stewart, M. P., and Tsakiri, M.,** 1999. Adaptive Kalman Filtering for Integration of GPS with GLONASS and INS. Proceedings of Geodesy Beyond 2000: the Challenges of the First Decade, 325-330, Birmingham, UK.

[22] **Sasiadek, J. Z, and Wang, Q.,** 1999. Sensor Fusion Based on Fuzzy Kalman Filtering for Autonomous Robot Vehicle. Proceedings of the 1999 IEEE International Conference on Robotics & Automation, **4**, 2970-2975, Detroit, Michigan, USA.

[23] **Zhang, S. T., and Wei, X. Y.,** 2003. Fuzzy Adaptive Kalman Filtering for DR/GPS. Proceedings of the Second International Conference on Machine Learning and Cybernetics, **5**, 2634-2637, Xi-an, PRC.

[24] **Escamilla-Ambrosio, P. J., and Mort, N.,** 2003. Hybrid Kalman Filter-Fuzzy Logic Adaptive Multisensor Data Fusion Architecture. Proceedings of the 42nd IEEE Conference on Decision and Control, **5**, 5215-5220, Hawaii, USA.

[25] **Hu, C., Chen, W., Chen, Y., and Liu, D.,** 2003: Adaptive Kalman Filtering for Vehicle Navigation. *Journal of Global Positioning Systems,* **2**, 42-47

[26] **Hide, C., Moore, T., and Smith, M.,** 2004. Adaptive Kalman Filtering Algorithms for Integrating GPS and Low Cost INS. Proceedings of the Position Location and Navigation Symposium, 227-233, Monterey, USA.

[27] **Ding, W., Wang, J., Rizos, C., and Kinlyside, D.,** 2007: Improving Adaptive Kalman Estimation in GPS/INS Integration. *The Journal of Navigation*, **60,** 517–529

[28] **Kim, K. H., Lee, J. G., and Park, C. G.,** 2006: Adaptive Two-Stage Kalman Filter in the Presence of Unknown Random Bias. *International Journal of Adaptive Control and Signal Processing*, **20**, 305-319.

[29] **Hajiyev, Ch.,** 2007: Adaptive Filtration Algorithm with the Filter Gain Correction Applied to Integrated INS/Radar Altimeter. *Proceedings of the Institution of Mechanical Engineers, Part G: Journal of Aerospace Engineering*, **221**, 847-885.

[30] **Jwo, D.J., and Weng, T.P.,** 2008: An Adaptive Sensor Fusion Method with Applications in Integrated Navigation. *The Journal of Navigation*, **61,** 705–721.

[31] **Geng, Y., and Wang, J.,** 2008: Adaptive Estimation of Multiple Fading Factors in Kalman Filter for Navigation Applications. *GPS Solutions*, **12,** 273-279.

[32] **Jiang, Z., Song, Q., He, Y., and Han, J.,** 2007. A Novel Adaptive Unscented Kalman Filter for Nonlinear Systems. Proceedings of the 46th IEEE Conference on Decision and Control, pp. 4293-4298, New Orleans, USA.

[33] **Xu, J., Jing, Y., Dimirovski, G. M., and Ban, Y.,** 2008. Two-Stage Unscented Kalman Filter for Nonlinear Systems in the Presence of Unknown Random Bias. Proceedings of the American Control Conference, 3530-3535, Seatle, USA.

[34] **Wertz, J. R.,** 1988: Spacecraft Attitude Determination and Control, Kluwer Academic Publishers, Dordrecht, Holland.

[35] **Bak, T.,** 1999. Spacecraft Attitude Determination – A Magnetometer Approach, *Ph.D.Thesis,* Aalborg University, Aalborg, Denmark.

[36] **Sidi, M. J.,** 1997: Spacecraft Dynamics & Control – Apractical Engineering Approach , Cambridge University Press, New York, USA.

[37] **Corno, M., and Lovera, M.,** 2009: Spacecraft Attitude Dynamics and Control in the Presence of Large Magnetic Residuals. *Control Engineering Practice*, **17**, 456-468.

[38] **Macmillan, S., and Maus, S., Bak, T.,** 2005: International Geomagnetic Field – the Tehth Generation. *Earth Planets Space,* **57**, 1135-1140.

[39] **Jiangi, W., Xibin, C., and Zhaowei, S.,** 2003: Attitude and Orbit Determination for Small Satellite Using Magnetometer Measurement. *Aircraft Engineering and Aerospace Technology*, **75**, 241-246.

[40] **Zarchan, P., and Musoff H.,** 2000: Fundamentals of Kalman Filtering; A Practical Approach, AIAA, Virginia, USA.

APPENDICES

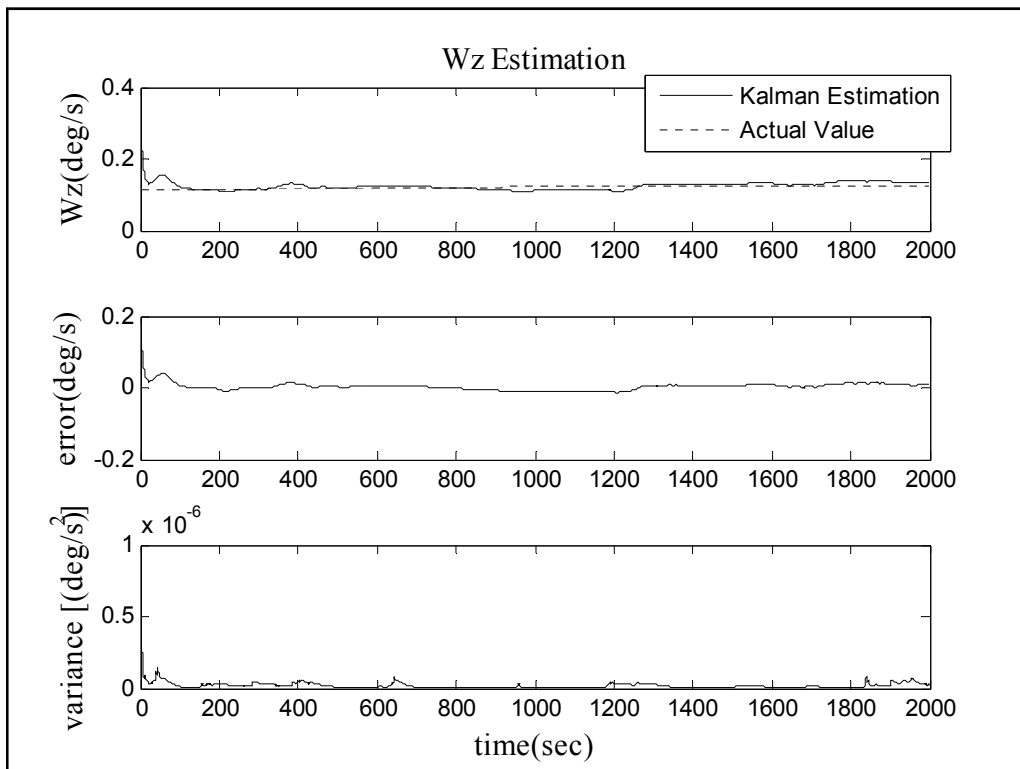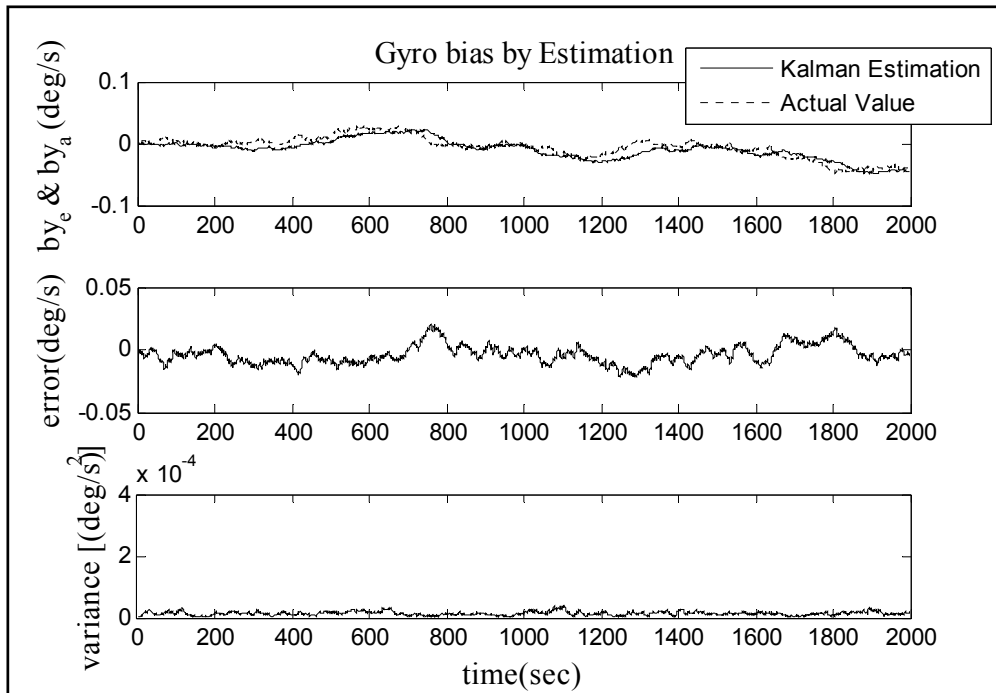**Figure A.1 :** Pitch angle estimation by UKF for torque estimation scenario.
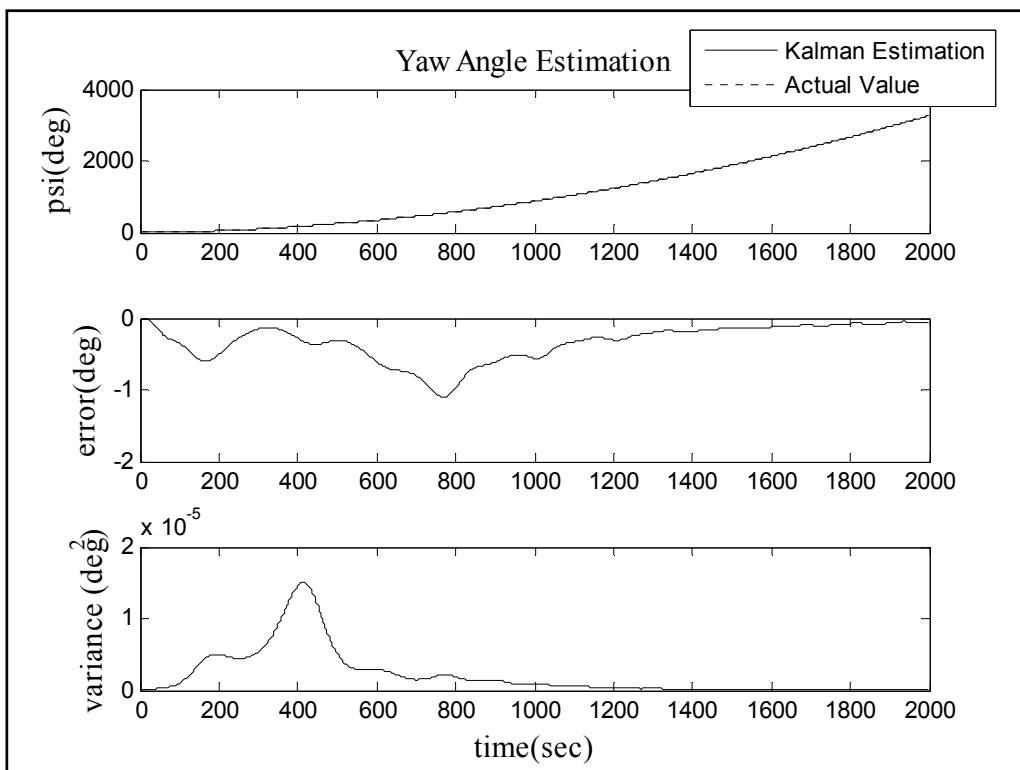
**Figure A.2 :** Yaw angle estimation by UKF for torque estimation scenario.
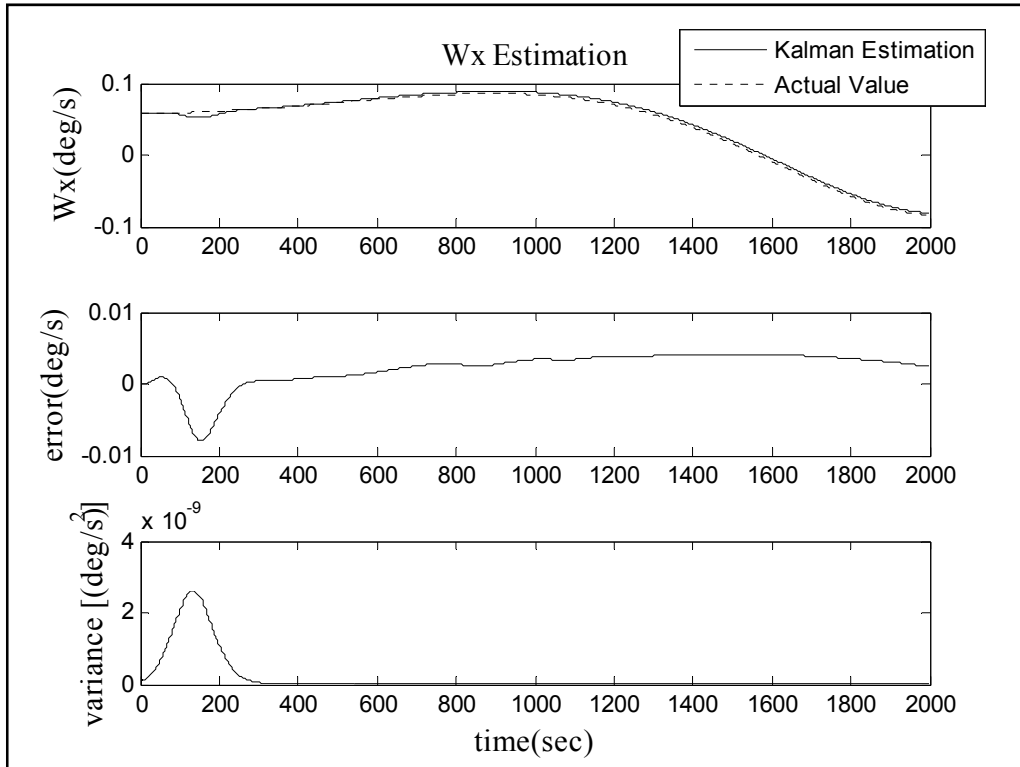
Figure A.3 : Estimation of angular velocity about "x" axis by UKF for torque estimation scenario.
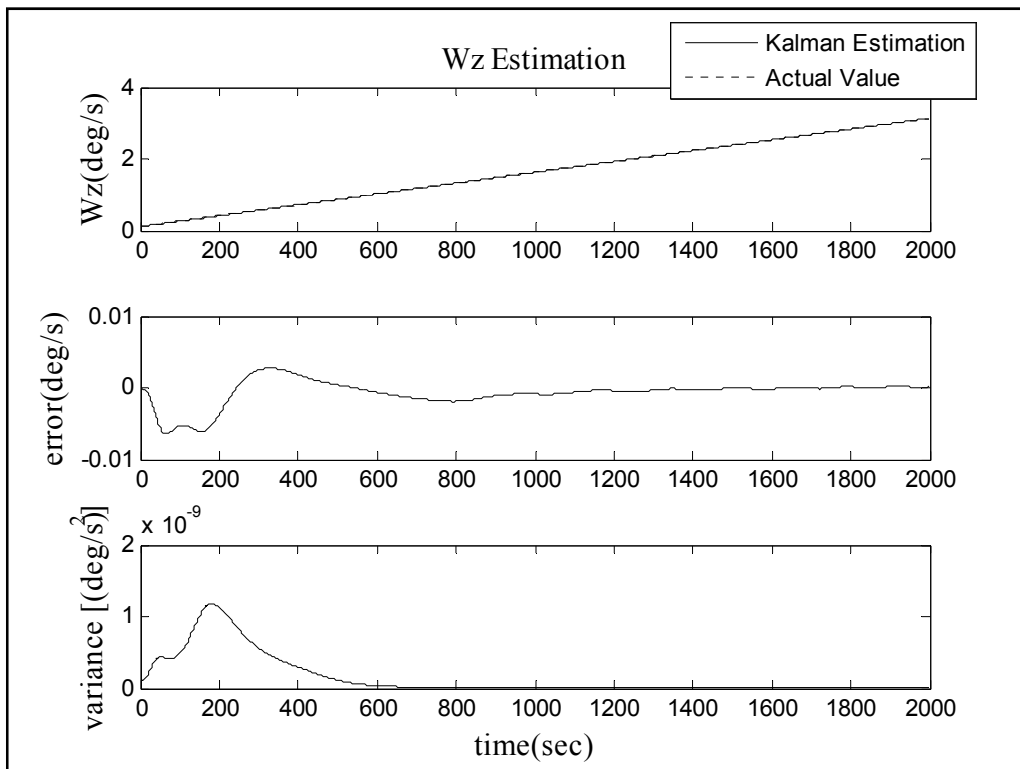
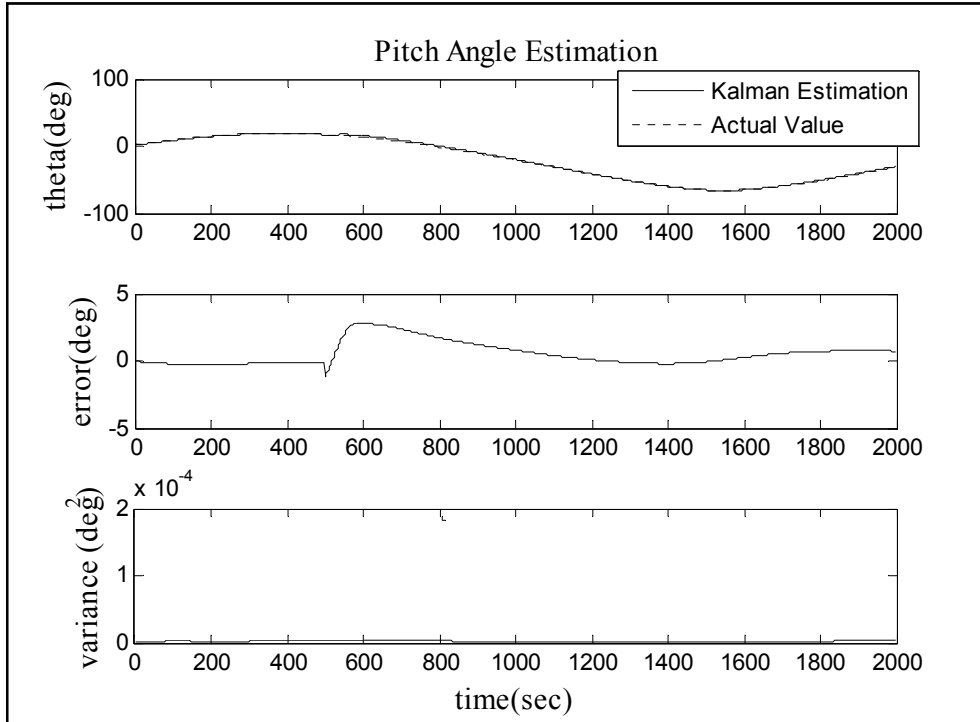**Figure A.4 :** Estimation of angular velocity about "z" axis by UKF for torque estimation scenario.
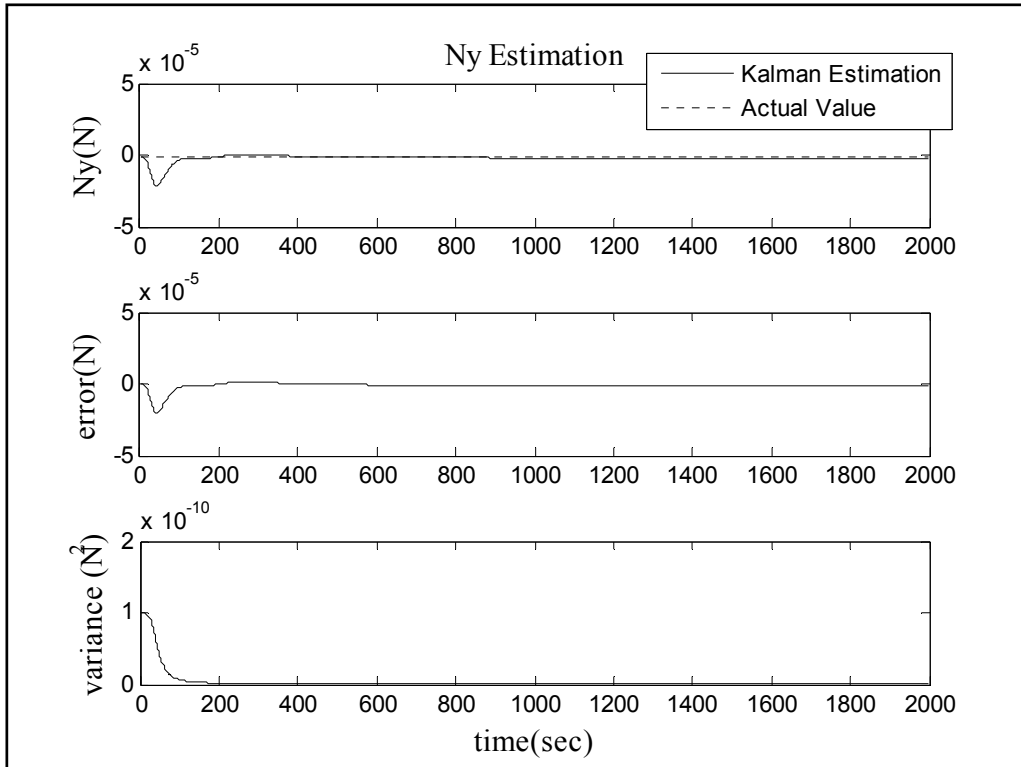
Figure A.5 : Estimation of constant external torque about "y" axis with UKF.
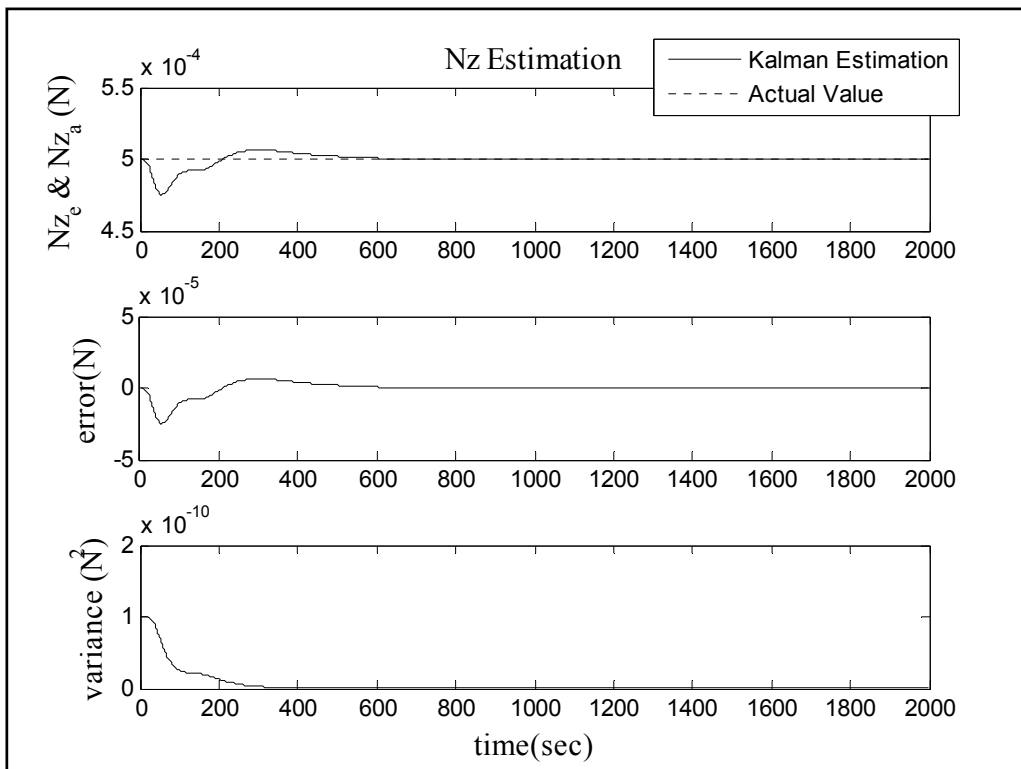
Figure A.6 : Estimation of constant external torque about "z" axis with UKF.

APPENDIX B
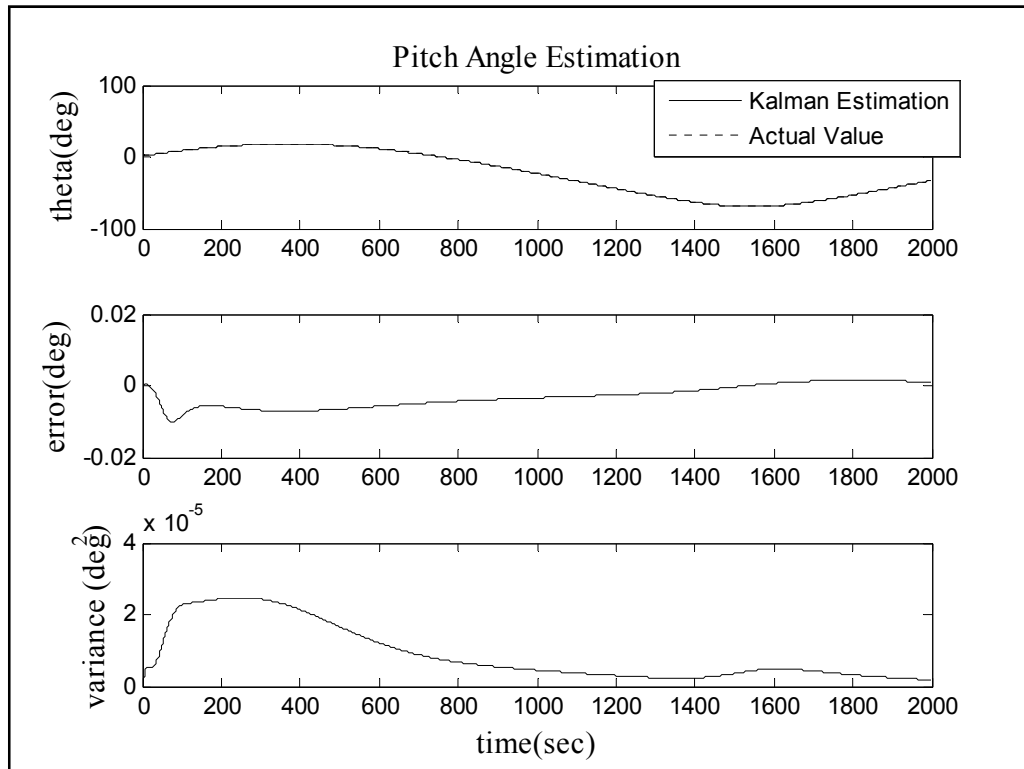
Figure B.1 : Pitch angle estimation by UKF for magnetometer bias estimation scenario.
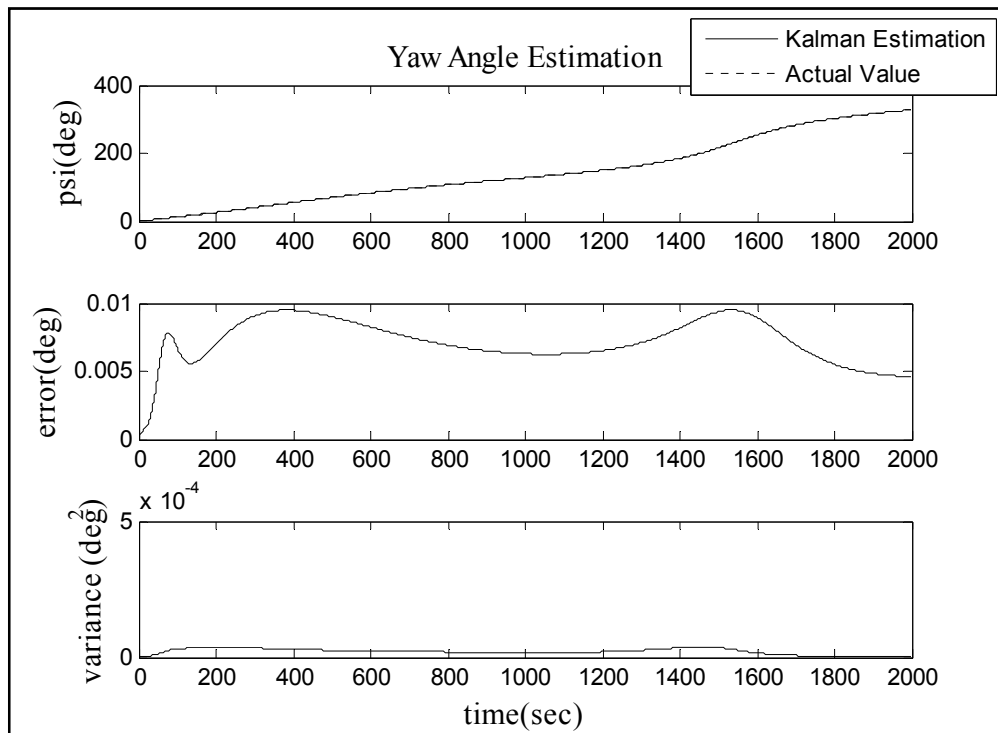
Figure B.2 : Yaw angle estimation by UKF for magnetometer bias estimation scenario.
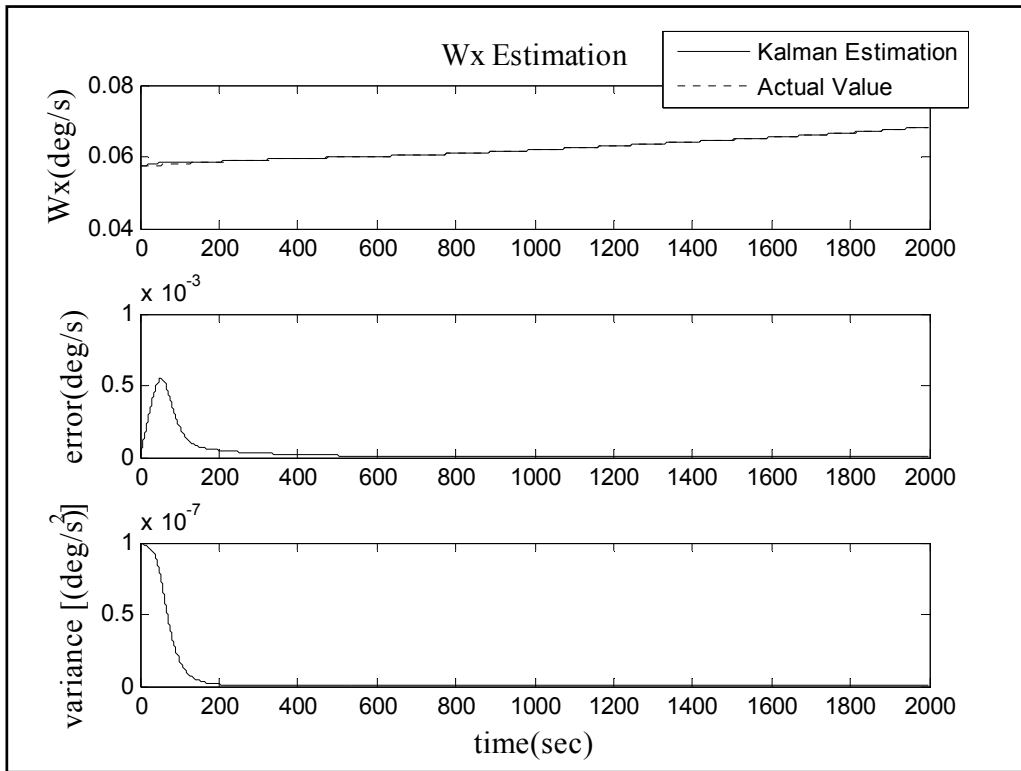
Figure B.3 : Estimation of angular velocity about "x" axis by UKF for
magnetometer bias estimation scenario.
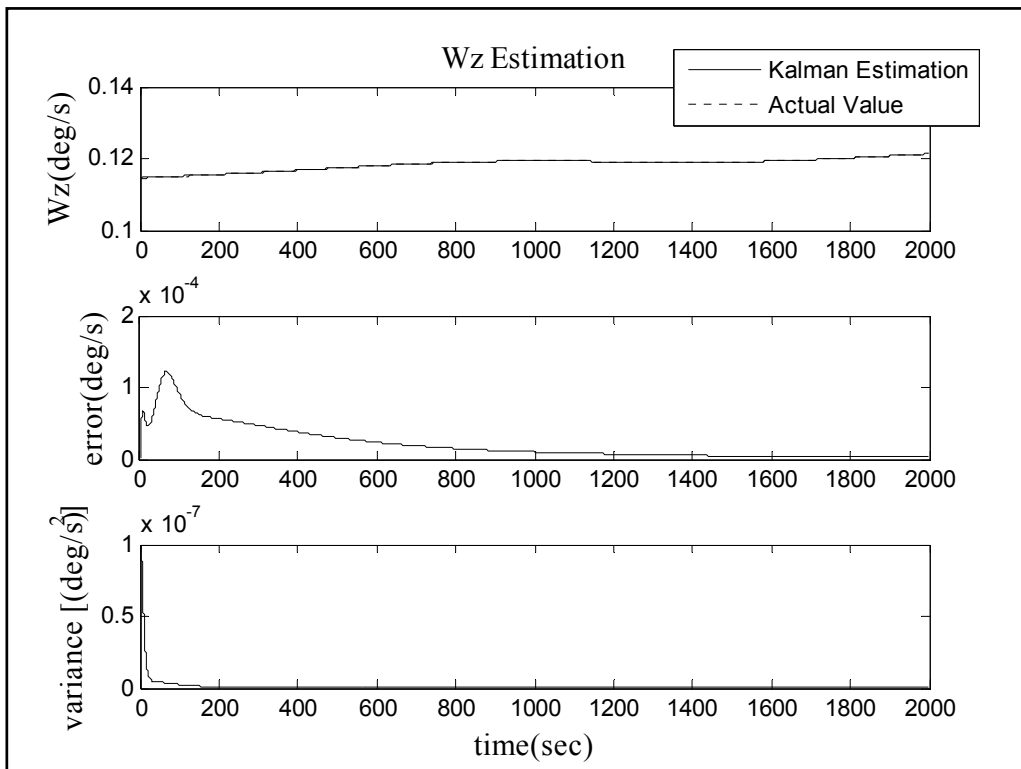
Figure B.4 : Estimation of angular velocity about "z" axis by UKF for
magnetometer bias estimation scenario.
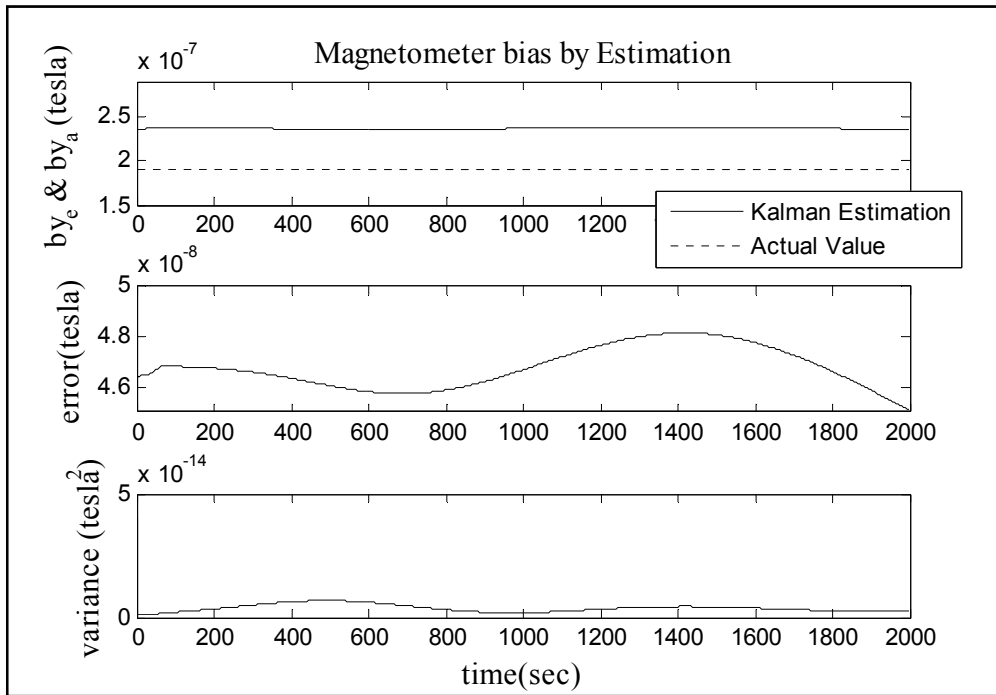
Figure B.5 : Estimation of bias of the magnetometer which is aligned in "y" axis.
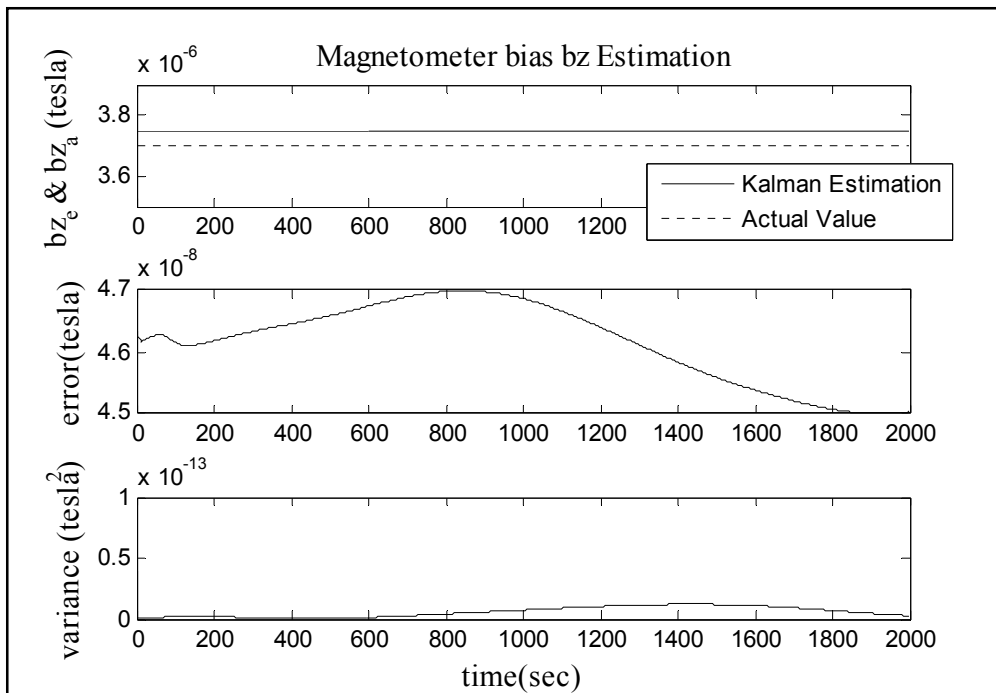
Figure B.6 : Estimation of bias of the magnetometer which is aligned in "z" axis.

Figure C.1 : Yaw angle estimation by UKF for gyro bias estimation scenario.
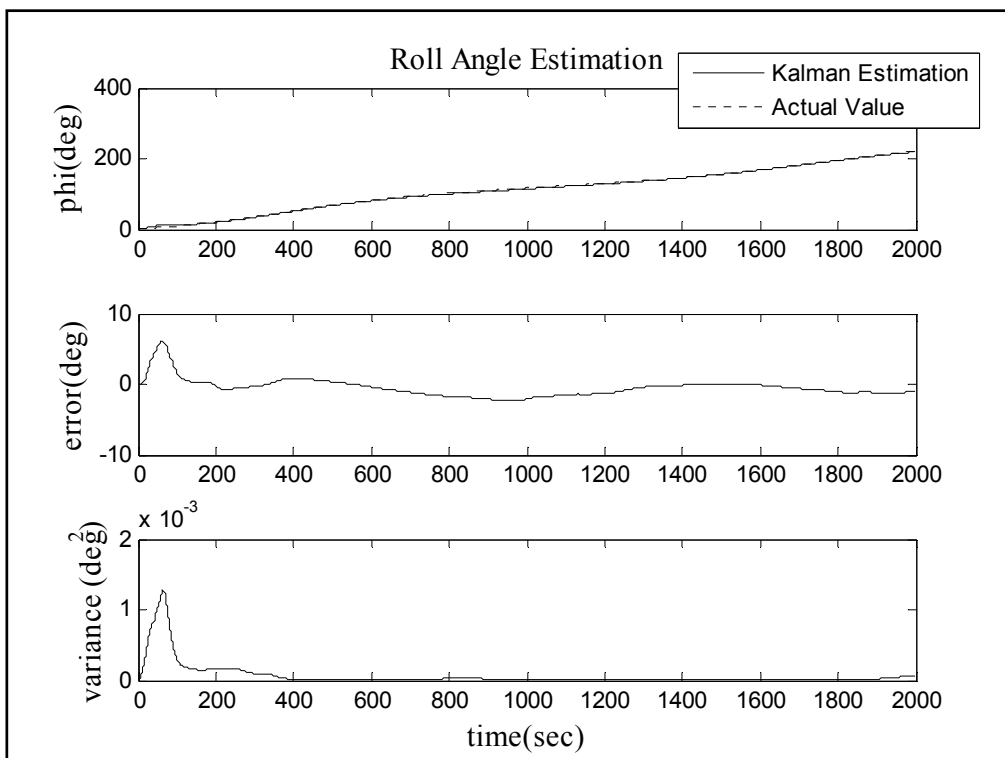
Figure C.2 : Roll angle estimation by UKF for gyro bias estimation scenario.
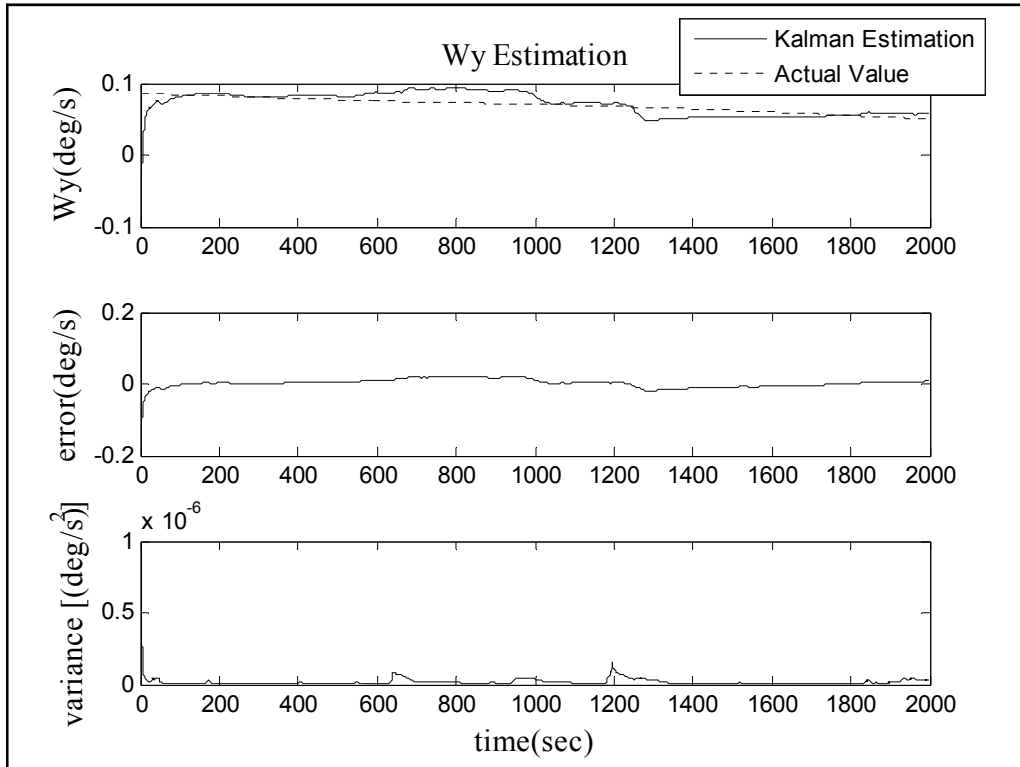
Figure C.3 : Estimation of angular velocity about "y" axis by UKF for gyro bias estimation scenario.

Figure C.4 : Estimation of angular velocity about "z" axis by UKF for gyro bias estimation scenario.

Figure C.5 : Estimation of bias of the gyro which is aligned in "y" axis.
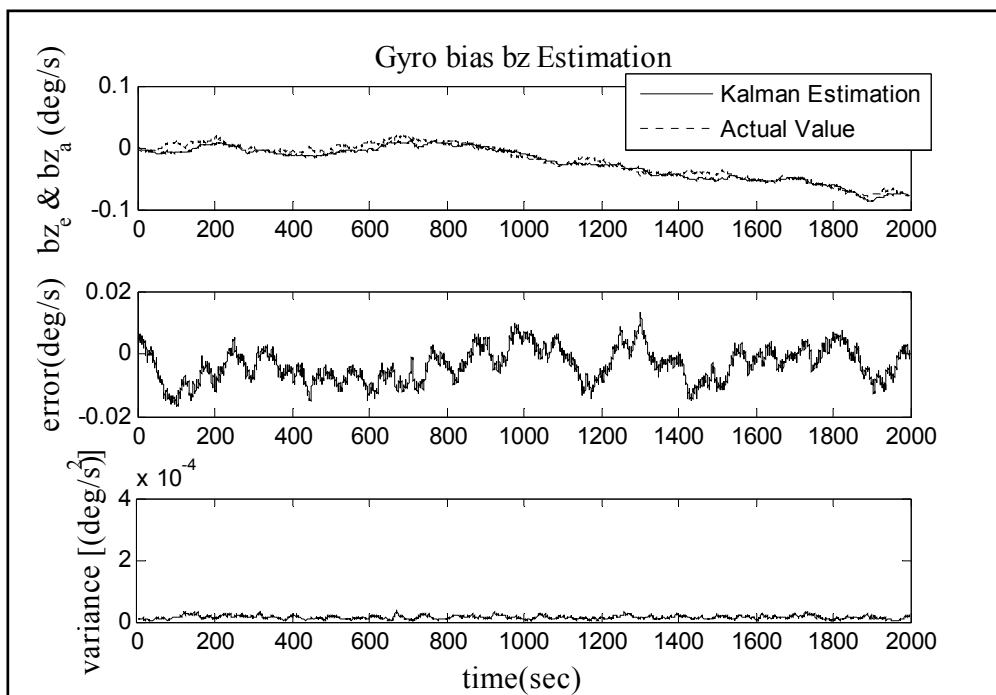
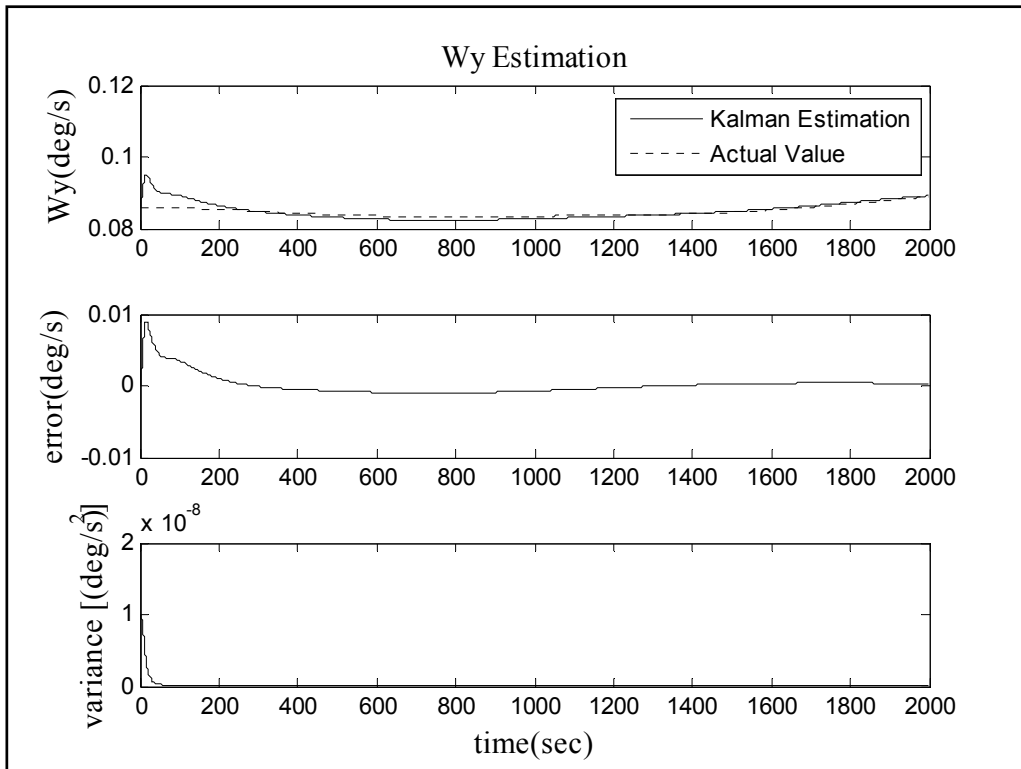**Figure C.6 :** Estimation of bias of the gyro which is aligned in "z" axis.

APPENDIX D

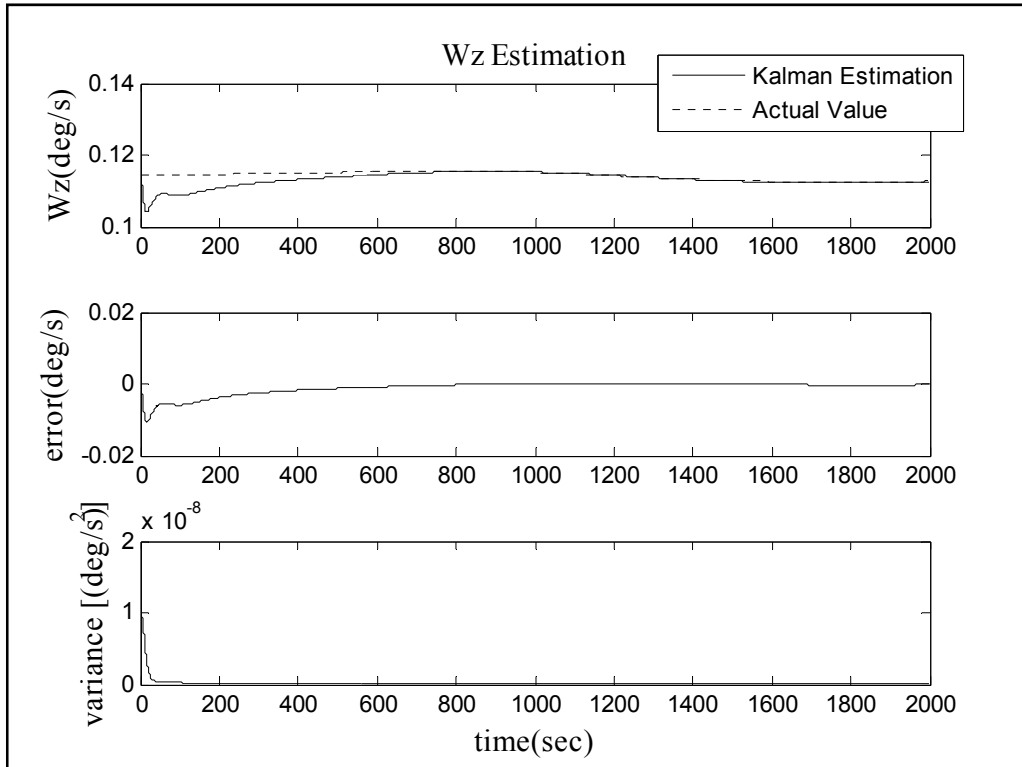**Figure D.1 :** Pitch angle estimation by optimal UKF in case of instantaneous abnormal measurements.
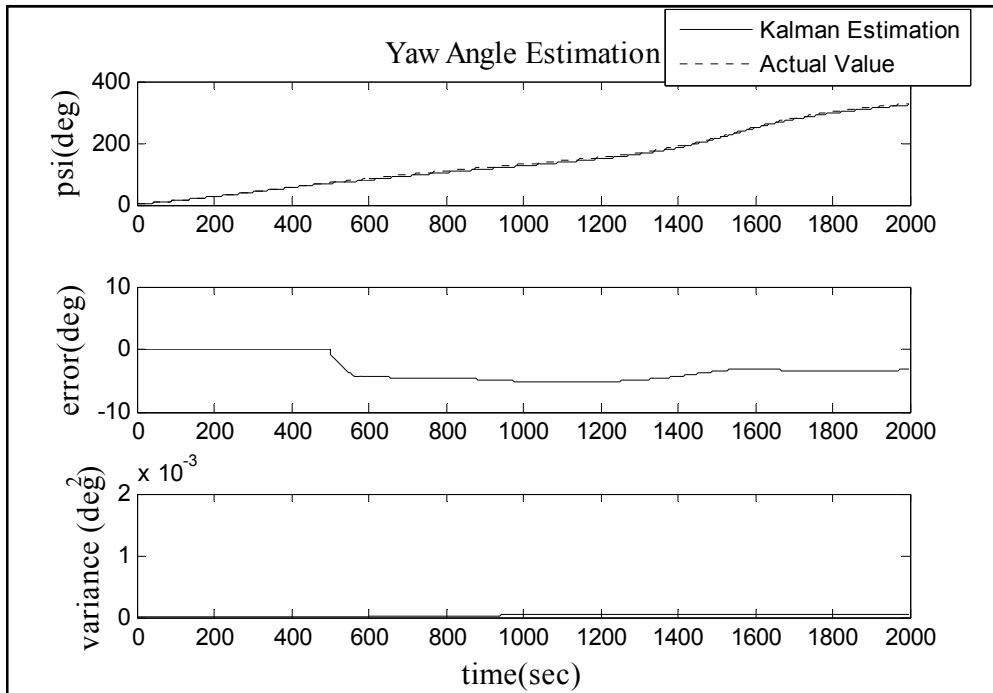
Figure D.2 : Yaw angle estimation by optimal UKF in case of instantaneous abnormal measurements.
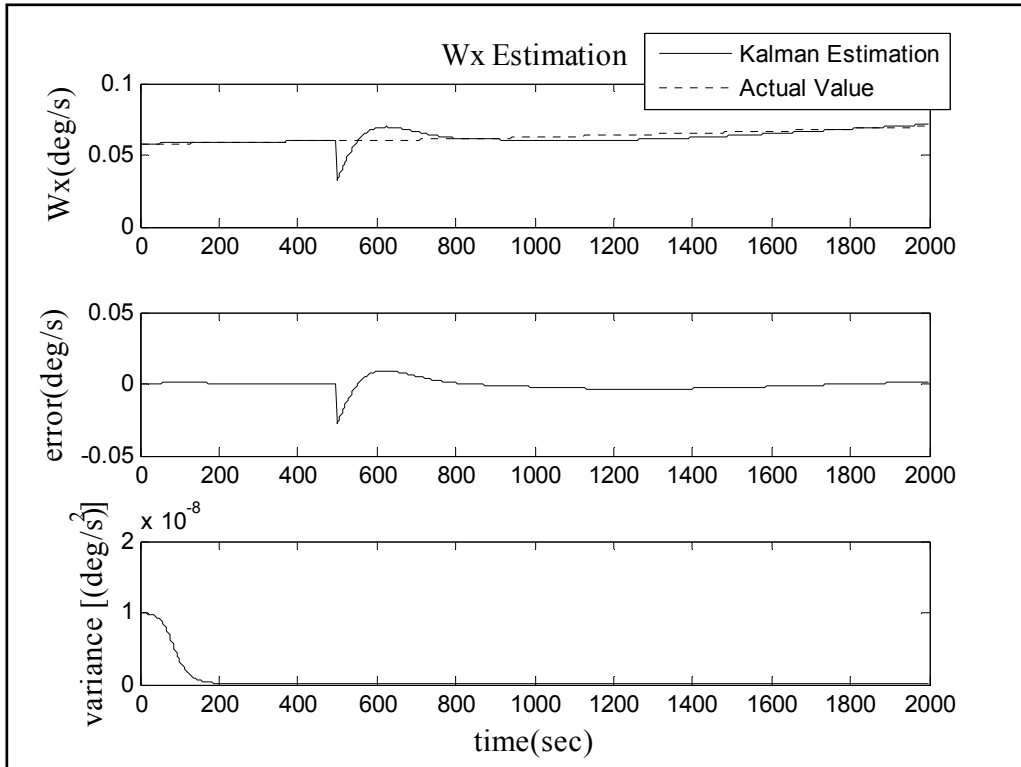
Figure D.3 :   Angular velocity about "x" axis estimation by optimal UKF in case of instantaneous abnormal measurements.
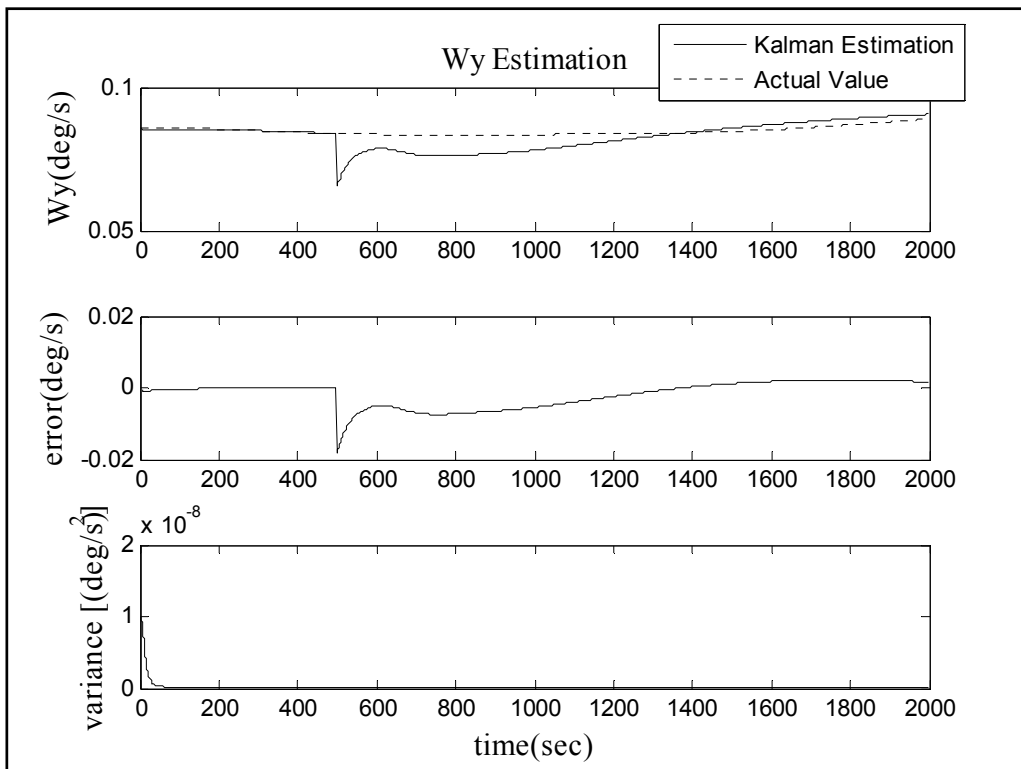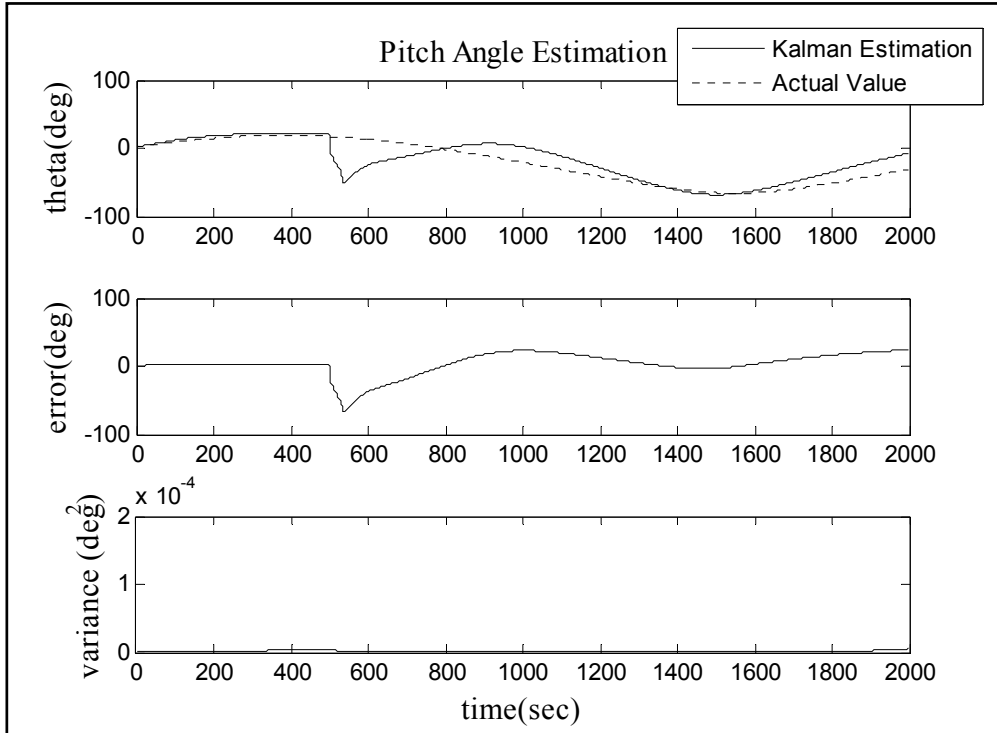

Figure D.4 :   Angular velocity about "y" axis estimation by optimal UKF in case of instantaneous abnormal measurements.
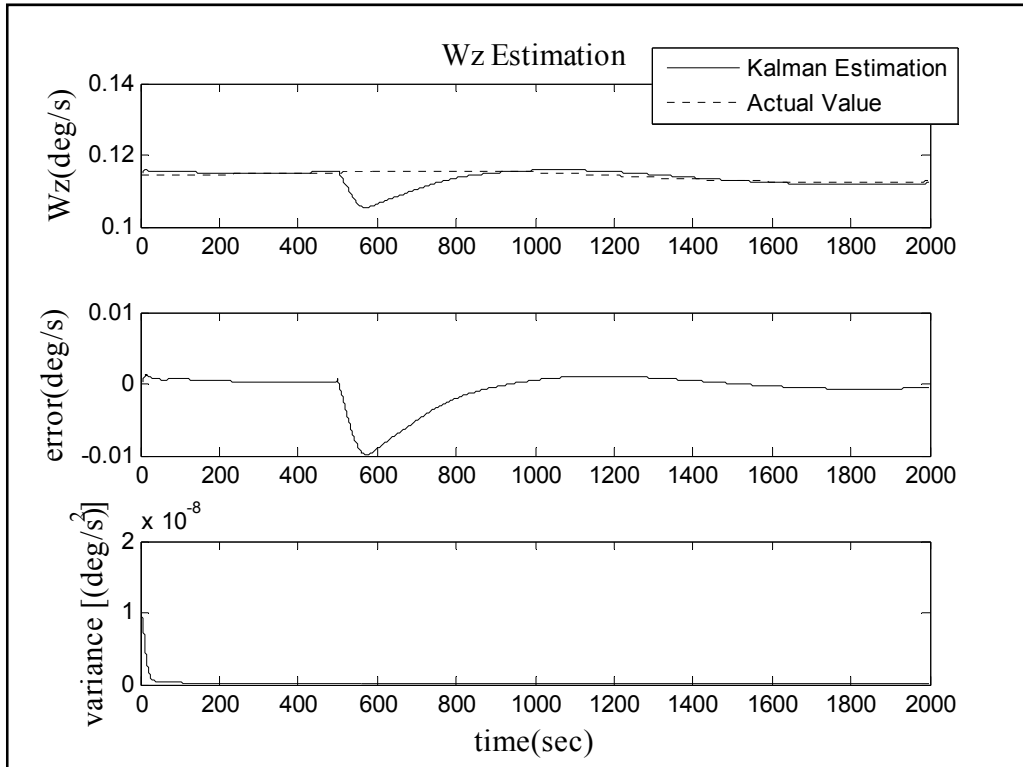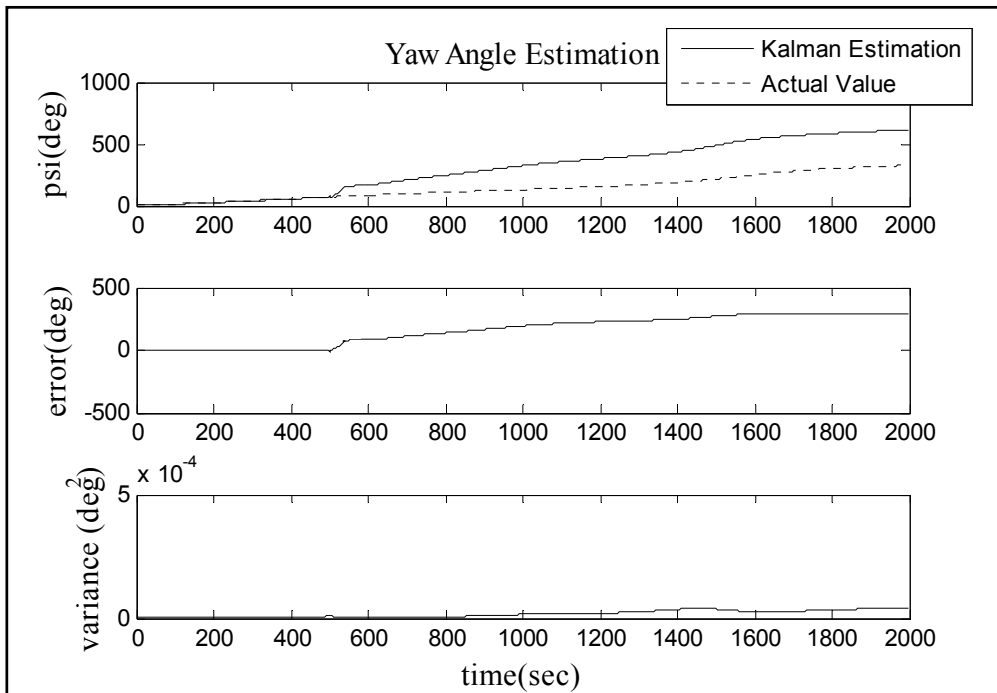
Figure D.5 : Angular velocity about "z" axis estimation by optimal UKF in case of instantaneous abnormal measurements.

APPENDIX E
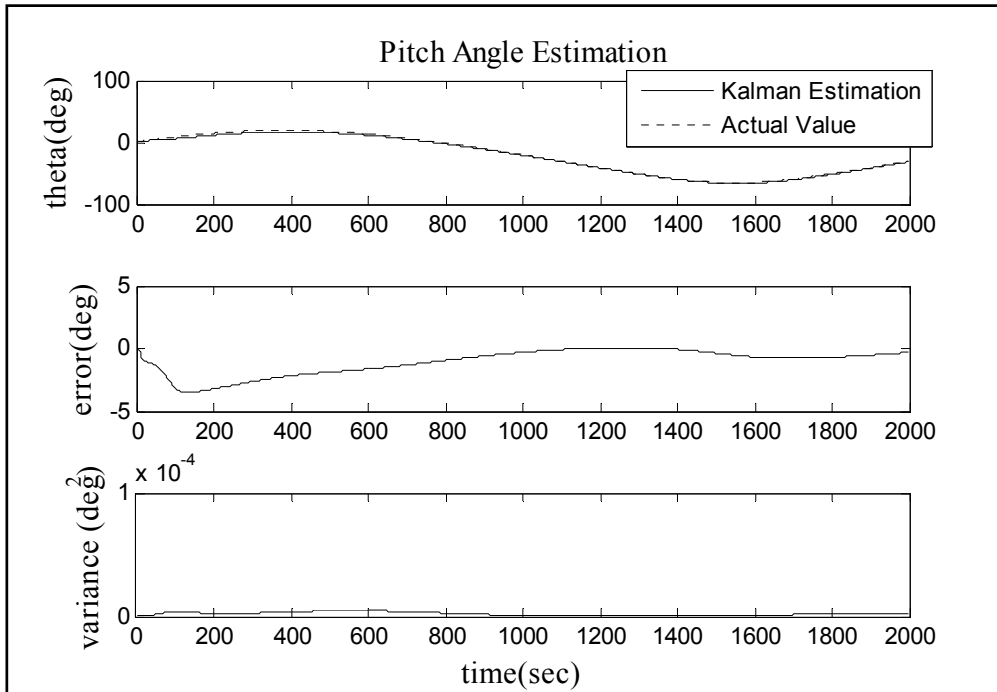
Figure E.1 : Pitch angle estimation by AUFKF with SFF in case of instantaneous abnormal measurements.
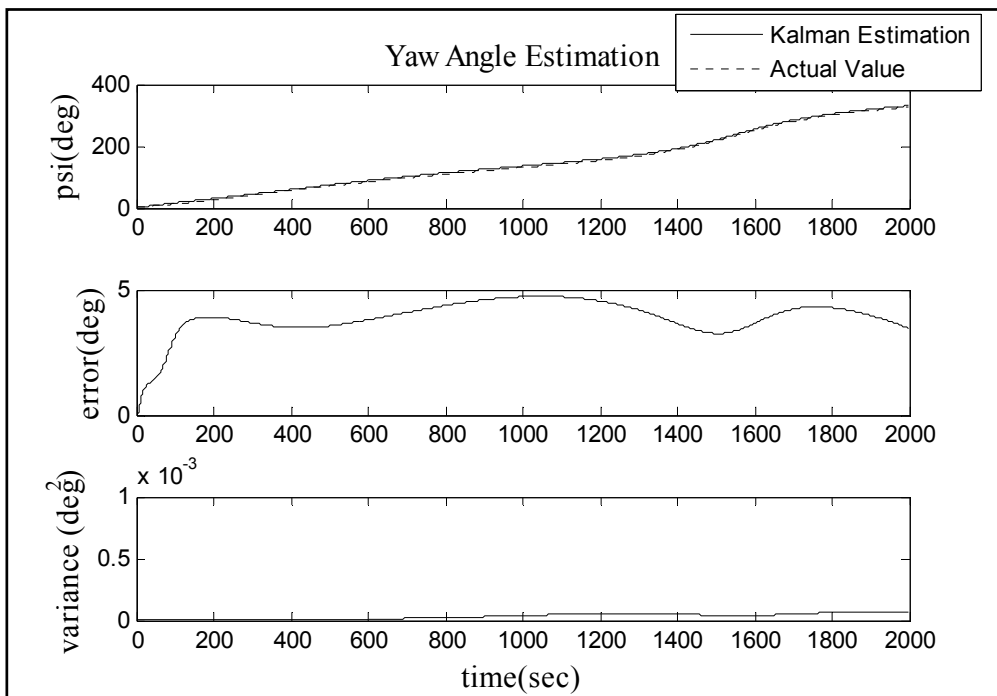
Figure E.2 : Yaw angle estimation by AUFKF with SFF in case of instantaneous abnormal measurements.
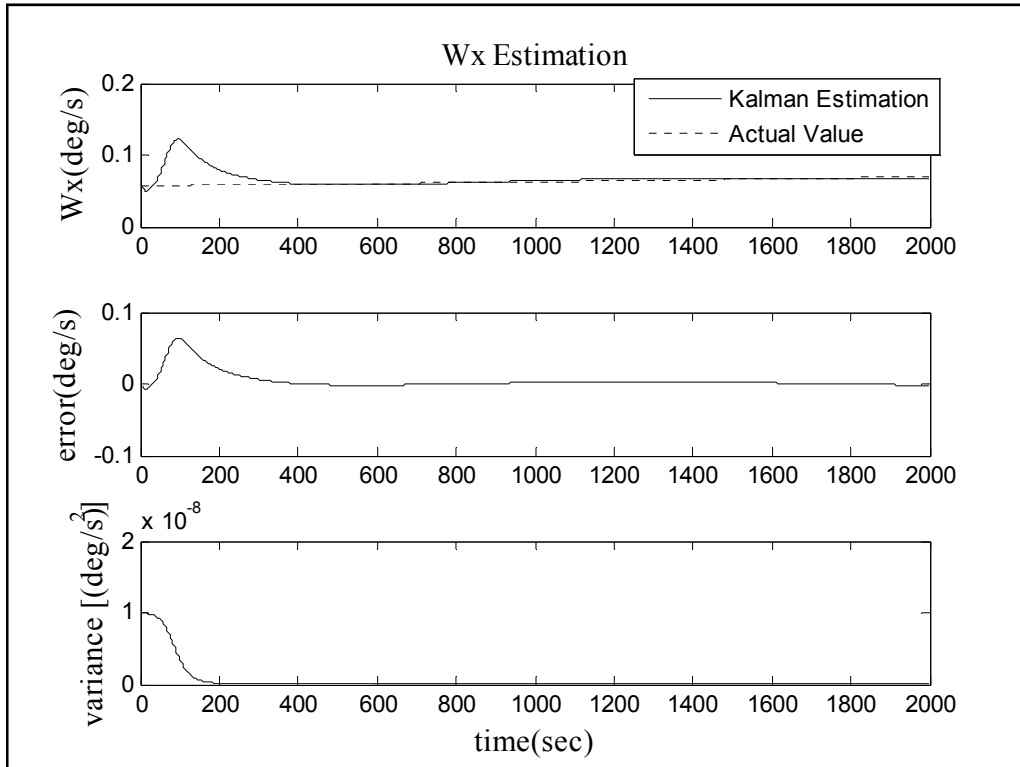
Figure E.3 : Angular velocity about "x" axis estimation by AUFKF with SFF in case of instantaneous abnormal measurements.
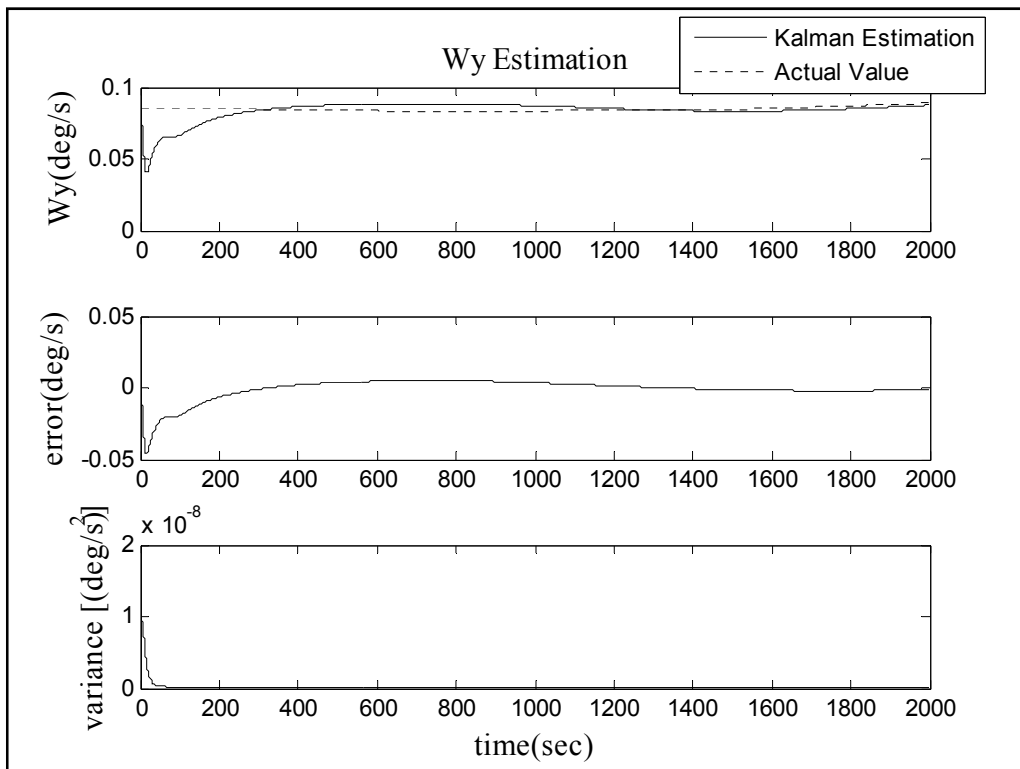
Figure E.4 : Angular velocity about "y" axis estimation by AUFKF with SFF in case of instantaneous abnormal measurements.
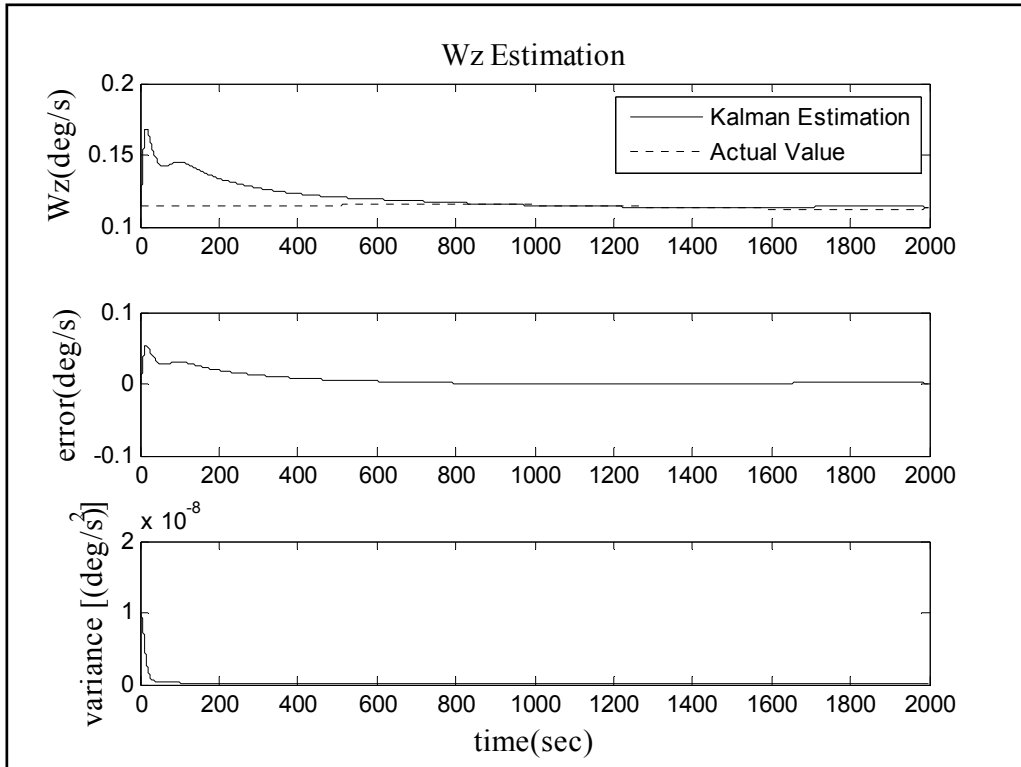
Figure E.5 : Angular velocity about "z" axis estimation by AUFKF with SFF in case of instantaneous abnormal measurements.
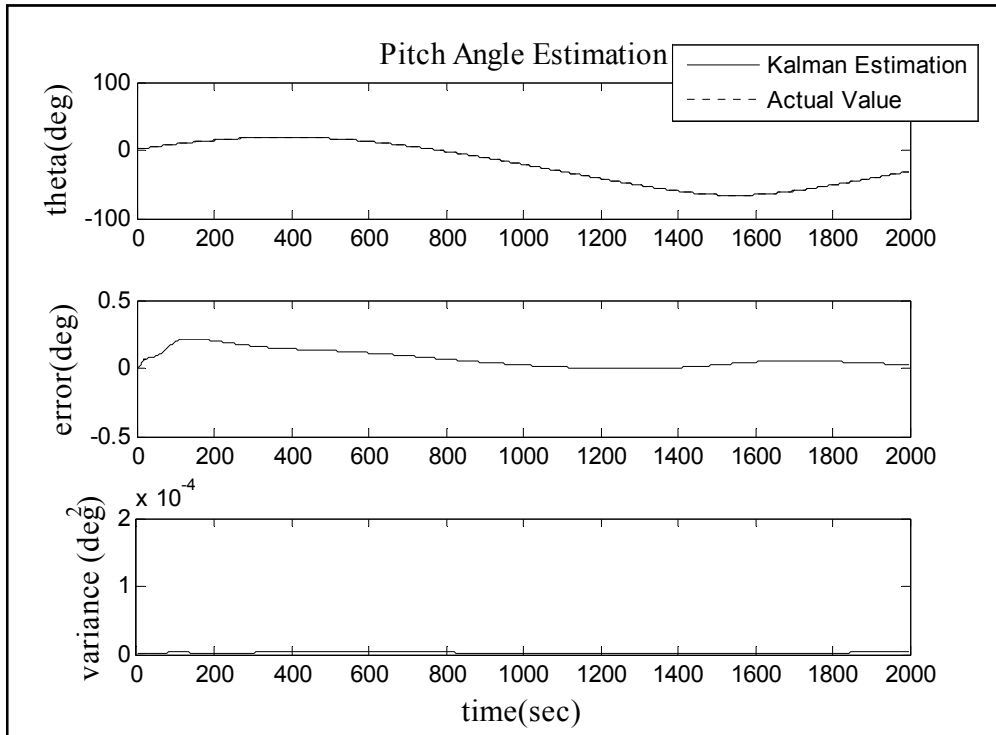
Figure F.1 : Pitch angle estimation by AUFKF with MFF in case of instantaneous abnormal measurements.
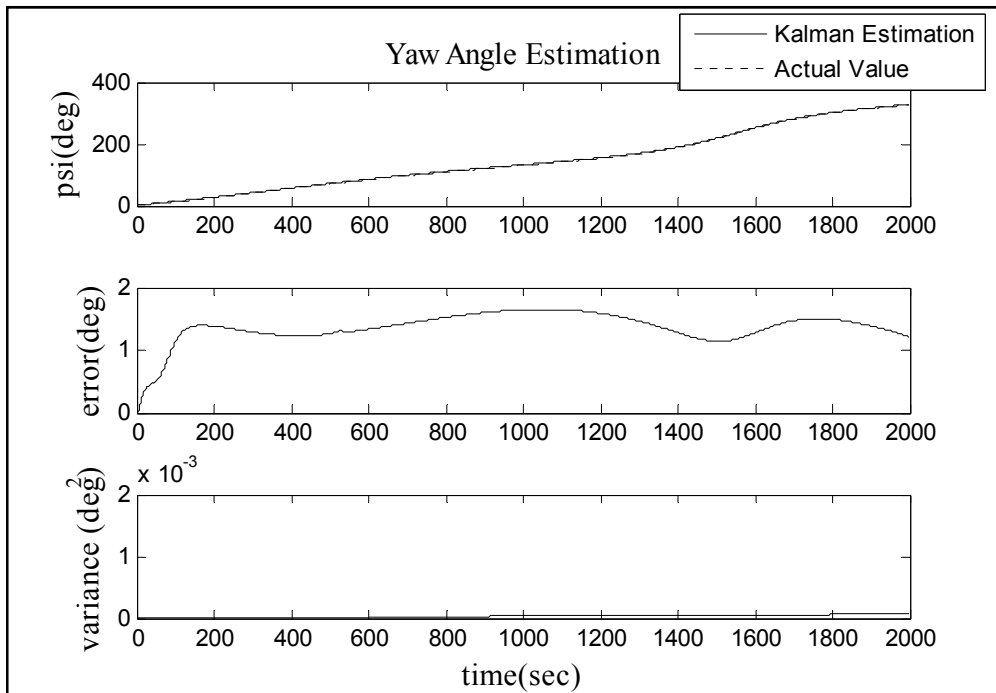
Figure F.2 : Yaw angle estimation by AUFKF with MFF in case of instantaneous abnormal measurements.
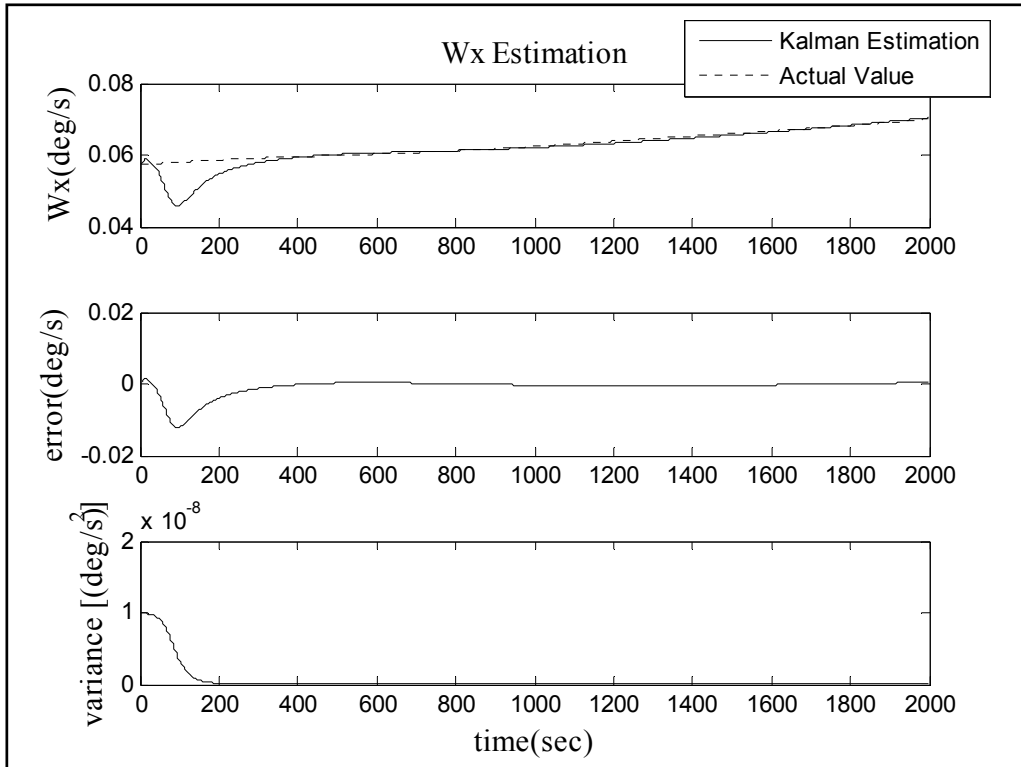
Figure F.3 : Angular velocity about "x" axis estimation by AUFKF with MFF in case of instantaneous abnormal measurements.

Figure F.4 : Angular velocity about "y" axis estimation by AUFKF with MFF in case of instantaneous abnormal measurements.

Figure F.5 : Angular velocity about "z" axis estimation by AUFKF with MFF in case of instantaneous abnormal measurements.

APPENDIX G

Figure G.1: Pitch angle estimation by optimal UKF in case of continuous bias at measurements.

Figure G.2: Yaw angle estimation by optimal UKF in case of continuous bias at measurements.
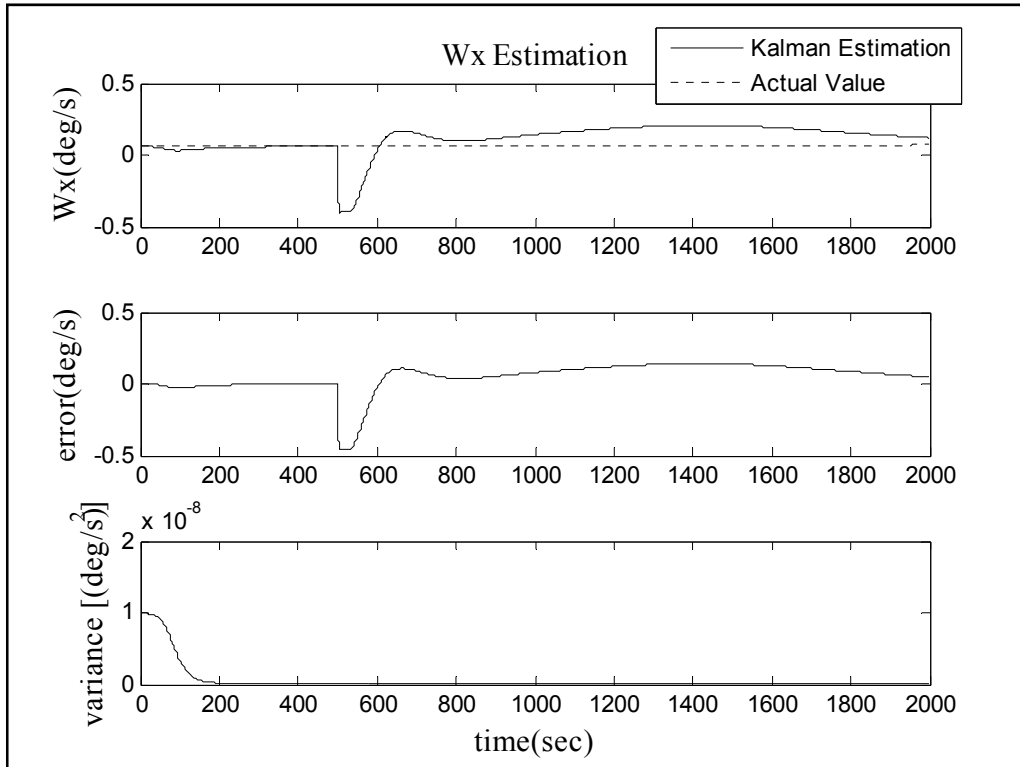
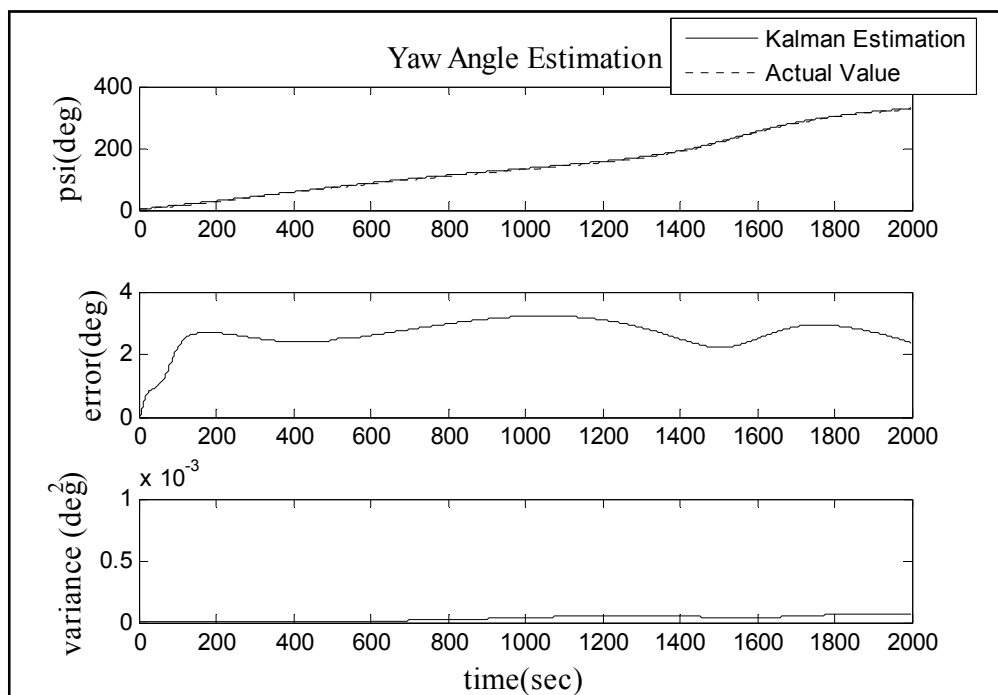**Figure G.3:** Angular velocity about "x" axis estimation by optimal UKF in case of continuous bias at measurements.
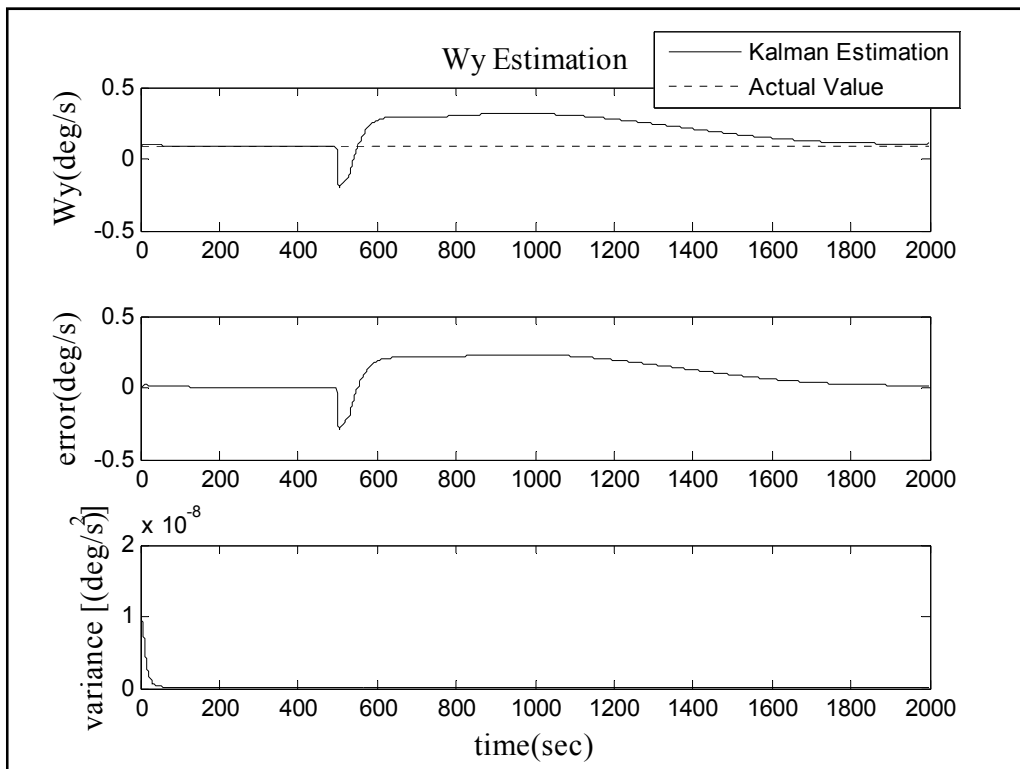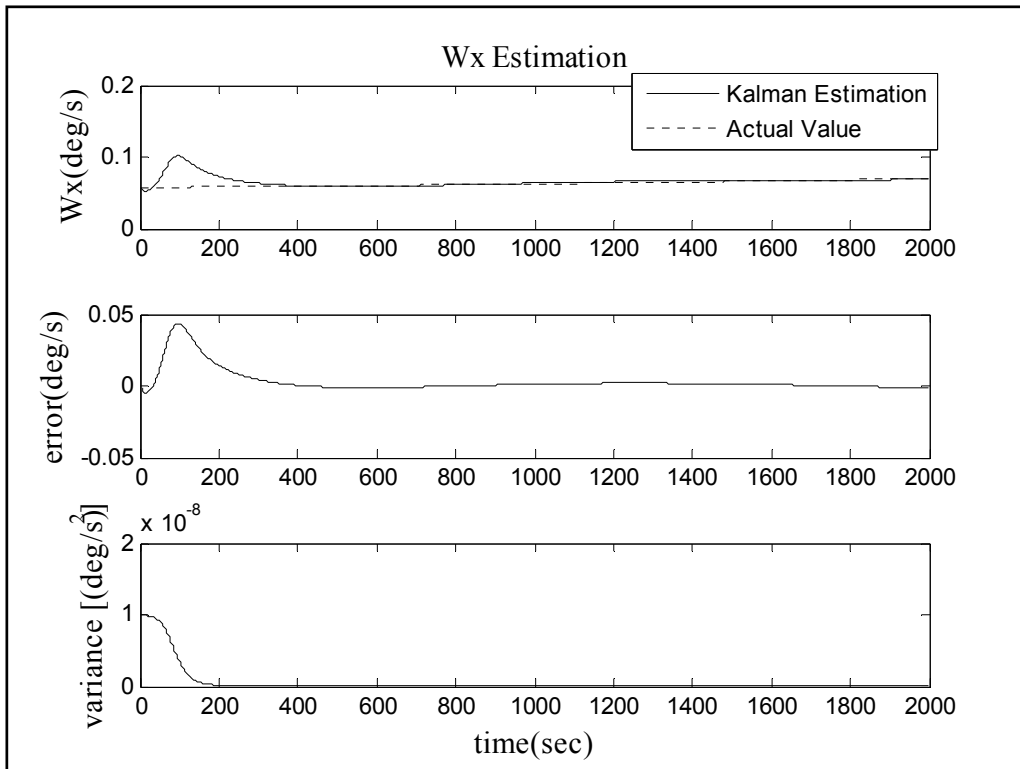

Figure G.4: Angular velocity about "y" axis estimation by optimal UKF in case of continuous bias at measurements.
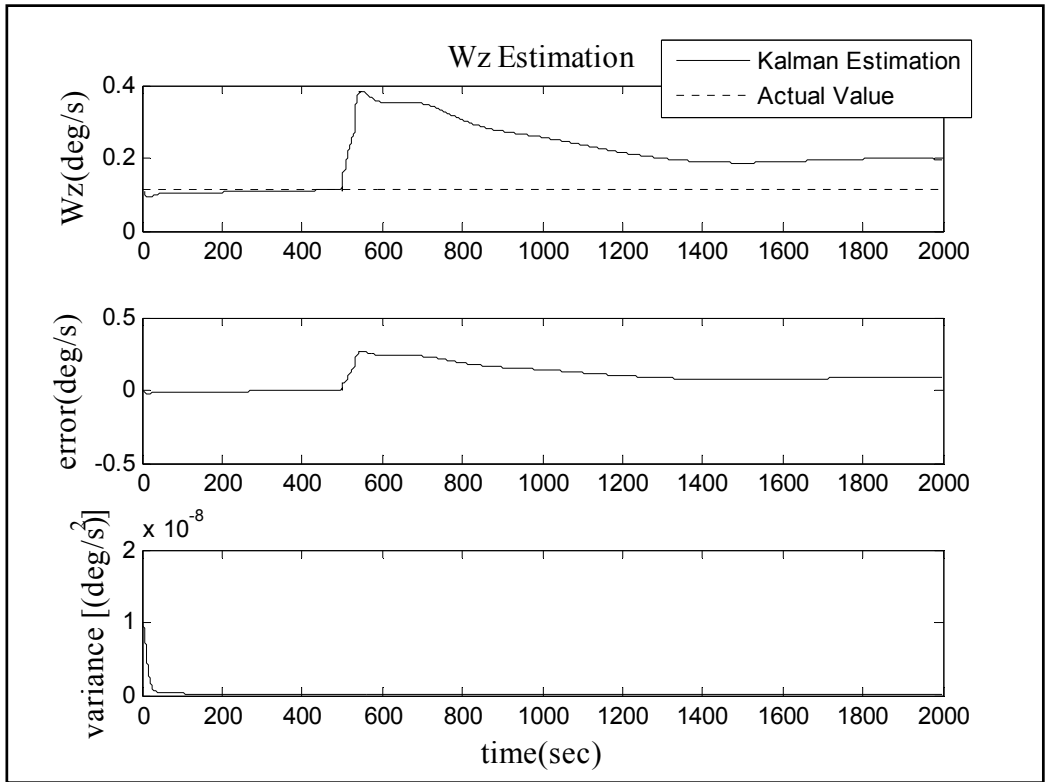
Figure G.5:   Angular velocity about "z" axis estimation by optimal UKF in case of continuous bias at measurements.
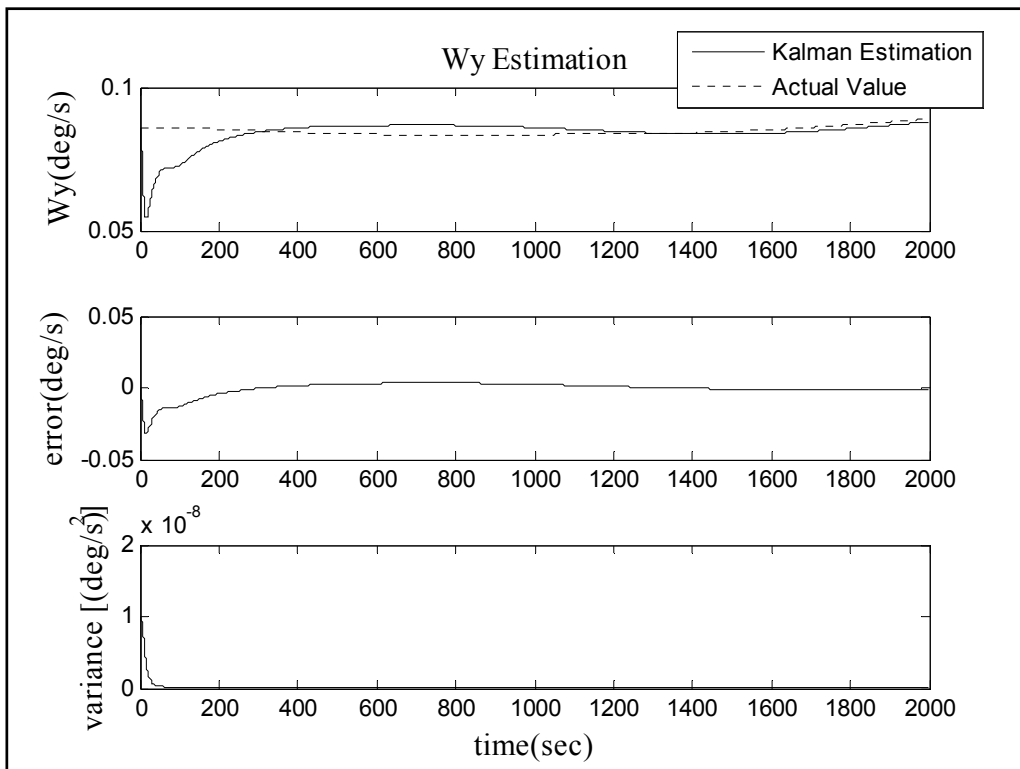
APPENDIX H
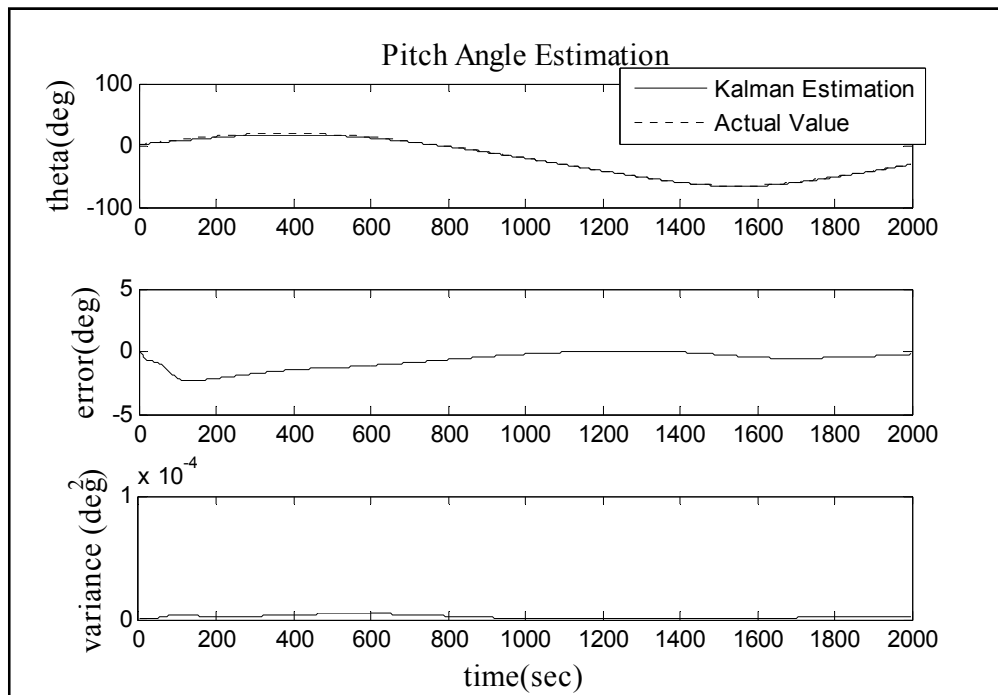
Figure H.1: Pitch angle estimation by AUFKF with SFF in case of continuous bias at measurements.
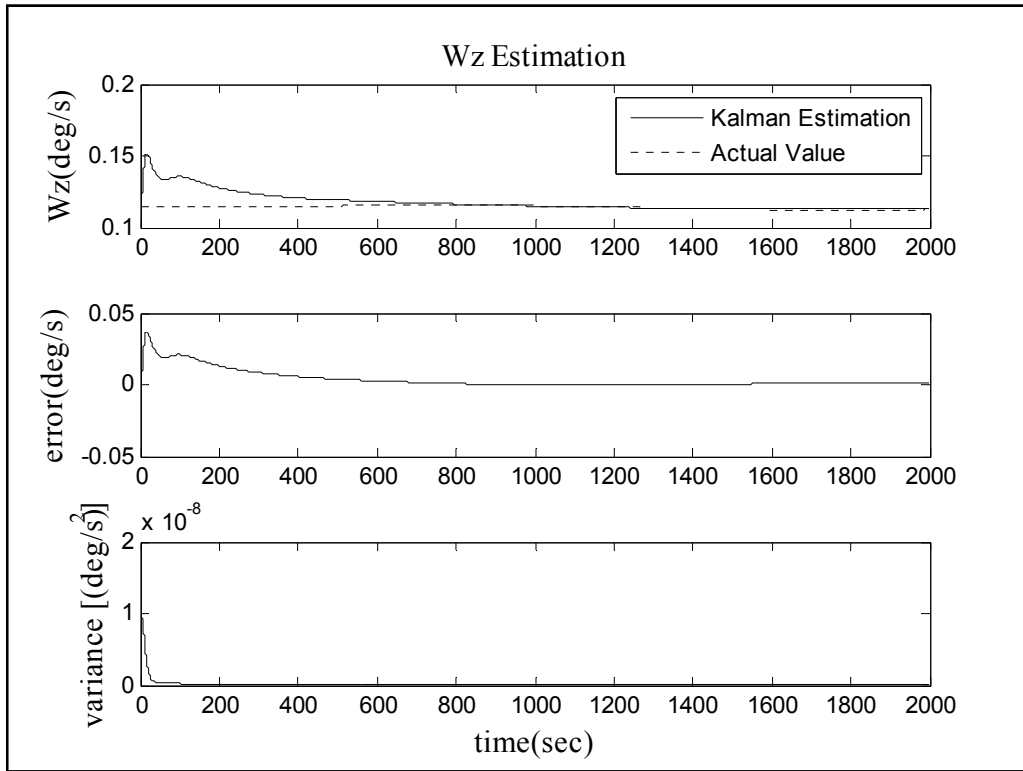

Figure H.2: Yaw angle estimation by AUFKF with SFF in case of continuous bias at measurements.

Figure H.3: Angular velocity about "x" axis estimation by AUFKF with SFF in case of continuous bias at measurements.
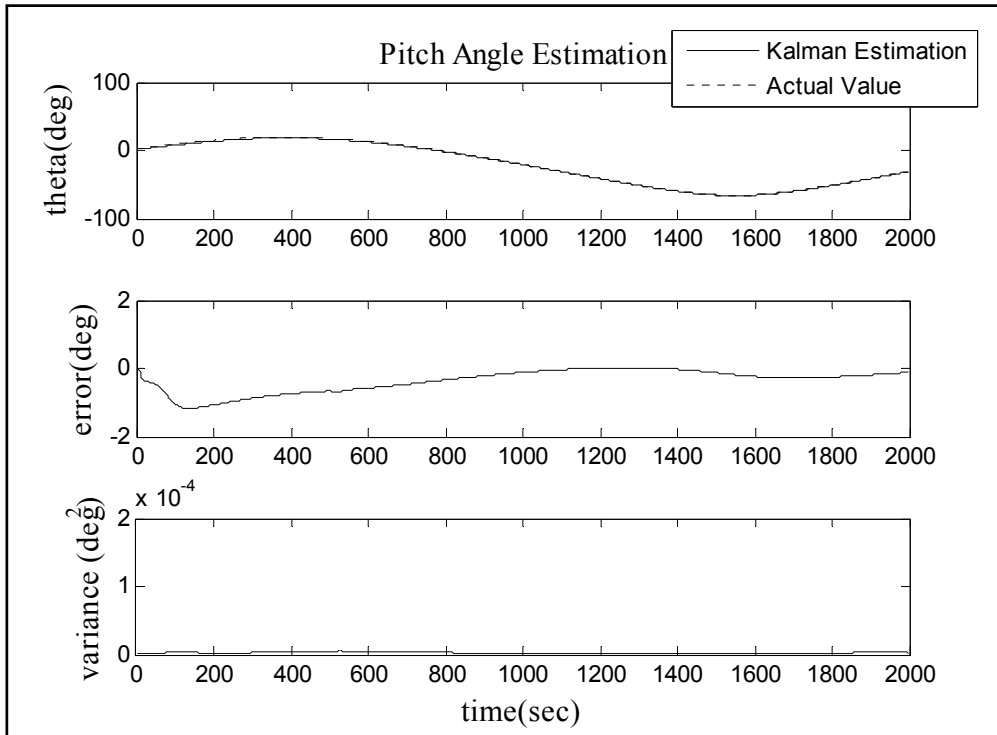

Figure H.4: Angular velocity about "y" axis estimation by AUFKF with SFF in case of continuous bias at measurements.
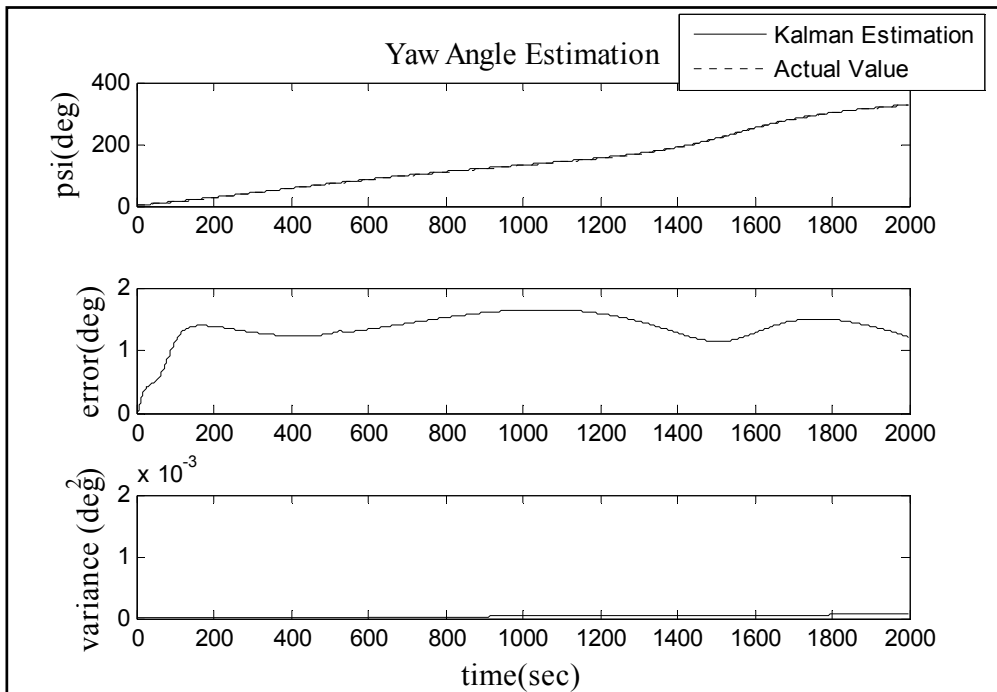
Figure H.5: Angular velocity about "z" axis estimation by AUFKF with SFF in case of continuous bias at measurements.
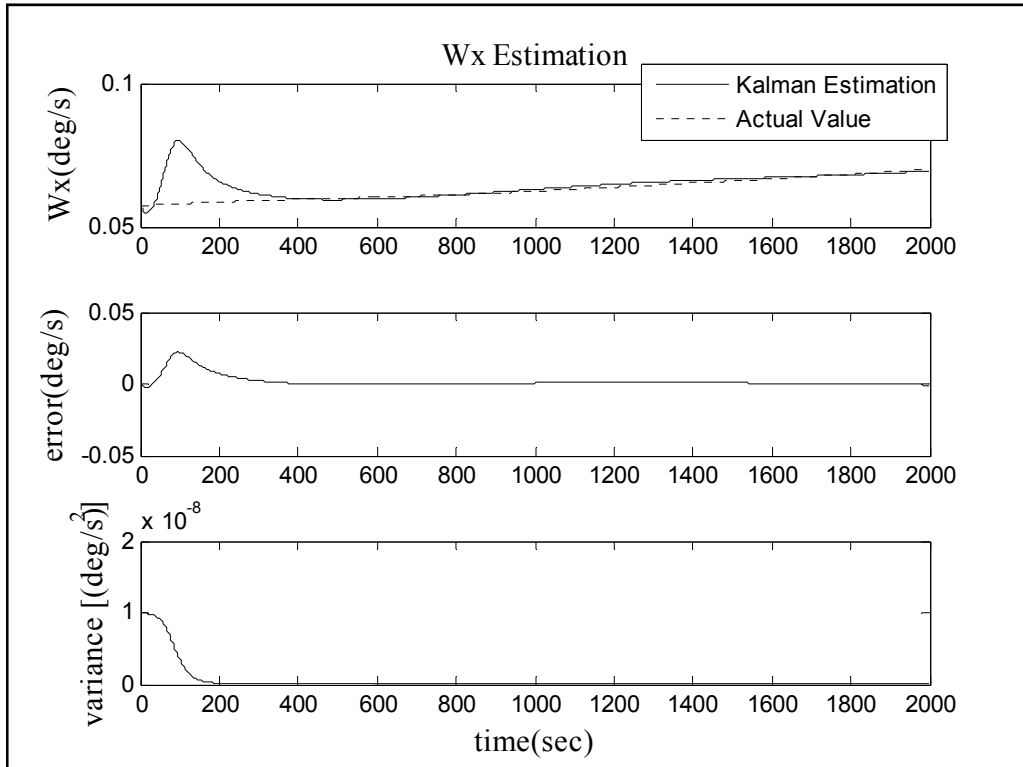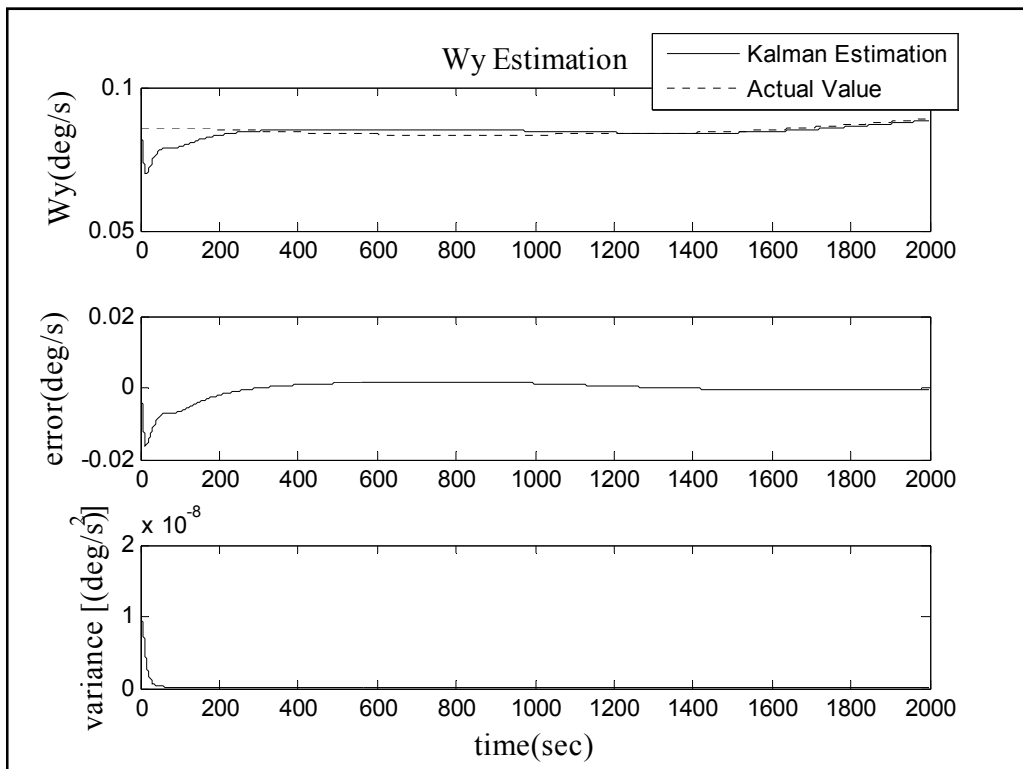
APPENDIX I

Figure I.1: Pitch angle estimation by AUFKF with MFF in case of continuous bias at measurements.
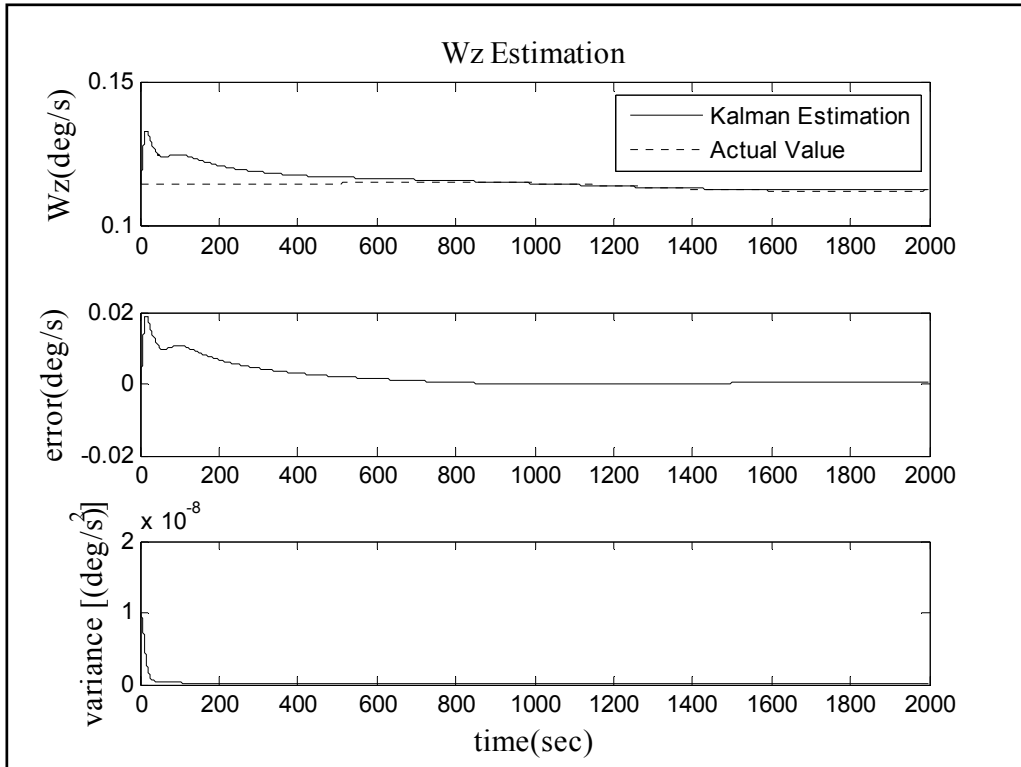

Figure I.2: Yaw angle estimation by AUFKF with MFF in case of continuous bias at measurements.

Figure I.3: Angular velocity about "x" axis estimation by AUFKF with MFF in case of continuous bias at measurements.
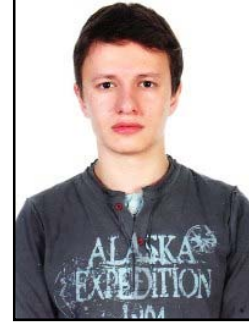

Figure I.4: Angular velocity about "y" axis estimation by AUFKF with MFF in case of continuous bias at measurements.

Figure I.5: Angular velocity about "z" axis estimation by AUFKF with MFF in case of continuous bias at measurements.

CURRICULUM VITA

Candidate's full name: Halil Ersin Söken

Place and date of birth: İstanbul / 1985

Permanent Address: Şehremini, İstanbul

**Universities and
Colleges attended:**

Bachelor of Science

2003 - 2008   Istanbul Technical University (ITU)
               Faculty of Aeronautics and Astronautics
               Department of Aeronautical Engineering (2. Major)

2003 - 2007   Istanbul Technical University (ITU)
               Faculty of Aeronautics and Astronautics
               Department of Astronautical Engineering (1. Major)

High School

1996 – 2003   Vefa Anatolian High School

Publications:

▪ Hajiyev, Ch., and **Söken, H.E.,** 2007: Attitude Estimation of ITU-PSAT I Satellite on Magnetometer Measurements. *Proceedings of: 4th Ankara International Aerospace Conference,* September 10-12, 2007 Ankara, Turkey.

▪ Hajiyev, Ch., and **Söken, H.E.,** 2008: Unscented Kalman Filter Based Attitude Estimation of ITU-PSAT I Satellite using Magnetometer Measurements. *Proceedings of: SSW 2008 International Workshop on Small Satellites, New Missions and New Technologies,* June 5-7, 2008 Istanbul, Turkey.

▪ **Söken, H.E.,** and Hajiyev, Ch. 2008: Adaptive EKF with the Filter Gain Correction Applied to Magnetometer Based Attitude Determination System of a LEO Satellite. *Proceedings of: SSW 2008 International Workshop on Small Satellites, New Missions and New Technologies,* June 5-7, 2008 Istanbul, Turkey.

▪ **Söken, H.E.,** and Hajiyev, Ch. 2008: İTÜ-PSAT I Yönelim Kestirim Uygulamaları için Genişletilmiş ve Sezgisiz Kalman Süzgeçleri Karşılaştırması. *II. Ulusal Havacılık ve Uzay Konferansı,* Ekim 15-17, 2008 İstanbul, Türkiye.

- Hajiyev, Ch., and **Söken, H.E.,** 2009: Adaptive Kalman Filter with Multiple Fading Factors for UAV State Estimation. *Proceedings of: 7th IFAC Symposium on Fault Detection, Supervision and Safety of Technical Processes,* June 30- July 2, 2009 Barcelona, Spain.

- **Söken, H.E.,** and Hajiyev, Ch. 2009: Adaptive Unscented Kalman Filter with Multiple Fading Factors for Pico Satellite Attitude Estimation. *Proceedings of: 4th International Conference on Recent Advances in Space Technologies,* June 11-13, 2009 Istanbul, Turkey.

- **Söken, H.E.,** and Hajiyev, Ch. 2009: UKF for Identification of the Pico-Satellite Attitude Dynamics Parameters and External Torques on IMU and Magnetometer Measurements. *Proceedings of: 4th International Conference on Recent Advances in Space Technologies,* June 11-13, 2009 Istanbul, Turkey.

- Hajiyev, Ch., and **Söken, H.E.,** 2009: Adaptive Kalman Filter with the Gain Correction Applied to UAV Flight Dynamics. *Proceedings of: 17th Mediterranean Conference on Control and Automation,* June 24-36, 2009 Thessaloniki, Greece.

- Hajiyev, Ch., and **Söken, H.E.,** 2009: Adaptive Fading Kalman Filters with UAV Flight Control System Applications. *Accepted for: International Symposium on Engineering and Architectural Sciences of Balkan, Caucasus and Turkic Republics,* October 22-24, 2009 Isparta, Turkey.